LEVEL

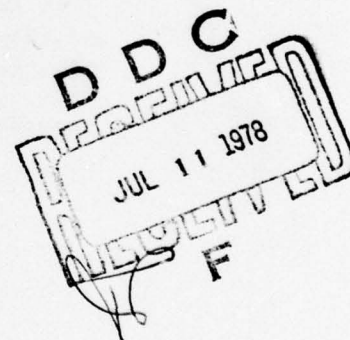Report No. FAA-RD-77-119

AD A056151

ID No. _____
JDC FILE COPY

GUST FRONT ANALYTICAL STUDY

R. C. Goff
J. T. Lee
E. A. Brandes

DDC

JUL 11 1978

F

December 1977

FINAL REPORT

Document is available to the U.S. public through
the National Technical Information Service,
Springfield, Virginia 22161.

Prepared for

U.S. DEPARTMENT OF TRANSPORTATION
FEDERAL AVIATION ADMINISTRATION
Systems Research & Development Service
Washington, D.C. 20590

78 07 06 064

NOTICE

This document is disseminated under the sponsorship of the Department of Transportation in the interest of information exchange. The United States Government ment assumes no liability for its contents or use thereof.

Technical Report Documentation Page

1. Report No.	2. Government Accession No.	3. Recipient's Catalog No.
FAA-RD-77-119		

4. Title and Subtitle		5. Report Date
GUST FRONT ANALYTICAL STUDY		December 1977
		6. Performing Organization Code

7. Author's)	8. Performing Organization Report No.
R. C. Goff, J. T. Lee and E. A. Brandes	

9. Performing Organization Name and Address	10. Work Unit No. (TRAIS)
U. S. Department of Commerce	154-451-014C
National Oceanic and Atmospheric Administration	11. Contract or Grant No.
National Severe Storms Laboratory	DOT-FA76WAI-622 Task II
1313 Halley Circle Norman, Oklahoma 73069	13. Type of Report and Period Covered

12. Sponsoring Agency Name and Address	
U. S. Department of Transportation	Final Report
Federal Aviation Administration	March 1976 - December 1977
Systems Research and Development Service, Airport Div.	14. Sponsoring Agency Code
Washington, D. C. 20590	FAA/ARD-450

15. Supplementary Notes

Prepared under FAA Interagency Agreement No. DOT-FA76WAI-622, managed by the Aviation Weather Branch, ARD-450

16. Abstract

Strong wind changes and turbulence encountered by aircraft arriving or departing an airport constitute hazards to safe flight. Most serious encounters are thunderstorm outflow related. The gust front structure as observed by Doppler radar, standard weather radar, a 461 m meteorologically instrumented tower, aircraft and other observations is presented. Gust front evolution as observed with a severe thunderstorm is shown. Turbulence and multiple surges are discussed.

17. Key Words	18. Distribution Statement
Thunderstorm Gust Front Wind Shear	Document is available to the U.S. public through the National Technical Information Service, Springfield, Virginia 22151.

19. Security Classif. (of this report)	20. Security Classif. (of this page)	21. No. of Pages	22. Price
Unclassified	Unclassified	140	

Form DOT F 1700.7 (8-72)   Reproduction of completed page authorized

iii

PREFACE

The authors are most grateful for the efforts of all who helped
in the preparation of this report.   In particular, we wish to recognize
Mr. Leonard Johnson and Mr. Jack Reece whose diligent and expert at-
tention to the meteorological tower operation was responsible for the
high quality data set.   We also would like to thank the staff members
of the National Severe Storms Laboratory and those of the U. S. Air
Force Aeronautical System Division whose participation in data acquisi-
tion made the project possible.   Miss Judi Stokes' assistance in the
tower data analysis, Mrs. Connie Hall and Mrs. Madelyn Priest's typing
of the manuscript, Mr. Charles Clark and Mrs. Jennifer Moore's prepara-
tion of the illustrations are all recognized and greatly appreciated.

METRIC CONVERSION FACTORS

Approximate Conversions to Metric Measures

Symbol	When You Know	Multiply by	To Find	Symbol
	LENGTH			
in	inches	*2.5	centimeters	cm
ft	feet	30	centimeters	cm
yd	yards	0.9	meters	m
mi	miles	1.6	kilometers	km
	AREA			
in^2	square inches	6.5	square centimeters	cm^2
ft^2	square feet	0.09	square meters	m^2
yd^2	square yards	0.8	square meters	m^2
mi^2	square miles	2.6	square kilometers	km^2
	acres	0.4	hectares	ha
	MASS (weight)			
oz	ounces	28	grams	g
lb	pounds	0.45	kilograms	kg
	short tons (2000 lb)	0.9	tonnes	t
	VOLUME			
tsp	teaspoons	5	milliliters	ml
Tbsp	tablespoons	15	milliliters	ml
fl oz	fluid ounces	30	milliliters	ml
c	cups	0.24	liters	l
pt	pints	0.47	liters	l
qt	quarts	0.95	liters	l
gal	gallons	3.8	liters	l
ft^3	cubic feet	0.03	cubic meters	m^3
yd^3	cubic yards	0.76	cubic meters	m^3
	TEMPERATURE (exact)			
°F	Fahrenheit temperature	5/9 (after subtracting 32)	Celsius temperature	°C

*1 in = 2.54 (exactly). For other exact conversions and more detailed tables, see NBS Misc. Publ. 286, Units of Weights and Measures, Price $2.25, SD Catalog No. C13.10:286.

Approximate Conversions from Metric Measures

Symbol	When You Know	Multiply by	To Find	Symbol
	LENGTH			
mm	millimeters	0.04	inches	in
cm	centimeters	0.4	inches	in
m	meters	3.3	feet	ft
m	meters	1.1	yards	yd
km	kilometers	0.6	miles	mi
	AREA			
cm^2	square centimeters	0.16	square inches	in^2
m^2	square meters	1.2	square yards	yd^2
km^2	square kilometers	0.4	square miles	mi^2
ha	hectares (10,000 m^2)	2.5	acres	
	MASS (weight)			
g	grams	0.035	ounces	oz
kg	kilograms	2.2	pounds	lb
t	tonnes (1000 kg)	1.1	short tons	
	VOLUME			
ml	milliliters	0.03	fluid ounces	fl oz
l	liters	2.1	pints	pt
l	liters	1.06	quarts	qt
l	liters	0.26	gallons	gal
m^3	cubic meters	35	cubic feet	ft^3
m^3	cubic meters	1.3	cubic yards	yd^3
	TEMPERATURE (exact)			
°C	Celsius temperature	9/5 (then add 32)	Fahrenheit temperature	°F

TABLE OF CONTENTS

LIST OF ILLUSTRATIONS

LIST OF TABLES

LIST OF ABBREVIATIONS AND SYMBOLS

AGL	=	Above ground level
c	=	Gust front propagation speed
C	=	Temperature degrees Celsius
CST	=	Central Standard Time
dBZ	=	Radar reflectivity factor in decibels
h_1	=	Unit depth of downdraft
h_2	=	Depth of outflow
INS	=	Inertial navigation system
km	=	Kilometers
K	=	Temperature degrees Kelvin
m	=	Meter
mb	=	Millibar
$m\ s^{-1}$	=	meter per second
M_1	=	Mass of downdraft air
M_2	=	Mass of outflow air
n mi	=	Nautical mile
P	=	Pressure
r_1	=	Downdraft radius
$r_2 r_3$	=	Outflow radius
RAD	=	Solar radiation
RH	=	Relative humidity
s	=	Second
t	=	Time
T	=	Dry bulb temperature
T_w	=	Wet-bulb temperature
u	=	Horizontal wind normal to gust frontal axis
v	=	Horizontal wind parallel to gust front
V	=	Wind speed
$\vec{V}$	=	Vector wind
w	=	vertical velocity
z	=	radar reflectivity factor
α	=	Gust front orientation angle
ρ_1	=	Density of downdraft air

ρ_2 =   Density of outflow air

∇ =   Del operator

GUST FRONT ANALYTICAL STUDY

1.0 Introduction

1.1 Nature of the Problem

Strong wind changes and turbulence encountered during landing or takeoff
are a hazard to aircraft. Change in effective air flow over the wing may be
manifested under severe conditions as unacceptable departures of the aircraft
from the glide slope. The hazard may be additionally compounded by turbu-
lence, downdrafts, and pilot input with a serious accident as the net result.
Most serious encounters have been related to thunderstorm produced outflow or
gust front. Uncertainty in gust front observation and prediction, severity,
and location appear as the main elements in continued loss of, or damage to,
aircraft due to gust fronts and it is toward understanding of these factors
that this program is directed.

The thunderstorm gust front is a line or zone extended horizontally,
along which the wind shifts abruptly. Ahead of the gust front the air is
often blowing into the storm. Behind the gust front rain-cooled descended air
is blowing out of the storm.

1.2 Objectives and Scope

Our study has two main objectives: 1) Gather and present a represent-
ative sample of gust front data, and 2) Develop a three-dimensional model of
thunderstorm gust fronts. The project is based on data acquired by airborne
and ground-based systems which measure the wind shear and turbulence in and
below thunderstorm cloud bases, primarily along the leading edge of the cold
air outflow or gust front.

1.3 Research Plan

The thunderstorm gust front is a transitory boundary and to characterize
it requires observations of many meteorological parameters in both time and

space domains. Many of the specific aspects have been observed before (Byers, Braham, 1949; Charba, 1974). In the Thunderstorm Project, for example, Byers and Braham called the outflow's leading edge the "First Gust" and noted that it appeared to result from cold downdraft air of a mature thunderstorm reaching the ground and spreading out in all directions. When the cell had motion relative to the earth, then the cell's translational velocity was added to the outflow with an increase in velocity relative to the surface on the leading edge and a decrease in velocity on the trailing edge. Surface manifestations, measured by a network of autographic meteorological instruments, were main considerations. Gust front characteristics above the ground were not defined and this requirement is paramount in the National Severe Storms Laboratory (NSSL) program design.

In an idealized case study, the observational sequence typically develops as follows: 1) a cumulus-congestus cloud is observed by weather radar and satellite; 2) as the cloud develops in a field of wind, temperature and moisture defined by rawinsonde observations, two Doppler radars are used with coordinated scans to delineate motions within the cloud; 3) during the transition into a thunderstorm, aircraft flying at or below cloud base, are directed to define the horizontal and vertical extent of the developing gust front; 4) as the gust front approaches the instrumented tower, the aircraft are concentrated on observing the turbulence and wind shear along the gust front boundaries while the Doppler radars are operating in a mode to acquire data in the clear air around and below the thunderstorm base; 5) as the gust front approaches the airport, the instrumented aircraft is flown to make repeated landing approaches while the gust front crosses the field. Data obtained during several such sequences of events would be melded for gust model development.

In practice, vagaries of nature and instruments precluded attainment of the ideal in observations. We have nevertheless substantially attained study objectives in gust front description and model development.

1.4 Observational Program

The 1976 National Severe Storms Laboratory (NSSL) observational program
utilized a number of sensing systems deployed as shown in Figure 1-1. These
systems are as follows:

1.4.1 Meteorologically Instrumented Tower

The 461 m KTVY television transmitter tower (Figure 1-2) has been used
by NSSL as a multi-level boundary layer sensor facility since 1966. The
tower is located in a rural area north of Oklahoma City. This location is
well surveyed by NSSL's Doppler radars at Norman and Cimarron Field.

In 1976 the tower was instrumented at six levels with various sensors
measuring wind, temperature, water vapor content, radiation, rainfall and
pressure. In addition, a standard 7 m surface site, located 60 m from the
tall tower, sensed certain near-ground level meteorological information.
Figure 1-3 is a schematic diagram of the tower facility and the surface
station. Table 1-1 gives sensor types.

Table 1-1. Tower Sensor Types

V: Bendix Aerovane Model 120 (3 bladed propeller)

T: Yellow Springs linearized thermistors (with aspirated radiation shield)

T_w: Same as T, except moistened muslin wick attached to probe. Water
reservoir attached.

RH: Vaisälä Humicap relative humidity sensors

W: R. M. Young Model 27100 vertical velocity sensor (4-bladed
polystyrene propeller.)

P: Belfort model 6068 aneroid barometer

Rainfall: Belfort Model 5-780 recording raingage

Radiation: Epply pyranometer

Data is routinely recorded on magnetic tape. A 10 second sample
interval is used during non-storm conditions and a 1.3 second interval
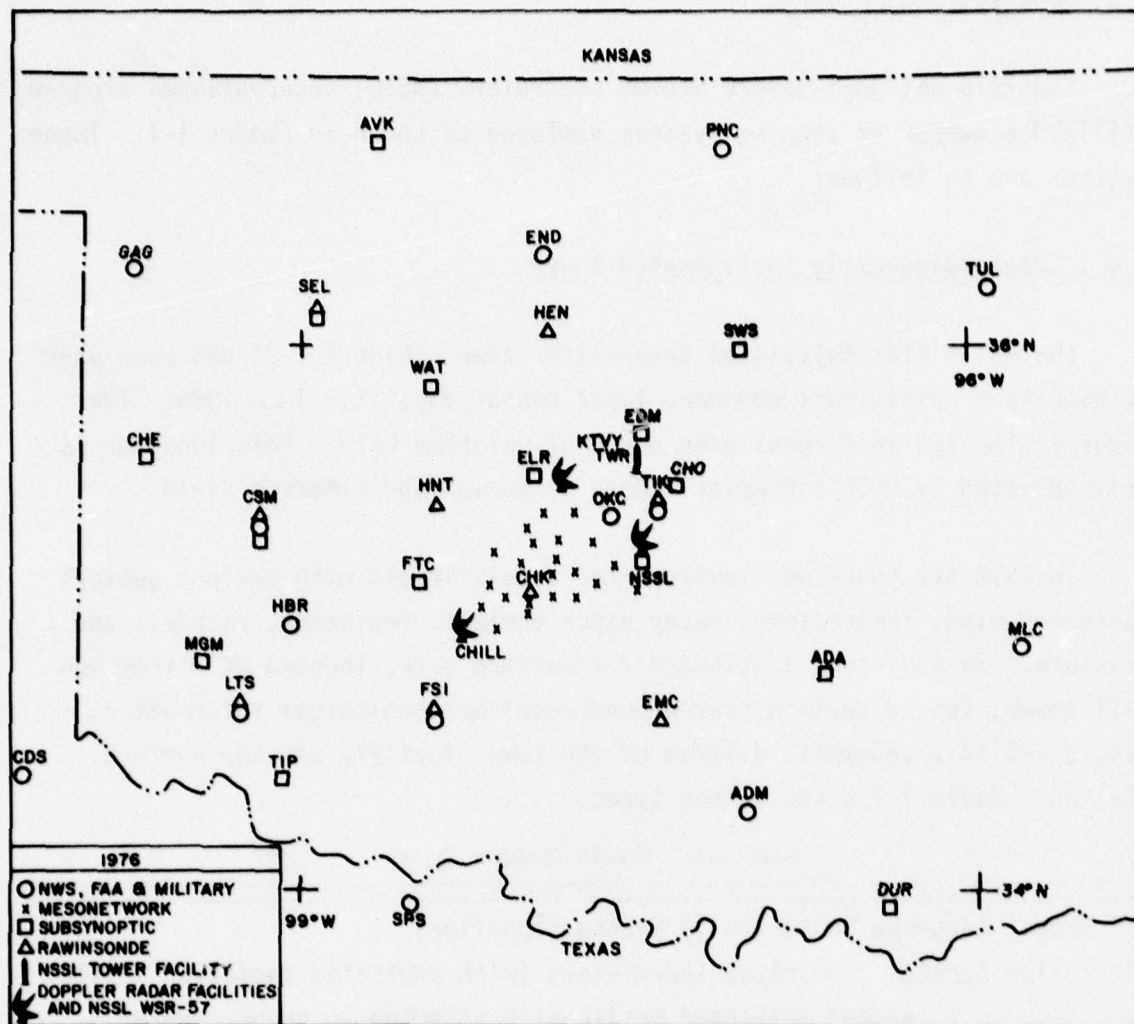during storm periods. Data are later edited and archived following rigorous

Figure 1-1 *National Severe Storms Laboratory's 1976 Spring Observational Program network.*

quality control procedures. Objective analysis of the tower data in time-height sections (see Appendices) is described in detail in Goff (1976).

1.4.2 Aircraft

To measure turbulence and wind shear along the glide slope and in the upper regions of the gust front above the tower, an F-4-C aircraft has been employed. Considerations in the aircraft selection were aircraft structural

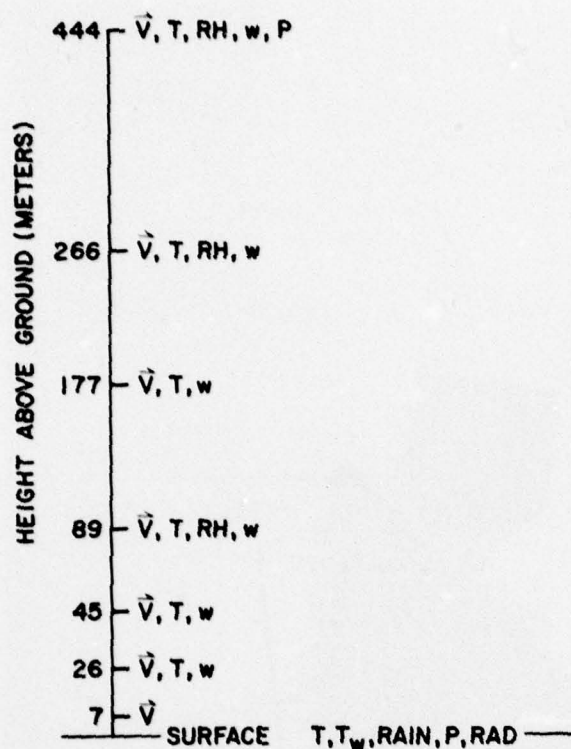Figure 1-2 View up southwest face of NSSL-KTVY meteorological tower. Conduit bridge is in left foreground.

Figure 1-3 *Schematic view of sensors and tower; figures at left indicate height of sensor systems.* $\vec{V}$ - *horizontal wind speed and direction;* T = *dry-bulb temperature;* T_w = *wet-bulb temperature;* RH = *relative humidity;* w = *vertical velocity;* P = *pressure;* Rad = *Solar radiation.*

HEIGHT ABOVE GROUND (METERS)

444 — $\vec{V}$, T, RH, w, P

266 — $\vec{V}$, T, RH, w

177 — $\vec{V}$, T, w

89 — $\vec{V}$, T, RH, w

45 — $\vec{V}$, T, w

26 — $\vec{V}$, T, w

7 — $\vec{V}$

SURFACE   T, T_w, RAIN, P, RAD

ruggedness, reserve power, instrumentation and availability. A fighter-type aircraft best meets the power and structural requirements. An F-4-C instrumented for thunderstorm turbulence measurements was available and with full utilization of the inertial platform aboard the aircraft, u, v, and w wind components as well as turbulence were determined. The F-4-C #744 (Figure 1-4) is operated by the USAF 3246 Test Wing (AFSC), Eglin AFB, Florida with equipment assistance by the 4950th Test Wing, Wright-Patterson AFB, and is flown in a joint program with FAA and NSSL. Basic characteristics of the F-4-C are given in Table 1-2 and meteorological instrumentation in Table 1-3.

Data are recorded in analog form by FM multiplexing using a Leech model MTR-3200A recorder. Records are converted from analog to digital format on the ground. Data are sampled at 1/50 second intervals and 5 data points are averaged to give 1/10 second data output values. The aircraft was stationed at Tinker AFB May 13 to June 18 during which seven flights were made. None were flown into a gust front since all storms occurring
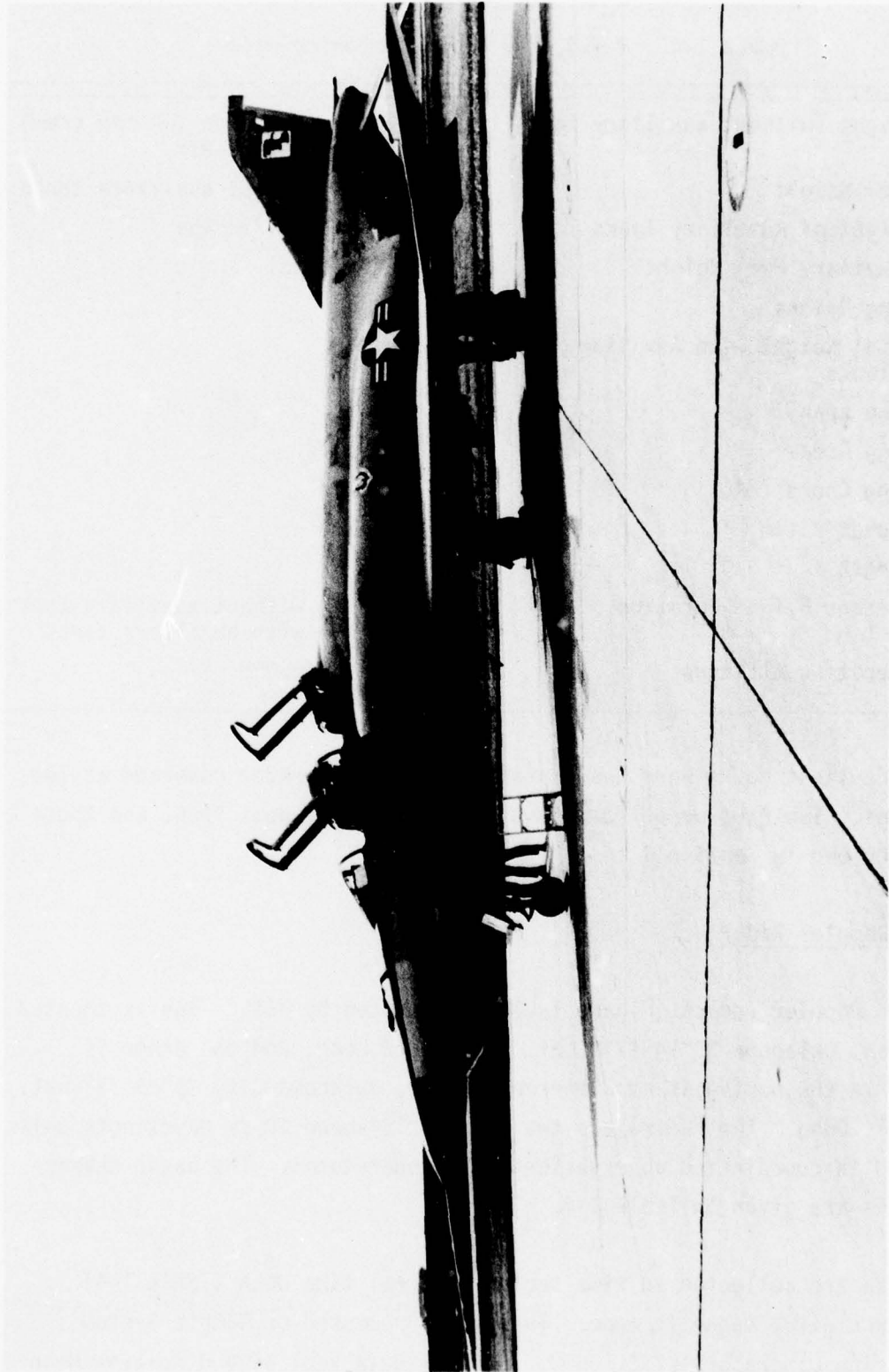
Figure 1-4 F-4-C Aircraft used for gust front and thunderstorm turbulence studies.

7

Table 1-2. F-4-C #744 Basic Characteristics

Weight (without auxiliary tank)	44,582 lbs (fuel and two man crew) at ramp for take-off
Fuel Weight	12,845 lbs without auxiliary tanks
Weight of Auxiliary Tanks	2 @ 616 lbs = 1232 lbs
Auxiliary Fuel Weight	5,032 lbs total
Wing Pylons	264 lbs
Total Weight with Auxiliary Tanks	51,110 lbs
Wing span	38 ft 5 in
Wing Area	538.34 sq ft
Wing Chord (MAC)	16 ft .5 in
Aspect Ratio	2.82
Length	56 ft
Average Flight Duration	1 hr 30 min without auxiliary tanks 2 hr 15 min with auxiliary tanks
Operating Altitude	Surface to 40,000

during daylight hours were too distant for adequate radar coverage at low altitudes. Two runs were flown just above a surface gust front and these are described in Section 4.

1.4.3 Doppler Radar

Two Doppler radars (Figure 1-5) are operated by NSSL. One is located at Norman, Oklahoma 35°14'11"N Lat. 97°27'48"W Long. and the other is 41.3 km to the northwest at Cimarron Airport, Oklahoma City 35°28'31" Lat. 97°48'47" Long. The radars are two similar "S"-band 10 cm wavelength units operated in coordinated observations of thunderstorms. The basic characteristics are given in Table 1-4.

Data are collected in time series and real time data (Table 1-4) format on digital magnetic tape. These are processed on NSSL's System Engineering Laboratory's SEL 8600. Doppler data real time displays--Mean

Table 1-3. Aircraft Instrumentation

Parameter	Instrument
Temperature	Rosemount 102CA2W peaks
Time	Time code generator
Angle of attack	
α-β vanes	Fiberglass
Pitch angle	
Pitch rate	
Normal accelerations	
Pressure altitude	Kistler Inst. Corp. model 314A001
Radar altitude	APN 159
Elevator position	
INS pitch attitude	INS Litton AN/ASN-56
Roll angle	INS
Airspeed	Kistler Inst. Corp. model 314D0001 pressure differential transducer
Groundspeed and direction	INS
Magnetic heading	
Tape recorder	Leech model MTR-3200A

Velocity Processor and Multi-Moment Display, described by Sirmans (1973) and Burgess, et al (1976) respectively--were used in addition to the spectrum display described in Section 4.2 of this report.

1.4.4 The WSR-57 Weather Radar

The WSR-57 is the basic weather surveillance radar used at NSSL. Charactistics are given in Table 1-5. Radar reflectivity (intensity) is digitized and time-and space-integrated and recorded at 200 range locations on a grid of 2° by 1 km. These values are displayed on a PPI scope, recorded on magnetic tape, and also photographed with a 35 mm camera on a repeater scope. There is also an MPX-7/UPX-6 aircraft transponder interrogator (IFF) and receiver whose trigger and antenna rotation is synchronized with the WSR-57. The IFF reply is superimposed on the WSR-57 PPI reflectivity display.

9

Figure 1-5 30 ft. diameter antenna
of NSSL 10 cm Doppler radar
Norman, Oklahoma.

1.4.5 Surface Observations

Two standard surface stations were operated on different sides of the
tower in 1976. These stations were roughly 6.5 mi northwest (North Pennsyl-
vania) and southeast (Coultrain Road) of the KTVY tower so that the stations
and the tall tower were all on the same straight line.

The two stations recorded horizontal wind, dry- and wet-bulb tempera-
ture, pressure and rainfall, using the same sensors as the tall tower.
Data were recorded on magnetic tape and analog stripchart. In addition,
the data were transmitted to NSSL via telephone line and displayed there on
a cathode ray tube to allow real time estimation of the timing of approaching
thunderstorms (in particular the gust front). Low-level aircraft runs past
the tower (and approaches to Tinker AFB) would then be well timed with
information from the surface sites and the tower. Unfortunately, meteorolo-
gical conditions allowing these experiments never occurred during the 1976
spring program.

10

TABLE 1-4   NSSL Doppler Radar Characteristics (1976)

PARAMETER	CIMARRON (CIM)	NORMAN (NRO)	NRO Hi PRF
Antenna			
Shape	Parabolic	Parabolic	Parabolic
Diameter	9.15 m	9.15 m	9.15 m
Half-Power Beam Width	0.85 deg	0.81 deg	0.81 deg
Gain	46 dB	46.8 dB	46.8 dB
First Side Lobe Level	21 dB	21 dB	21 dB
Polarization	Horizontal	Vertical	Vertical
RMS Surface Deviation	2.5 mm	2.8 mm	2.8 mm
Transmitter			
Wavelength	10.94 cm	10.52 cm	10.52 cm
Frequency	2735 MHz	2850 MHz	2850 MHz
Pulse Repetition Time	768 μsec	768 μsec	288 μsec
Pulse Width	1 μsec (150 m)	1 μsec (150 m)	0.30 μsec (52 m)
* Peak Power	500 kW	750 kW	200 kW
Receiver			
*/**System Noise Figure	4 dB	4 dB	4 dB
Transfer Function	Doppler - linear; Intensity - logarithmic	Doppler - linear; Intensity - logarithmic	Doppler - linear; Intensity - logarithmic
* Dynamic Range	70 dB	80 dB	80 dB
Band Width: 3 dB; 6 dB	.6; .85 MHz	.6; .85 MHz	.45; .63 MHz
Intermediate Frequency	30 MHz	30 MHz	30 MHz
* Min. Detectable Signal (SNR = 1)	-105 dBm	-108 dBm	-107 dBm
Doppler Time Series Data Acquisition			
No. of Simultaneous Range Gates	16	16	6
No. of Blocks Along Radial	Unlimited	8	8
Range Gate Spacing	300, 450,...1200, 1350 m	150, 300, 600, 1200 m	150, 300, 600, 1200 m
Azimuthal Sample Spacing	0.1 to 9.9 deg	0.1 to 9.9 deg	0.1 to 9.9 deg
Automatic Elevation Increment	0.5 to 9.9 deg	0.1 to 9.9 deg	0.1 to 9.9 deg
***Number of Samples in Time Series	2^n; n = 1, 2,...13	2^n; n = 1, 2,...13	2^n; n = 1, 2,...13
Complex Video Digital Word Length	10 bits (binary)	12 bits (binary)	12 bits (binary)

*Representative value.

**Measured at receiver calibration port.

***Practically all data taken with n = 6, i.e., 64 samples for normal PRF and n = 7, i.e., 128 samples for Hi PRF.

TABLE 1-4   (Continued).

PARAMETER	CIMARRON (CIM)	NORMAN (NRO)	NRO Hi PRF
Mean Velocity and Spectrum Width			
Data Acquisition			
No. of Range Gates	762	762	192
Range Gate Spacing	150 m	150 m	225 m
***Number of Samples in Estimate	2^n; n = 5, 6, 7, 8	2^n; n = 5, 6, 7, 8	2^n; n = 5, 6, 7, 8
Recorded Word Length			
Velocity	6 bits (2's comp)	6 bits (2's comp)	6 bits (2's comp)
Width	6 bits, 0-32 (binary)	6 bits, 0-32 (binary)	6 bits, 0-32 (binary)
Intensity Data Acquisition			
No. of Range Gates	762	762	192
Range Gate Spacing	150 m	150 m	225 m
****Number of Samples in Estimate	$2^n - 1$ (exp); 2^n (linear) n = 3, 4,...10	$2^n - 1$; 2^n n = 3, 4,...10	$2^n - 1$; 2^n n = 3, 4,...10
Time Window Function	Linear or exponential	Linear or exponential	Linear or exponential
Recorded Word Length	6 bits (binary)	6 bits (binary)	6 bits (binary)
General Features			
****Azimuthal Antenna Rotation Rate	0.1 to 24.0 deg sec^{-1}	0.1 to 10 deg sec^{-1}	0.1 to 10 deg sec^{-1}
***Maximum Unambiguous Range	115 km	115 km	43 km
Maximum Unambiguous Velocity	$\pm$35.6 m sec^{-1}	$\pm$34.2 m sec^{-1}	$\pm$91 m sec^{-1}
PPI Capability	Yes	Yes	Yes
RHI Capability	Yes	Yes	Yes
Coplane Capability	No	No	No

* High PRF real time estimates are with an equivalent PRF of 870 Hz; V_m = 22.7 m s^{-1}
** Practically all data taken with n = 7, i.e., 128 samples in estimate.
*** Practically all data taken with n = 7, i.e., 127 samples in estimates.
**** Practically all data taken in exponential mode with n = 7, i.e., 127 samples in estimates.

12

Table 1-5. NSSL WSR-57 Radar Characteristics

Antenna

Shape	Parabolic
Diameter	3.66 m
Half-power beamwidth	2.0°
Gain	40 dB
First side lobe level	20 dB
Polarization	Horizontal

Transmitter

Wavelength	10.6 cm
Frequency	2840 mHz
Pulse repetition time	6144 s
Pulse width	4 sec (600 m)
Peak power	2.26×10^5 watts

Intensity Data Acquisition

No. of range gates	200 (recorder) 512 (display)
Range gate spacing	Variable .5, 1, 2 km (normally 1 km)
Azimuthal sample spacing	2 deg

General Features

Azimuthal rotation rate	3 RPM
Maximum unambiguous range	921.6 km
Normal recording range	200 km
Normal surveillance range	512 km

Additional surface observation mesonetwork stations (Figure 1-6) were in operation, mostly southwest of Norman, as indicated on the map in Figure 1-1. These 38 stations recorded wind, temperature, humidity and rainfall in analog format. The records were changed weekly and archived at Norman. These records supplement the radar and satellite observations.

1.4.6 Radiosondes

The rawinsonde network utilized during the observational program is a flexible system uniquely designed each year to address specific experiments. The 1976 system shown in Figure 1-1 employed a net of nine stations spaced an average of 50 km apart. The U.S. Air Force supplied four teams and the U.S. Army five. GMD-1 equipment was used. Balloons were 600 gram with a normal rise rate of 350 m/min. Radiosonde instruments were made by VIZ. Corp.

Figure 1-6 Typical surface mesonetwork station.

Soundings were made twice each day at 0900 CST and 1430 CST to augment the national rawinsonde network data. Soundings were also made at 1.5 hr intervals whenever severe storms were expected to develop or were in the area. A total of 1002 runs were made during the operation May 10 to June 17. Data are computer processed and archived on magnetic tape for analysis.

2.0 DOPPLER RADAR OBSERVATIONS OF SEVERE THUNDERSTORM GUST FRONTS

2.1 Introduction

In this section Doppler radar observations are used to describe gust front evolution and the radar reflectivity structure of large steady-state thunderstorms with rotating updrafts. Here, the gust front is defined as the convergent boundary between storm outflow and inflow, and as such differs slightly from the definition used by Goff (1976).

The data are coordinated volumetric sampling sequences from two S-band pulsed Doppler radars. Generally, measurements are spaced 1 deg in azimuth,

14

1 deg in elevation, and 0.6 km in radial range. Assuming conservation of storm structure during sampling (a period usually less than 2 min), all observations are adjusted for mean storm motion to a common reference time near the midpoint of data collection.

Radial velocity and reflectivity measurements from both radars are interpolated to common horizontal planes with a Gaussian weighting function having an oblately spheroidal influence region with horizontal and vertical influence radii 1.5 and 1.0 km, respectively (Barnes, 1964). Observation weights varied from 1.0 for measurements coincident with grid point locations to 0.02 for measurements at the periphery of the influence region.

Procedures used to determine wind components have been given by Brandes (1977). Analysis parameters include the horizontal perturbation wind [level-mean flow removed, i.e., for a particular velocity field, the average of all velocities is subtracted from each data point leaving the perturbation field ($V^1 = V - \bar{V}$)], vertical velocity, horizontal divergence, and vertical vorticity fields. The perturbation wind presentation is chosen to aid visualization of eddy motion. To reduce errors that arise in the vertical wind component (due to errors inherent in the numerical solution and the Doppler measurements), this component is smoothed with a nine point filter (Shuman, 1957).

2.2 Observations

Severe thunderstorms typically form along cyclonically sheared and convergent boundaries (fronts, for example) and are often organized in squall lines. In the Doppler measurements, primary updrafts, located on southern storm flanks, often appear along an amplified and perturbed convergent boundary separating air entering forward and rear storm quadrants. Storm rotation, if it exists, is first detected aloft (usually below 5 km), then lowers to ground during severe development. Examples of important evolutionary and structural features of squall line storms which contained rotating cells will now be given. These squall lines are to be distinguished from so-called straight (wind) squall lines which comprise most of the tower data.

2.2.1 Oklahoma City Storm: June 8, 1974

On June 8, 1974, a major outbreak of tornadic storms developed in central and northeastern Oklahoma. A squall line formed ahead of a dry line and west of a tropospheric wind jet. The "first echo" of a multiple tornado producing storm that struck Oklahoma City and neighboring communities appeared on radar at 1210 (all times CST). Although the radar reflectivity pattern grew rapidly and was well formed by 1314, the storm's velocity structure had still not attained maximum amplitude. At 0.3 km (all heights AGL)[1], weak shear and convergence are evident in flow entering the storm's western and eastern quadrants (Figure 2-1a). Peak wind shears and strongest updrafts reside near the storm's developing mesocyclone and weak downdrafts are located on the western and northern storm (echo) fringes. Reflectivity appendages and hook echoes were observed continuously in the radar reflectivity patterns from 1314 (right rear flank) until 1440 (right forward flank).

As mesocyclone wind flow increased, the low-level wind discontinuity between air entering the forward and rear storm quadrants became more pronounced and perturbed. It is noteworthy that the mesocyclone circulation plays a significant role in shaping this discontinuity. In all, three tornadoes were spawned by this storm (beginning at 1342); the remaining discussion focuses on storm structure during the last tornado. The resultant wave-like pattern (Figure 2-1b), with a sharply defined psuedo-cold front or gust front (extending southward) and diffuse warm front (extending northward), resembles extratropical cyclone development on a polar front. Highest shear and maximum vertical velocities are situated within the mesocyclone and near the gust front. Downdrafts had formed within the reflectivity core and behind the gust front (east of the tornado). The outflow from both downdraft regions merges to intensify the gust front. Fastest horizontal winds are close to the axis of rotation and are contained in a layer several kilometers deep. A well defined hook echo, a characteristic of many rotating severe thunderstorms, now is evident in the radar PPI

---

[1]For MSL add 0.37 km.
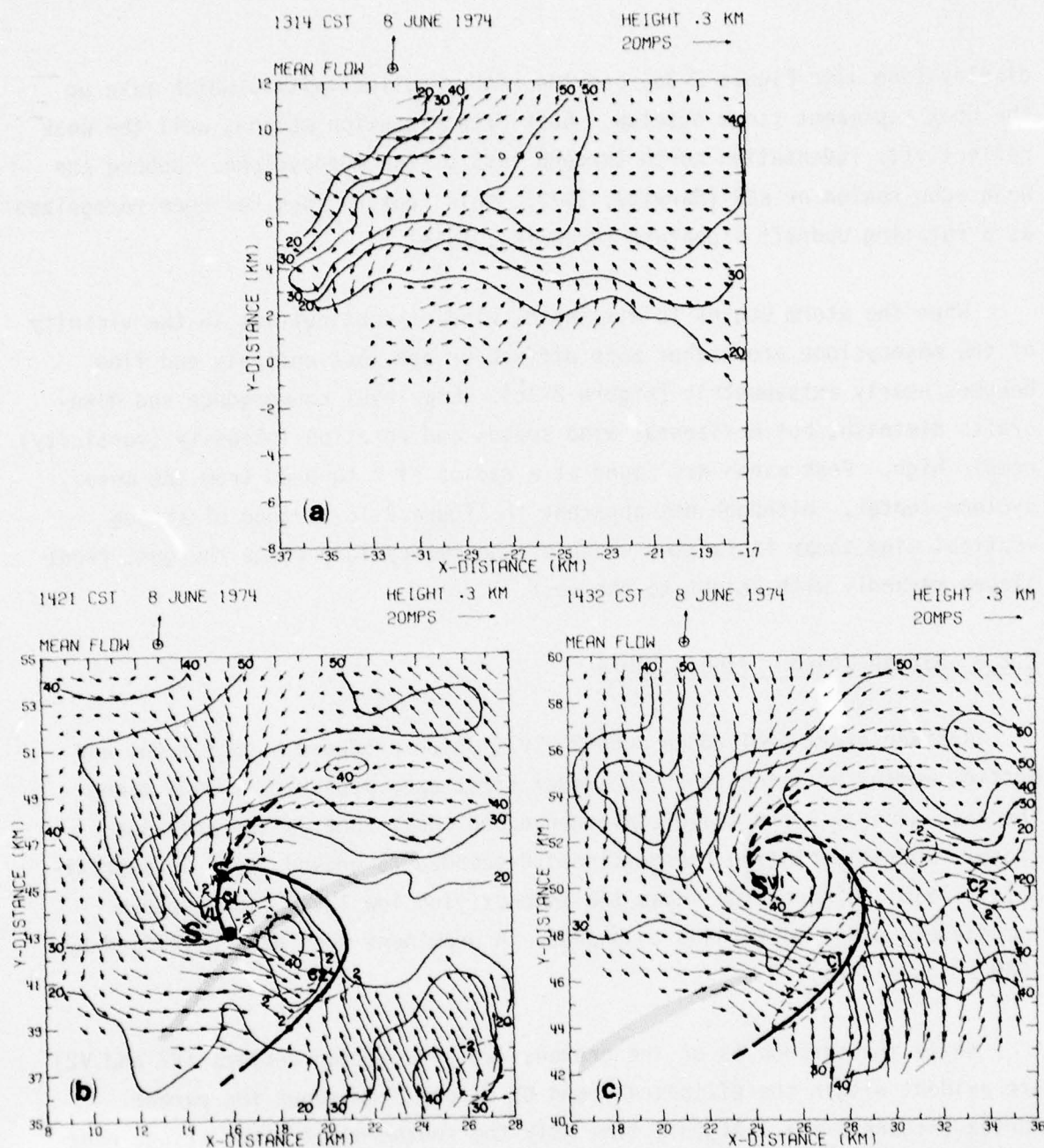
Figure 2-1 Horizontal perturbation wind field analysis of Oklahoma City storm (June 8, 1974) as deduced by Doppler radar. Mean flow has been removed. Contoured radar reflectivity (dBZ, solid lines) and distances pertain to Norman radar. Velocities < 0.5 m s⁻¹ are shown as circles. Select contours of vertical velocity (m s⁻¹) are shown as dashed lines. Vorticity (V) and convergence (C) maxima > 10⁻² s⁻¹ are indicated. Tornado is shown by solid circle and damage path is stippled. Gust front and convergence boundaries are shown by heavy lines. Shear zones are indicated by "S". Heights are AGL (for MSL height add 0.37 km) and north is toward the top of the figure. Storm motion is from 230° at 15 m s⁻¹.

17

display (see also Figure 2-2a) and the higher reflectivities which make up the hook represent storm outflow. Gust front location matches well the weak reflectivity indentation north through east of the mesocyclone. Dubbed the weak echo region or WER (Marwitz, 1972), this feature long has been recognized as a rotating updraft signature (Browning, 1964).

When the storm begins to dissipate, wind discontinuities in the vicinity of the mesocyclone are either more diffuse or are lost entirely and flow becomes nearly axisymmetric (Figure 2-1c). Low-level convergence and down-drafts diminish, but horizontal wind speeds and rotation intensity (vorticity) remain high. Peak winds are found at a radius of 2 to 3 km from the meso-cyclone center. Although not apparent in Figure 2-1c, a zone of strong vertical wind shear is located south of the mesocyclone where the gust front slopes markedly with height to the west.

2.2.2 Harrah Storm: June 8, 1974

Another storm evolved on June 8, 1974 which produced a gust front and outflow worthy of attention. The radar first echo appeared at 1406 along the same general large scale convergence and shear zone as the previous storm. Updraft rotation (mesocyclone) descended to ground level at approxi-mately 1515. Figure 2-3a shows the intensifying low level flow pattern immediately prior to tornado touchdown. A prominent hook echo developed by 1549 (Figure 2-2b).

While the tornado is on the ground, two circulation centers (V1 and V2) are evident within the elliptical band of strong flow about the parent vortex (Figure 2-3b). At this time only the southernmost circulation, near the region of strongest relative surface wind, has height continuity (Figure 2-3c). The other circulation coincides with strong cyclonic shear on the gust front. Intense downdrafts appear within the radar reflectivity core. Strong outflow west of the mesocyclone center may have driven the tornadic circulation in an easterly direction and perhaps contributed to dissipation. Note also the intense outflow surge (dashed line) in the vicinity of a weakening portion of the leading gust front in Figure 2-3c

18
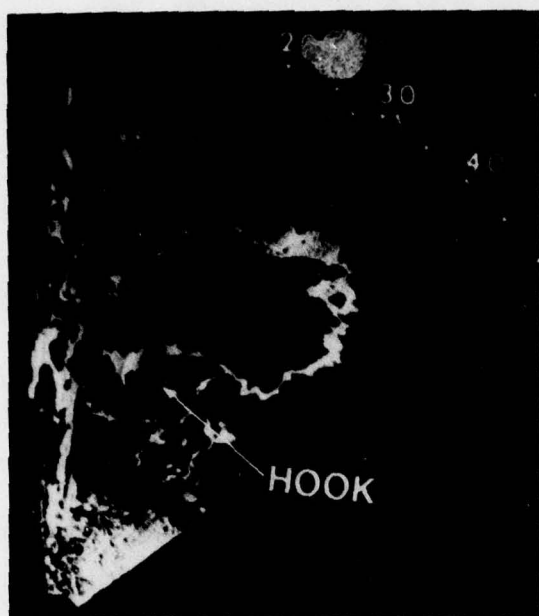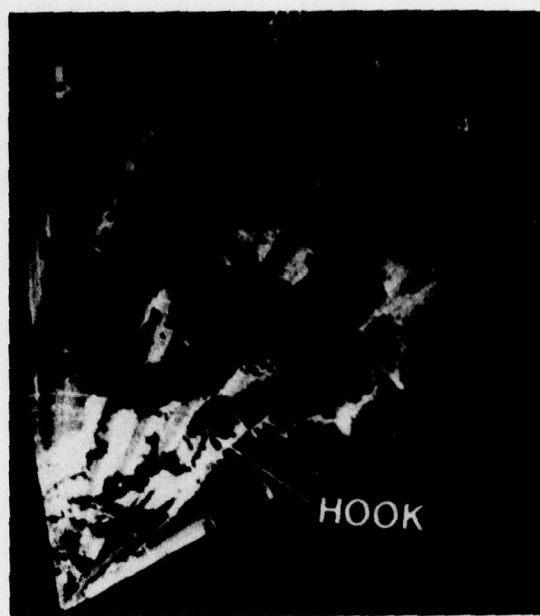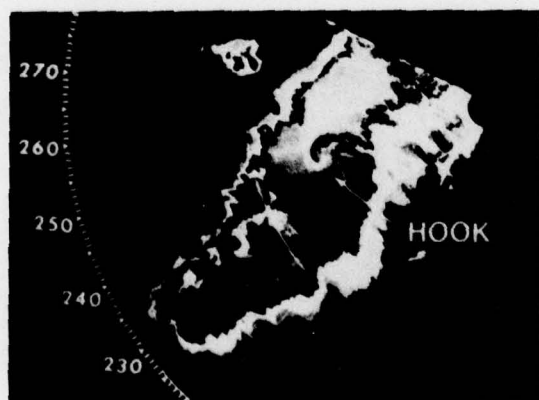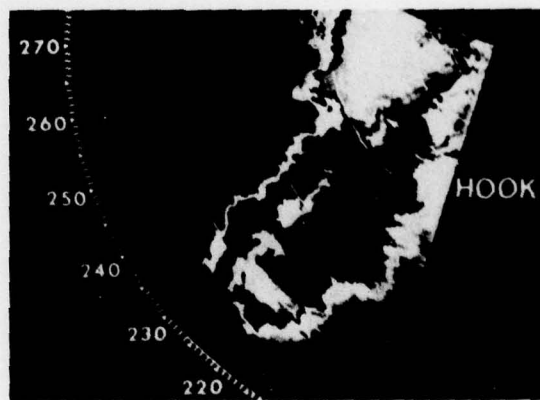
Figure 2-2 Contoured PPI display of Norman Doppler radar (not range normalized) for a) Oklahoma City storm (1419 CST; June 8, 1974); b) Harrah storm (1553 CST; June 8, 1974); c) Tabler storm (1605 CST; June 6, 1974); and d) Tabler storm (1624 CST). Range marks are 20 km.

19
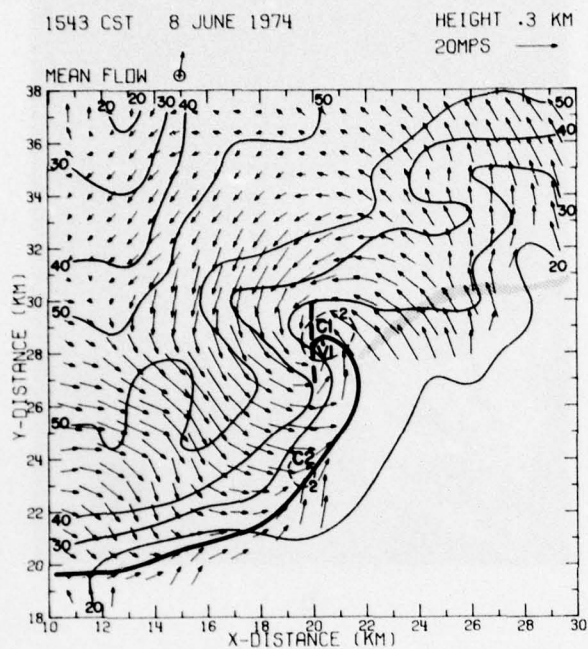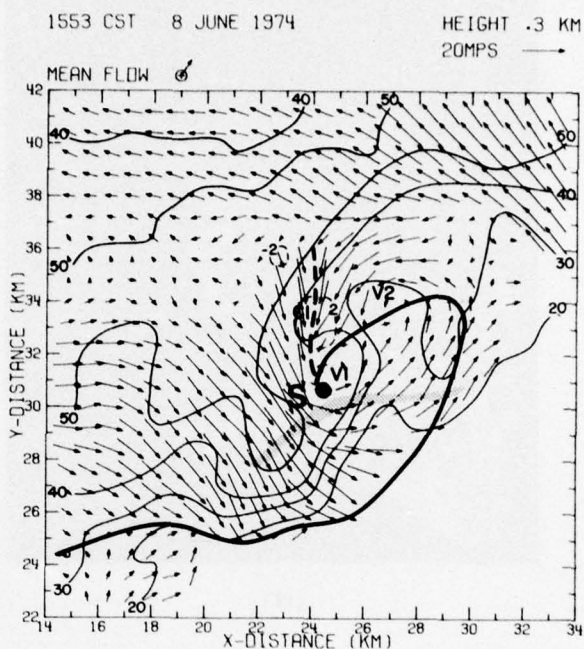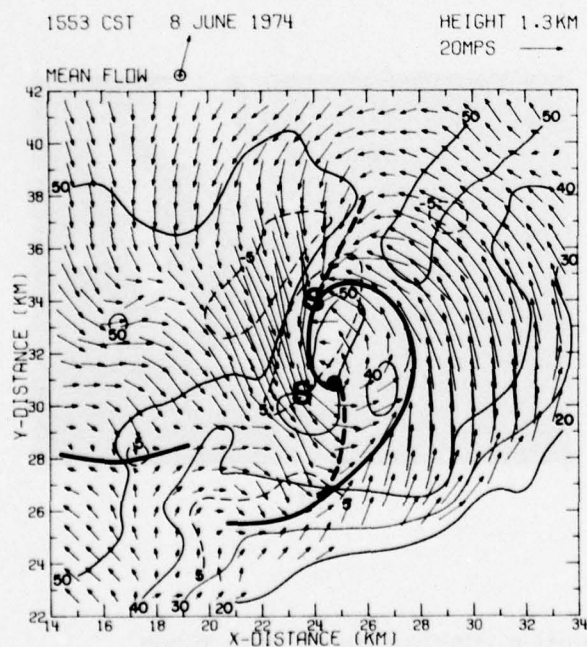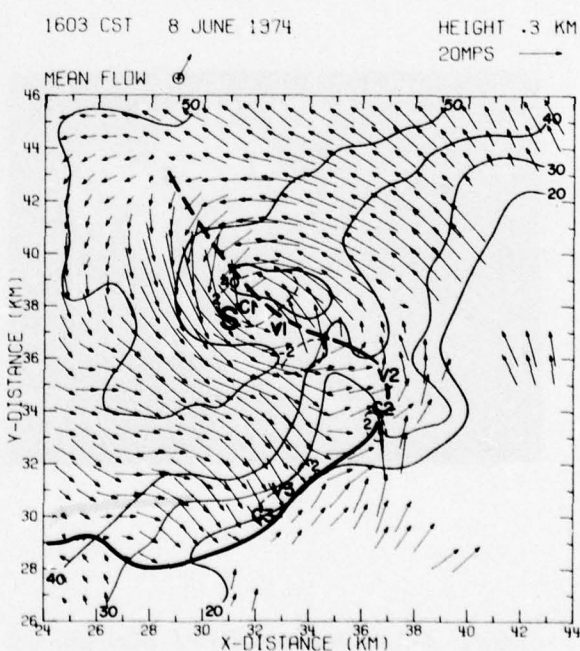
Figure 2-3 *Same as Figure 2-1 except for Harrah storm (June 8, 1974). Storm motion is from 230 deg at 13 m s⁻¹.*

20

which is not so obvious at ground level (Figure 2-3b). Strongest horizontal and vertical wind shears are within the mesocyclone and to the south near the gust front.

The tornadic circulation center dissipates by 1603 (Figure 2-3d), and the second vortex intensifies and becomes linked directly with the upper level mesocyclonic circulation. Surface relative horizontal wind speeds attain their maximum values at this time. Although no further tornadic activity was reported, the storm persisted and its outflow remained strong until at least 1800 when it moved beyond the radar surveillance region.

2.2.3 Tabler Storm: June 6, 1974

On June 6 1974 a short line of severe thunderstorms developed in central Oklahoma, moved across NSSL's mesonetwork and through the dual-Doppler surveillance region. Doppler measurements obtained in two merging storm cells at 1525 reveal cyclonically converging flow at low-levels (0.3 km elevation, Figure 2-4a). At higher elevations (e.g., z = 2.3 km, Figure 2-4b) cyclonic rotation is clearly evident along a magnified convergence zone (dashed line) separating inflow entering forward and rear quadrants. As the storms combine, an intense mesocyclone with damaging horizontal surface winds evolves.

Derived storm flow patterns at 1616 (Figure 2-4c) show an intense low level wind pattern with an attendant gust front that extends approximately 20 km from the meso-vortex center. At this time maximum radar echo tops and highest radar reflectivity aloft were close to the mesocyclone center and hail as large as 3/4" was falling along the mesocyclone path. Although not now in evidence an embedded hook echo had been observed briefly from 1600 to 1607 (Figure 2-2c).

From 1616 to 1625 the mesocyclone intensified further (Figure 2-4d) and the hook echo reformed (Figure 2-2d). (Analysis smoothing obliterates the hook features in Figure 2-4d). As in previous examples strong horizontal and vertical wind shears exist within the mesocyclone core and along the gust

21
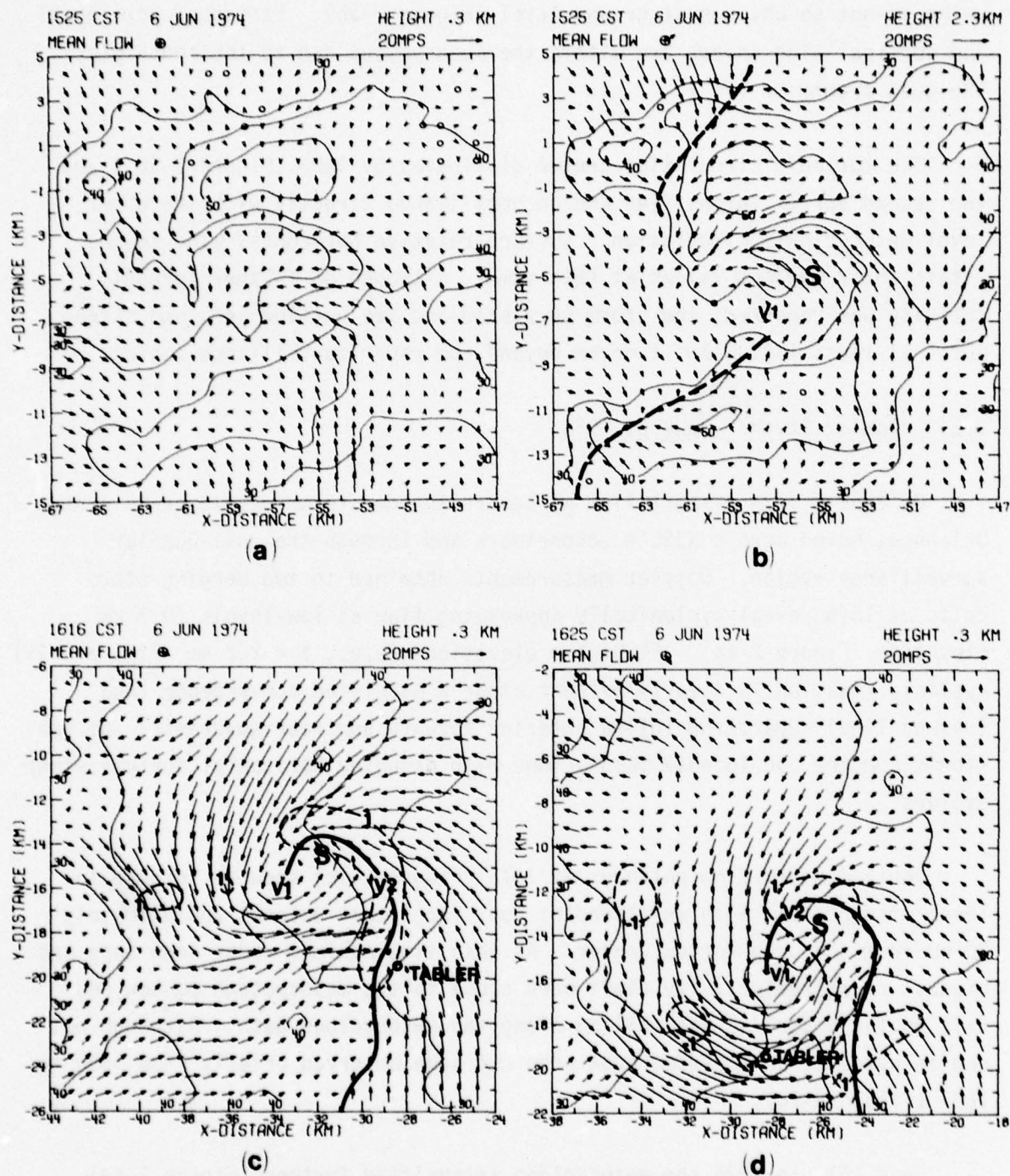
Figure 2-4 Same as Figure 2-1 except for Tabler, Oklahoma storm (June 6, 1974). Location of NSSL Tabler mesonetwork site shown by an open circle. Storm motion is from 280 deg at 13 m s^{-1}.

22

front. An abbreviated sequence of meteorological events recorded at NSSL's
Tabler, Oklahoma mesonet site (Table 2-1) attests to gust front severity.
Wet-bulb potential temperatures (<17°C) at Tabler during peak winds and heavy
rain indicate this outflow originated above 600 mb (4 km). On the other
hand, wet-bulb potential temperatures approaching 23°C beneath the central
reflectivity core suggest the outflow here contained primarily surface air.

Although a tornado was not reported with the Tabler storm a distinctive
shear anomaly (V1) approaching 6×10^{-2} s^{-1} and having several kilometers
vertical extent was observed aloft at 1616 and near ground at 1625 (Figure 2-4d).

Table 2-1. *Meteorological events recorded at Tabler, Oklahoma.
Winds are relative to ground. Times $\pm$ 1 minute.*

1600	Temperature 28 C.
1610	Minimum mesoscale pressure recorded.
1615	Wind shift, east-southeast to west-northwest.
1615	Pressure jump of .04 in. in 5 min.
1617	Onset of temperature break.
1624	Step increase in wind speed to 23 m s^{-1}, onset of heavy rainfall.
1628	Minimum microscale pressure recorded, pressure drop 4 mb. Minimum temperature 18 C.
1629	Peak wind gust, west-northwest at 42 m s^{-1}.
1632	Pressure rise of 7 mb.
1650	Rainfall ends, accumulation 11.2 mm.

3.0 THUNDERSTORM OUTFLOW OBSERVATIONS FROM A TALL MULTI-LEVEL TOWER

3.1 1976 Data Cases: Specific Features and Outflow Dynamics

Data collected from NSSL's 461 m meteorological tower during the 1976
spring thunderstorm season essentially agree with results of earlier studies
by Goff (1975, 1976). These early cases are reproduced in Appendix A. Most
outflow gust fronts, in 1976, fit into groups 2 and 3 (Table 3-1): gust
fronts associated with mature storms (quasi-steady outflow) or gust fronts

Table 3-1. Grouping of Gust Front Cases

1.	Gust fronts associated with intensifying storms or accelerating outflow
2.	Gust fronts associated with mature intense storms or strong outflow
3.	Gust fronts associated with dissipating storms or outflow decelerating with respect to the storm
4.	Gust fronts in the final stage of life cycle

associated with dissipating storms, respectively. However, those gust fronts falling into group 2 were not generally extremely severe in terms of frontal horizontal shear or temperature contrast, because the 1976 Oklahoma storms were typically weaker than those observed in previous years.

Speed and orientation of outflows' leading edge were more accurately determined this year since the surveillance radar (NSSL's WSR-57) was configured to detect weaker returned signals. This permitted frequent detection of so called radar thin lines which, if present ahead of an advancing storm, were found to coincide with the leading edge of the outflow.[1]

The 1976 tower data corroborates results shown in Table 3-2 (reproduced from Goff, 1976) for gust front speed, distance of the gust front from the leading edge of the precipitation and maximum pre-frontal updrafts. The relationship between gust front propagation speed (c) and the maximum smoothed

---

[1] The exact nature of radar thin lines is not known although it is widely believed that they are due to discontinuities of refractive index. The tracking of thin lines appears, at first, to be an attractive means of locating the gust front and determining its horizontal shape. However, thin lines do not always appear when strong gust fronts are known to exist and conversely, thin lines may appear when there are no thunderstorms in proximity. Thin line presence, if associated with outflows, appears to be a function of the depth of the outflow, the orientation of the gust front axis relative to the radar beam, the horizontal thickness of the gust front from the radar and the minimum detectable signal of the radar. With present radar and so many variables, some difficult to measure, use of thin lines as gust front detectors remains questionable.

Table 3-2. *General quantitative gust front information.*
[Δt is the time between tower gust front passage
and precipitation onset. Δx is the distance
between these two events using the gust front
speed (c); i.e., Δx = c Δt.]

Type	Gust front average speed ($m\ s^{-1}$)	t (min)	x (km)	Smoothed 444 m w max ($m\ s^{-1}$)	Number of cases
1	8.1	12.8	7.5	5.0	4
2	11.3	17.7	11.8	6.2	8
3	9.0	3.6	1.7	4.3	4
4	18.6	9.0*	4.7*	2.3	4

*Inconclusive results: large variance from case to case.

(turbulent gusts removed) horizontal wind u_1 normal to the frontal axis and behind the front (in the cold air)

$$C = 0.67u_1$$

is also verified. In fact, this relationship is so consistent, regardless of frontal stage, it is an excellent way to estimate maximum sustained near surface winds once the frontal speed and orientation are known. Of course speed and orientation can often be determined from radar data. The data presented by Goff (1975) and in this report (Figure B-A-1 through B-J-2). Also show that the cold air outflow is typically directed normal to the gust front axis. With the speed and orientation of the gust front known, one might expect near surface winds in the outflow to come from a direction normal to the frontal axis, at a speed roughly 1.5 times faster than the gust front propagation speed.

No important differences were observed between the character of displaced warm air ahead of the gust front in the Charba (1974) and Goff (1975, 1976) models and in the 1976 cases. The warm air is always displaced upward by the more dense cold air in the outflow and results in a local updraft 1 to 1.5 km

25

wide just ahead of the gust front. As stated in earlier studies, the magnitude of the updraft is a function of the speed of the gust front, the slope of the frontal surface and the depth of the outflow. The updraft is a maximum just above the tower layer on the average (about 600 m). However, aircraft probes of an outflow in southwestern Oklahoma on May 29, 1976, indicated the gust front updraft was not strong at 1.2 km AGL or higher. The data from 35 outflow cases now at our disposal, allows us to state unequivocally, that the pre-gust front updraft is typically nonturbulent and only rarely exceeds 7 m s^{-1}.[2]

In 1976, tower data were digitized at 1.3 sec intervals to obtain a detailed description of gust front shape and outflow undercurrent. Our observations consistently show the protruding nose feature (Appendix B). This bulge of the gust front into the warm air is characteristically elevated 100-200 m, allowing a thin layer of warm air to be entrained under the gust front into the cold air mass. This process is believed to be a major dissipative mechanism when the outflow becomes deprived of cold air from the parent thunderstorm and it loses its forward momentum. Though the nose feature does not appear to be a major concern for pilots, it is an important boundary layer phenomenon for outflow models.

Conversely, the undercurrent observed directly behind the gust front in the cold air is of prime concern to pilots and has not been adequately addressed in prior studies. The undercurrent is partly a manifestation of the direct circulation observed in the cold air head which results from frontal baroclinicity. In the head region, pressure surfaces intersect isentropic (potential temperature) surfaces producing a positive circulation (see Goff, 1975, 1976 or Mitchell and Hovermale, 1977). This circulation transports high-momentum air downward, most of the time slowly, but occasionally, rapidly. If the transport is rapid, strong downdrafts may be observed in the cold air just behind the gust front. Strong downdrafts so close to the ground are of major concern when aircraft inadvertently enter

---

[2]In the June 27, 1972 case described by Goff (1975), the updraft was turbulent and maximum positive vertical velocities exceeded 10 m s^{-1} (unsmoothed observations taken at 10 sec intervals.)

26

this portion of the outflow. While these downdrafts are associated with collapse of the nose (Goff, 1975, 1976; Charba, 1974 and Mitchell and Hovermale, 1977), another factor may also be present.

In addition to strong downdrafts occasionally observed near the surface behind the gust front, the surface layer connecting with the downdraft zone is typically a region of high speed horizontal flow. In fact, analog records clearly show that following the wind shift, wind near the surface is strong at first and then decreases gradually. Aloft but still in the outflow, the strong winds are sustained and do not decrease. This behavior is clearly shown in Figures 3-1 a-f. These are tower strip chart records for a gust front case in 1969. In each chart a wind maximum close to 60 kts occurs at about 2338 CST. [The maximum at the surface (66 kts) is higher than at other levels.] Closer to the surface the wind decreases shortly after 2340 but remains at a fairly constant speed until 0005. To explain the nature of the unsteady surface wind, we must picture the outflow air moving from the base of a thunderstorm out toward the gust front. In Figures 3-1 a-f, this would be simulated by moving in the direction of decreasing time. In the cold air, well behind the gust front the wind generally increases from the surface to the top of the tower. This is expected since surface friction decelerates the air near the surface.

A key to the behavior of the near surface outflow wind in proximity to the gust front is sometimes found in the pressure. Figure 3-2, depicts a case similar to the one shown in Figure 3-1, except the data is objectively analyzed in time-height sections and pressure records are available (coincidentally, the case occurs two years later to the day). In the panel for the relative windspeed component normal to the front, a well defined vertical shear layer exists in the cold air (left side of the panel). Closer to the gust front, the vertical shear is reduced and the surface winds are higher, as in Figure 3-1a. Notice that as the cold air approaches the front, it goes from higher pressure to lower pressure; i.e., with respect to a parcel, the pressure is decreasing but with respect to time, the pressure increases locally after the gust front passes. It is the action of the pressure on the parcel that is important here. Implicit in this scenario is action of pressure

27
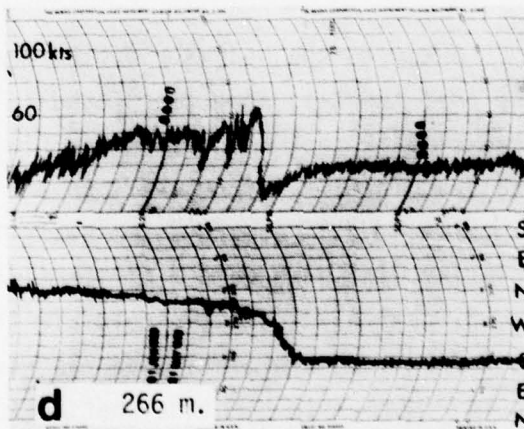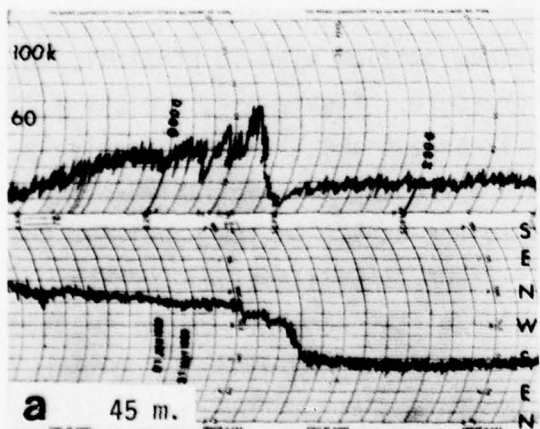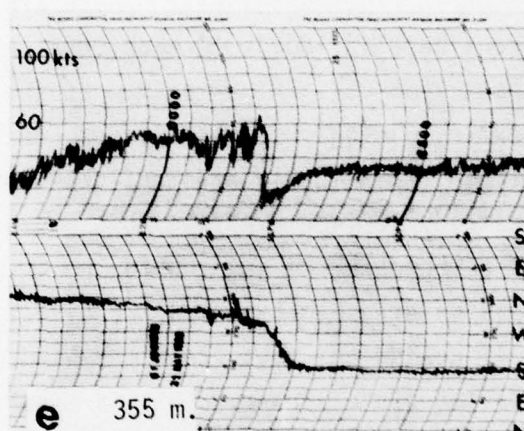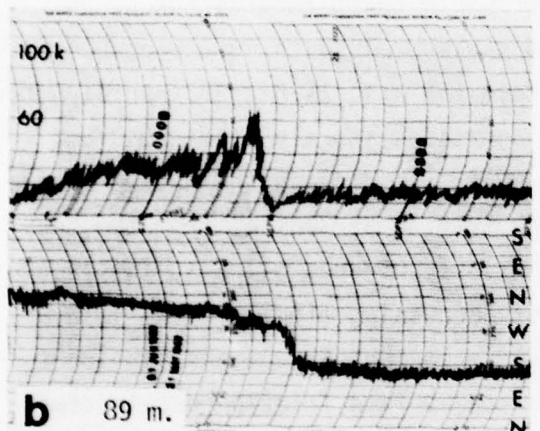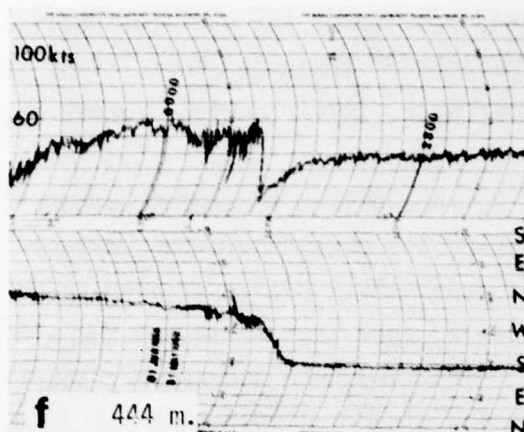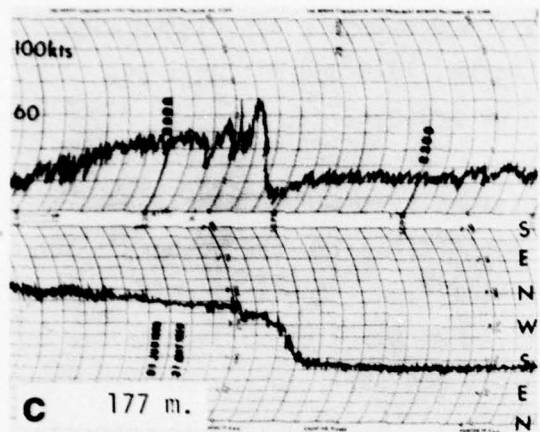
Figure 3-1 Wind records for a thunderstorm passage at the KTVY-TV tower site May 31 - June 1, 1969. Speed units are in knots. (a) 45 m level, (b) 89 m level, (c) 177 m level, (d) 266 m level, (e) 355 m level, and (f) 444 m level.
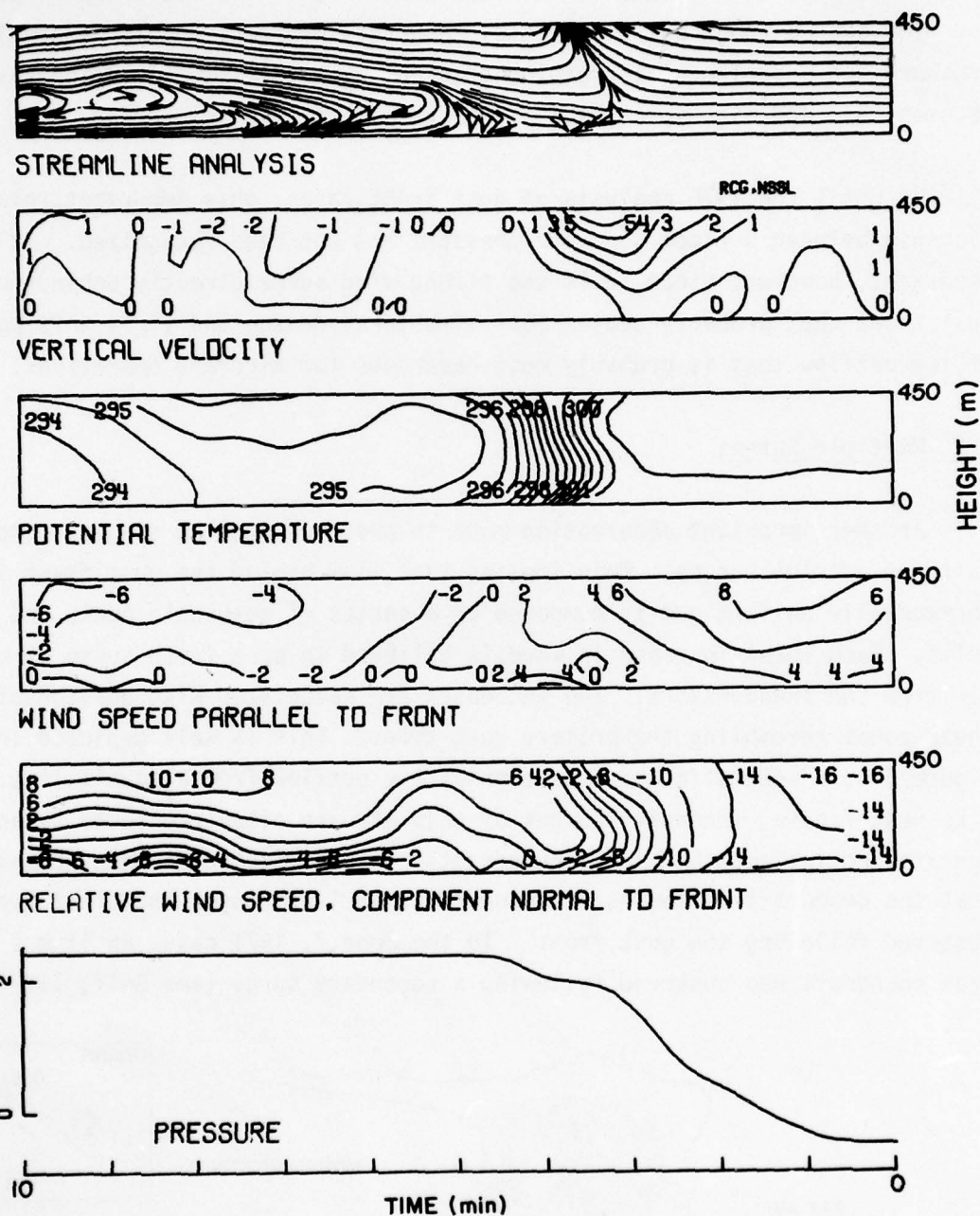
Figure 3-2 Objective analysis of quasi-steady thunderstorm outflow. Units
are m s^{-1} and °K. Streamline analysis is combination of second
(u) and fifth (v) panels. 1 km length scale using conversion
$\Delta x = -c \, \Delta t$ is shown at top.

29

on the depth of the separation layer in viscous boundary layers. When the
pressure gradient is constant, the separation layer thickness remains constant
for flow over a rough but flat plate. However, where air blows toward low
pressure and experiences increasing gradient with time, the friction layer
becomes thin and high speed flow is observed closer to the surface.

Up until the 1976 analysis of gust front cases, this important rela-
tionship between surface wind and pressure had not been recognized. It is
important, however, since it is the strong wind surge directly behind the
gust front that probably causes most structural damage and it is this portion
of the outflow that is probably most hazardous for aircraft operations.

3.2 Multiple Surges

Another important observation made in previous outflow studies concerns
multiple outflow surges. This implies that flow behind the gust front is not
horizontally uniform but is composed of a series of mesoscale peaks and
lulls. Each local increase in wind is believed to be a fresh surge of cold
air from the thunderstorm. The increases are associated with horizontal
shear zones resembling the primary gust front. This is well depicted in
Figure 3-3, a schematic cross section of the outflow from a squall line.
Like gust fronts, secondary surges of cold air are often preceded by an
updraft and followed by strong downdrafts. We have found, in many cases,
that the downdraft following a secondary surge is stronger than that typically
observed following the gust front. In the June 7, 1971 case, an 11 m s^{-1}
peak downdraft was observed following a secondary surge (see Goff, 1977).
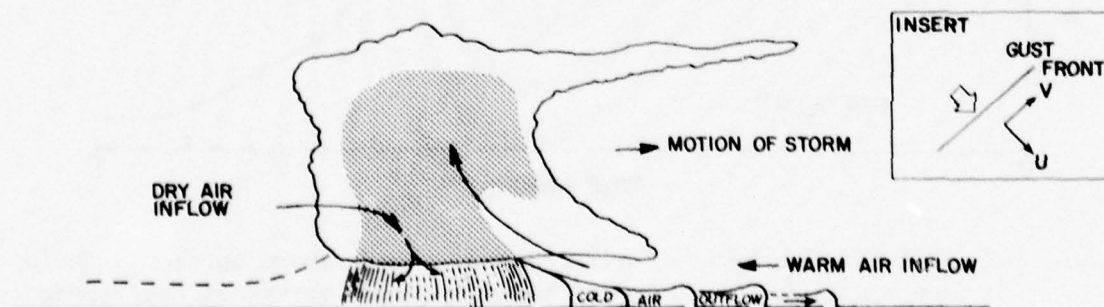
Figure 3-3 Model gust front.

30

The origin of these secondary surges is not precisely known. Obviously, they are a result of in-cloud microphysical processes that have not been well documented because they are beyond present capability of state-of-the-art instrumentation. What we have been able to glean from the near-surface observations is that these surges probably represent pulsations in the thunderstorm downdraft. Apparent negatively buoyant parcels of air origi- nating at midtropospheric levels in the storm descend to the ground in discrete pools, rather than in a continuous fashion. After the storm empties itself of the cold air, the process is renewed. Whether this implies juxta- posed discrete updrafts is not known, but it appears that a continuous up- draft could exist concurrently with discrete downdrafts.

Most of the tower data at our disposal to date, has been from squall line type thunderstorms. Tower data from Great Plains supercell type thunder- storms is not available in great quantity and, thus, it has not been possible to investigate the multiple surge phenomenon in these 3-dimensional storms using tower data. However, a few cases mentioned in Section 2.1 using dual microwave Doppler radar show that multiple surges are common in these storms also. Whereas in squall lines, the multiple surge discontinuities are nearly straight lines in plan view (see May 30, 1976 radar diagram), in supercell storms the outflow discontinuities are curved bands, like spiral bands, emanating from the mesocyclcone. In both types of storms horizontal wind- shear, strong sustained updrafts and downdrafts, and turbulence associated with multiple surge lines are potentially hazardous to aircraft. Further, they are often difficult to detect and predict. They are only rarely observed as thin lines on weather surveillance radar, and are infrequently associated with pressure jumps of the same magnitude as typically observed at the gust front.

As indicated in the case history cross-sections, the gust front is often well ahead of the precipitation. The gust front moves faster than the storm, and thus moves quite rapidly over the ground. If we consider a simplified case wherein the thunderstorm outflow is equated to the downdraft flow or $M_1 = M_2$ where M_1 is the downdraft mass and M_2 = outflow mass (Figure 3-4), then in a single cell storm with circular downdraft and outflow

31
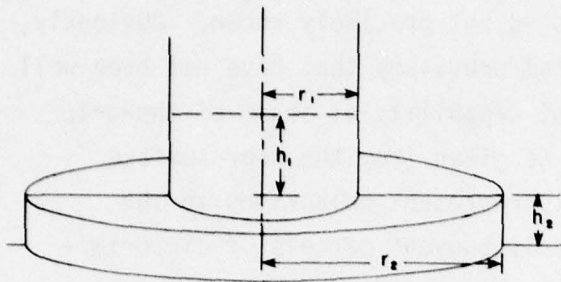
Figure 3.4 *Schematic single cell outflow.* Figure 3.5 *Schematic squall line outflow.*
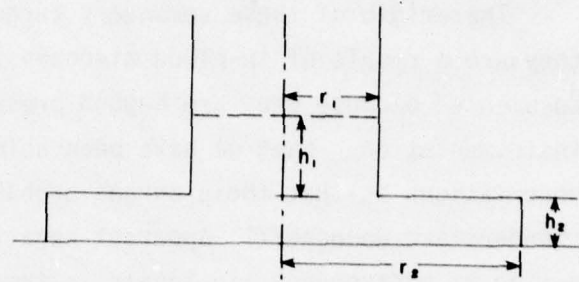
$$M_1 = \rho_1 \pi r_1^2 h_1 \text{ and } M_2 = \rho_2 (\pi r_2^2 h_2 - \pi r_1^2 h_2)$$

where r_1 = radius of downdraft

r_2 = radius of outflow

h_1 = depth of specific amount of downdraft

h_2 = depth of gust front

ρ_1 & ρ_2 = density of the downdraft and gust front air, respectively.

Since we are considering only the lower portions of the thunderstorm we assume $\rho_1 = \rho_2$ and $M_1 = M_2$. We thus have

$$\pi r_1^2 h_1 = \pi r_2^2 h_2 - \pi r_1^2 h_2$$

$$\text{or } r_2^2 = \frac{r_1^2 h_1 + r_1^2 h_2}{h_2}$$

We can equate h_1 to the downdraft velocity (w) and the duration t or $h_1 = wt$. Thus,

$$r_2 = (r_1^2 wt + r_1^2 h_2)^{1/2} h_2^{-1/2}$$

Lee (1972) shows the mean diameter of downdrafts measured during thunderstorm penetrations to be 2 km. Based on tower data we assume a gust front depth of 500 m. Tables 3-3 and 3-4 illustrate the time dependence of the gust front location for downdrafts of radius 1 km and 2 km and downdraft speeds of 6, 10 and 20 m s^{-1}.

32

Table 3-3. *Single Cell Case: movement speed and distance of gust front leading edge to center of storm for a downdraft radius of 1 km. (single cell)*

Time (m) from impact of downdraft with ground	when $w = 6$ m s^{-1}		when $w = 10$ m s^{-1}		when $w = 20$ m s^{-1}	
	r_2 (km)	dr_2/dt (m^{2}s^{-1})	r_2 (km)	dr_2/dt (m^{2}s^{-1})	r_2 (km)	dr_2/dt (m^{2}s^{-1})
1	1.3	4.6	1.5	6.7	1.8	10.8
2	1.6	3.8	1.8	5.4	2.4	8.3
4	2.0	3.1	2.4	4.2	3.3	6.1
6	2.3	2.6	2.9	3.5	3.9	5.1
8	2.6	2.3	3.3	3.1	4.5	4.5
10	2.9	2.1	3.6	2.8	5.0	4.0
20	3.9	1.5	5.0	2.0	7.0	2.9
30	4.0	1.3	6.1	1.6	8.5	2.3
40	5.5	1.1	7.0	1.4	9.8	2.0

Table 3-4. *Single Cell Case: movement speed and distance of gust front leading edge to center of storm for a downdraft radius of 2 km.*

Time (m) from impact of downdraft with ground	when $w = 6$ m s^{-1}		when $w = 10$ m s^{-1}		when $w = 20$ m s^{-1}	
	r_2 (km)	dr_2/dt (m^{2}s^{-1})	r_2 (km)	dr_2/dt (m^{2}s^{-1})	r_2 (km)	dr_2/dt (m^{2}s^{-1})
1	2	9.2	3.0	13.5	3.7	21.7
2	3.1	7.7	3.7	10.9	4.8	16.6
4	3.9	6.1	4.8	8.3	6.5	12.3
6	4.6	5.2	5.7	7.0	7.9	10.2
8	5.2	4.6	6.5	6.1	9.0	8.9
10	5.7	4.2	7.2	5.6	10.0	8.0
20	7.8	3.1	10.0	4.0	14.0	5.7
30	9.5	2.5	12.2	3.3	17.1	4.7
40	10.0	2.2	14.0	2.9	19.7	4.1

For the gust front speed we have

$$\frac{dr_2}{dt} = 0.5(r_1 w)(h_2)^{-1/2}(wt + h_2)^{-1/2} \quad .$$

Representative values are given in Tables 3-3 and 3-4.

For a squall line situation the interaction between downdrafts may be considered as limiting the lateral movement of the outflow so that only fore and aft displacement is in evidence. Under this condition (Figure 3-5)

$$r_1 h_1 = (r_2 - r_1)h_2$$

$$r_2 = \frac{r_1 wt + h_2 r_1}{h_2} = \frac{r_1 wt}{h_2} + r_1$$

$$\text{and } \frac{dr_2}{dt} = \frac{r_1 w}{h_2}$$

and as seen in Tables 3-5 and 3-6 the movement is more rapid than in the single cell situation. A portion of these tables are combined in Figures 3-6 and 3-7. In a real situation, the outflow is probably somewhere between these two simplified cases.

Since Doppler radar is not yet available as a real-time forecast tool for gust fronts, a surface network of anemometers appears to be the desired sensor system currently available to warn of their imminent danger.

4.0 AIRCRAFT AND DOPPLER DATA

4.1 Aircraft Observations

On May 29, 1976 storms originally formed about 240° 140 km from Norman. The storms moved northeastward about 10 m s^{-1} (20 kts) and by 1730, it became apparent that the storms would not reach the Norman area until after sunset. A decision was made to launch the F-4-C and obtain data along the

34

Table 3-5. *Squall Line Case: Movement speed and distance of gust front leading edge to center of storm for a downdraft radius of 1 km.*

Time (m) from impact of downdraft with ground	when $w = 6$ m s^{-1}		when $w = 10$ m s^{-1}		when $w = 20$ m s^{-1}	
	r_2 (km)	dr_2/dt (m^2s^{-1})	r_2 (km)	dr_2/dt (m^2s^{-1})	r_2 (km)	dr_2/dt ($m s^{-1}$)
1	1.7	12	2.2	20	3.4	40
10	8.2	12	13.0	20	25.0	40
20	15.4	12	25.0	20	49.0	40
30	22.6	12	37.0	20	73.0	40
40	29.8	12	49	20	97.0	40

Table 3-6. *Squall Line Case: Movement speed and distance of gust front leading edge to center of storm for a downdraft radius of 2 km.*

Time (m) from impact of downdraft with ground	when $w = 6$ m s^{-1}		when $w = 10$ m s^{-1}		when $w = 20$ m s^{-1}	
	r_2 (km)	dr_2/dt ($m s^{-1}$)	r_2 (km)	dr_2/dt ($m s^{-1}$)	r_2 (km)	dr_2/dt ($m s^{-1}$)
1	3.4	24	4.4	40	6.8	80
10	16.4	24	26.0	40	50.0	80
20	30.8	24	50.0	40	98.0	80
30	45.2	24	74.0	40	146.0	80
40	59.6	24	98.0	40	194.0	80

eastern edge of the thunderstorms as they came within first trip range of the Doppler (115 km). The sharp leading edge of the radar echo seemed favorable for a gust front. In accordance with previously determined flight procedures, the initial run was made below and parallel to the leading edge of the thunderstorm base but above the gust front itself. Each successive run was to be made at increasingly lower altitudes until the flight was wholly within the outflow air.
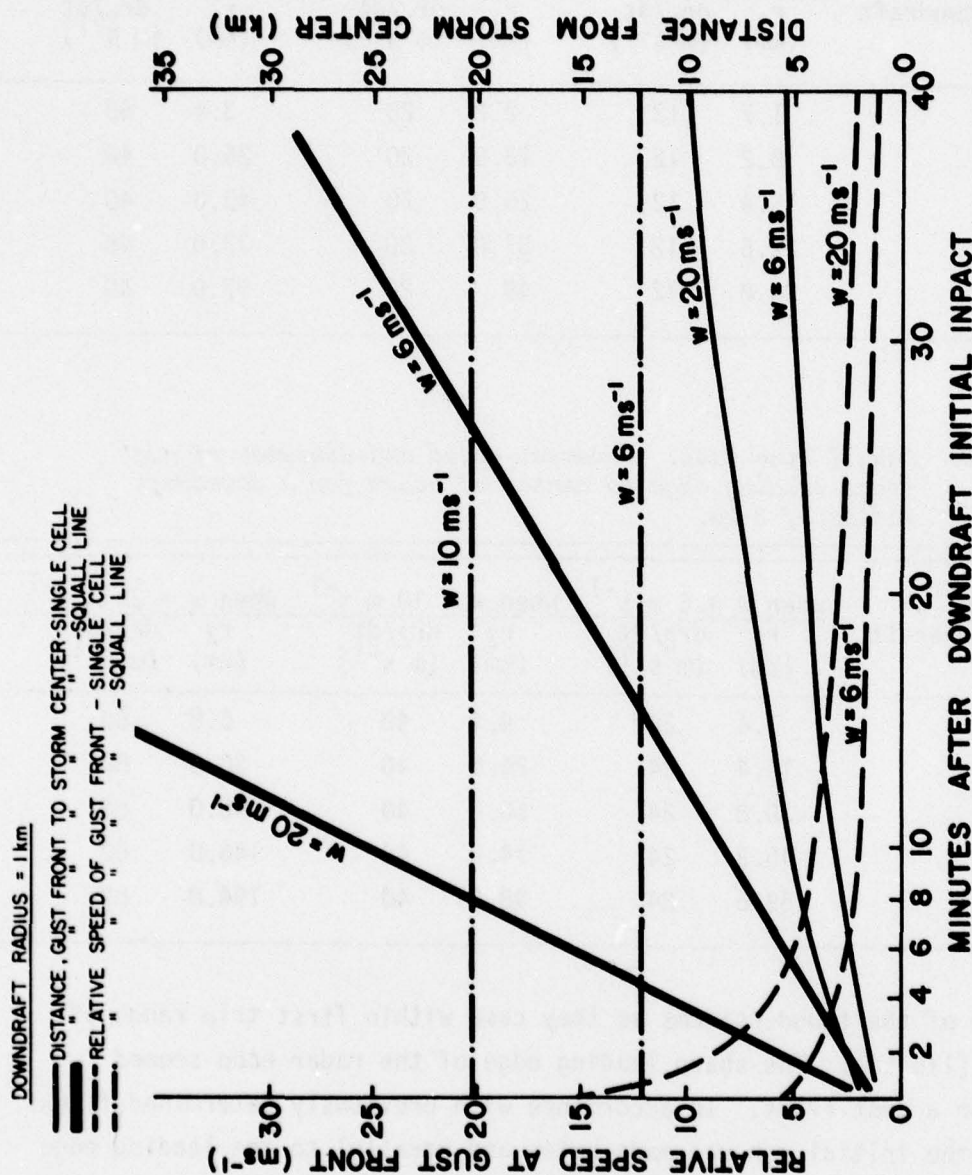
Figure 3-6 Time history graph of model gust front—1 km radius downdraft. Thin solid line is distance from gust front to storm center as a function of time for the single cell case; the heavy solid line - squall line case. The thin dashed line is the speed of the gust front relative to the downdraft center for the single cell; dot-dashed line is speed as a function of time for the squall line case.

36
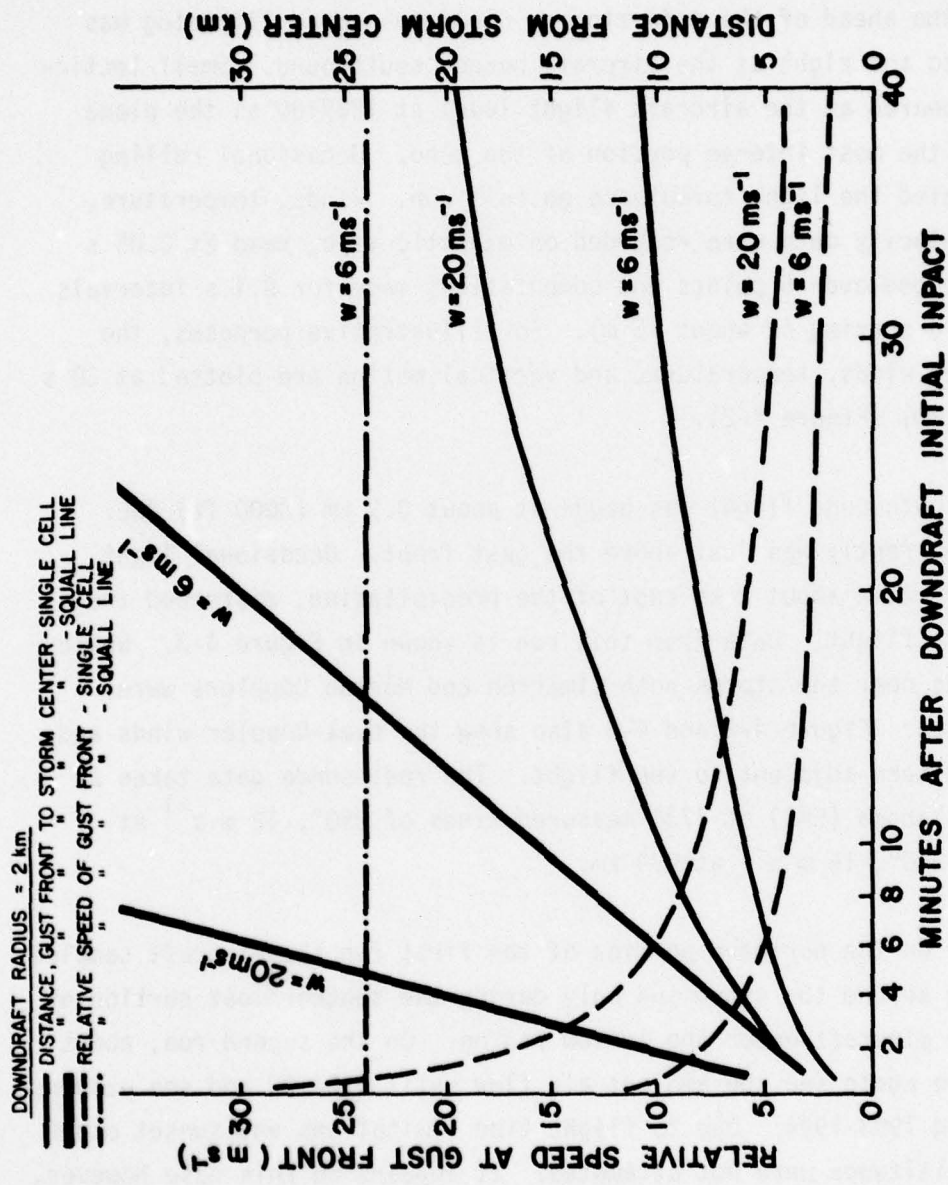
Figure 3-7 Time history graph of model gust front--2 km radius downdraft. Thin solid line is distance from gust front to storm center as a function of time for the single cell case; the heavy solid line - squall line case. The thin dashed line is the speed of the gust front relative to the downdraft center for the single cell; dot-dashed line is speed as a function of time for the squall line case.

37

The first run was conducted at 1.2 km (4000 ft) AGL and paralleled the echo edge (Figure 4-1). The flight altitude placed the aircraft 90 to 150 m (300-500 ft) below the clouds and about 4 km east of the heavy precipitation. The flight was generally smooth with a few bumps (1835:00) in the vicinity of a growing echo ahead of the main storm. Cloud-to-ground lightning was very frequent to the right as the aircraft headed southbound. Small lenticular clouds appeared at the aircraft flight level at 1839:00 as the plane passed east of the most intense portion of the echo. Occasional rolling motion accompanied the light turbulence on this run. Winds, temperature, and vertical velocity data were recorded on magnetic tape, read at 0.05 s intervals, averaged over 5 points and computations made for 0.1 s intervals (approximately a spacing of about 15 m). For illustrative purposes, the aircraft-derived winds, temperature, and vertical motion are plotted at 30 s intervals (3.9 km) (Figure 4-2).

A second southbound flight was begun at about 0.9 km (3000 ft) AGL. The aircraft apparently was just above the gust front. Occasional light turbulence, this time about 2 km east of the precipitation, disturbed the otherwise smooth flight. Data from this run is shown in Figure 4-3. While the aircraft was near the storms both Cimarron and Norman Dopplers were scanning the area. Figure 4-2 and 4-3 also show the dual-Doppler winds and reflectivity pattern adjacent to the flight. The radiosonde data taken at Elmore City, Oklahoma (EMC) at 1730 measured winds of 250°, 12 m s^{-1} at 1.2 km AGL and 210°, 15 m s^{-1} at 0.9 km.

Apparently on the northern portion of the first run the aircraft sampled the air flowing around the storm and only during the southernmost portion of the run did the aircraft enter the inflow region. On the second run, about 25 min later, we again see the ambient air flow until 1904:00 and see evidence of inflow around 1903-1904. Due to flight time limitations and sunset other runs at lower altitudes were not attempted. It appears in this case however, that the gust front was much shallower than the gust front on May 26, discussed in section 4.2.

38
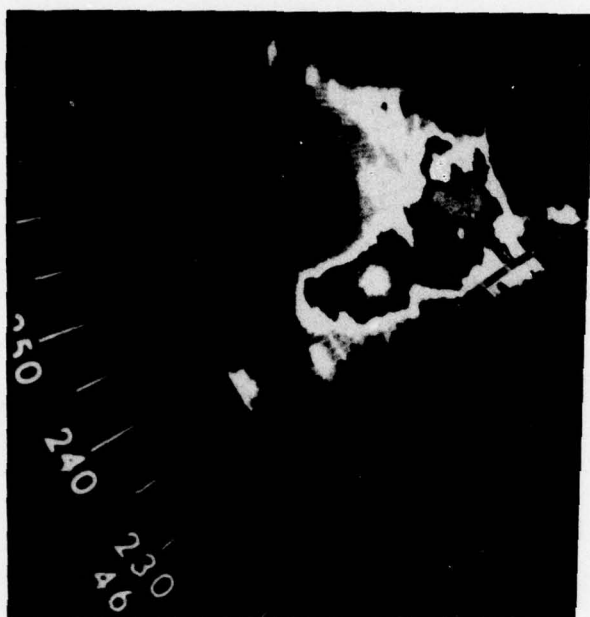
Figure 4-1 WSR-57 radar PPI display
for 1839:43 CST May 29,
1976 with aircraft track
superimposed. Radar
contours are approximately
10 dBZ intervals.

4.2 Doppler Radar: Clear-Air Study

A squall line-associated gust front accompanied by a zone of strong
shear and turbulence (Figure 4-4) passed the tower the morning of May 26.
The storm outflow produced strong surface winds (25 m s^{-1}) and very strong
(8 m s^{-1}) pre-gust front updrafts. After the gust front passed the tower
(at 0728), the remainder of the outflow contained little turbulence and only
a thin shear zone near the surface. However, at Wiley Post Airport 15 km WSW
of the tower a pilot reported heavy rain and moderate turbulence on take-off
(0720). When the outflow reached NSSL some 40 km south, the Norman Doppler
was used to obtain data prior to the onset of precipitation.

The use of the NSSL Doppler to obtain data in clear air had been under
trial for several months. A report of this early experimentation and the
real time display (Figure 4-5) is given by Hennington et al. (1976). Since
this is the first clear air gust front observed by Doppler, experimental
techniques were employed. Data were obtained from eight to twelve elevation
angles scanned at selected azimuths. Recording started at 0819 or 20 min
after the windshift but 30 min before rain started in Norman. Data were
abstracted at 1 km intervals along each elevation angle, analyzed, and
cross-sections (Figure 4-6) produced. Negative numbers indicate motion

39
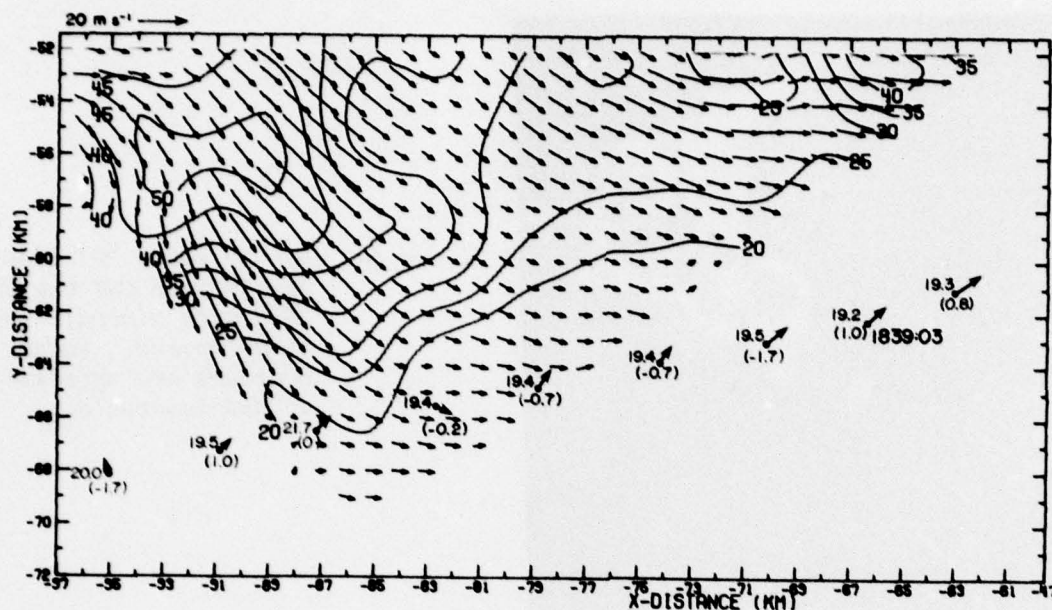
Figure 4-2   Dual-Doppler and F-4-C measured winds at 1.0 km May 29, 1976, 1845 CST.   Reflectivity contours are solid lines.   F-4-C flight track relative to storm at 1845 CST shows aircraft derived winds (base of arrow is observation point).   Aircraft measured temperature plotted above wind.   Calculated vertical motion (m s^{-1}) is enclosed with parentheses.   Aircraft altitude 1.2 km.
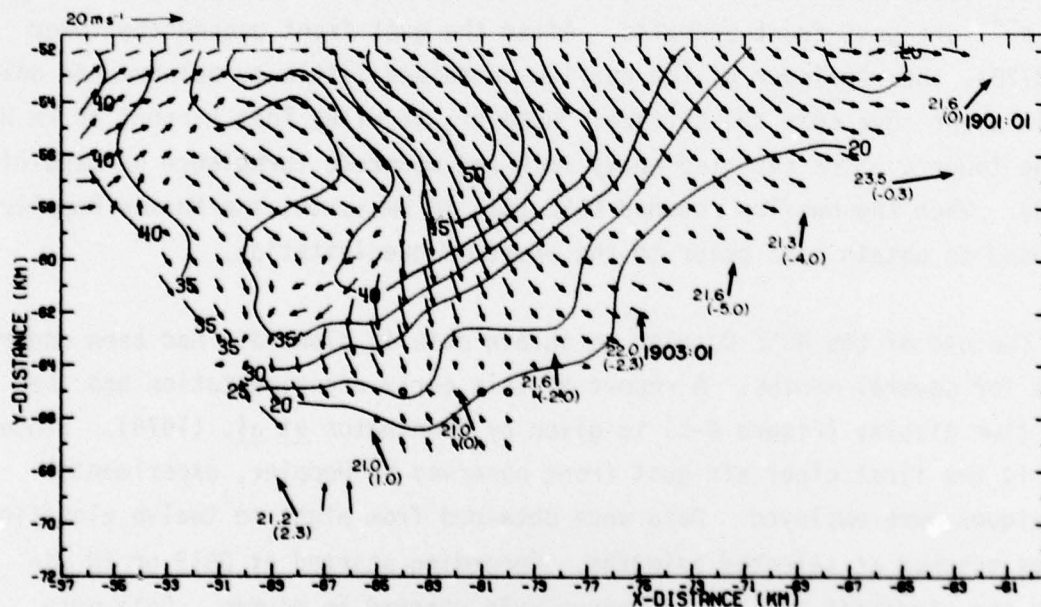
Figure 4-3   Dual-Doppler and F-4-C measured winds at 1.0 km May 29, 1976, 1853 CST.   Aircraft altitude was 0.8 km.
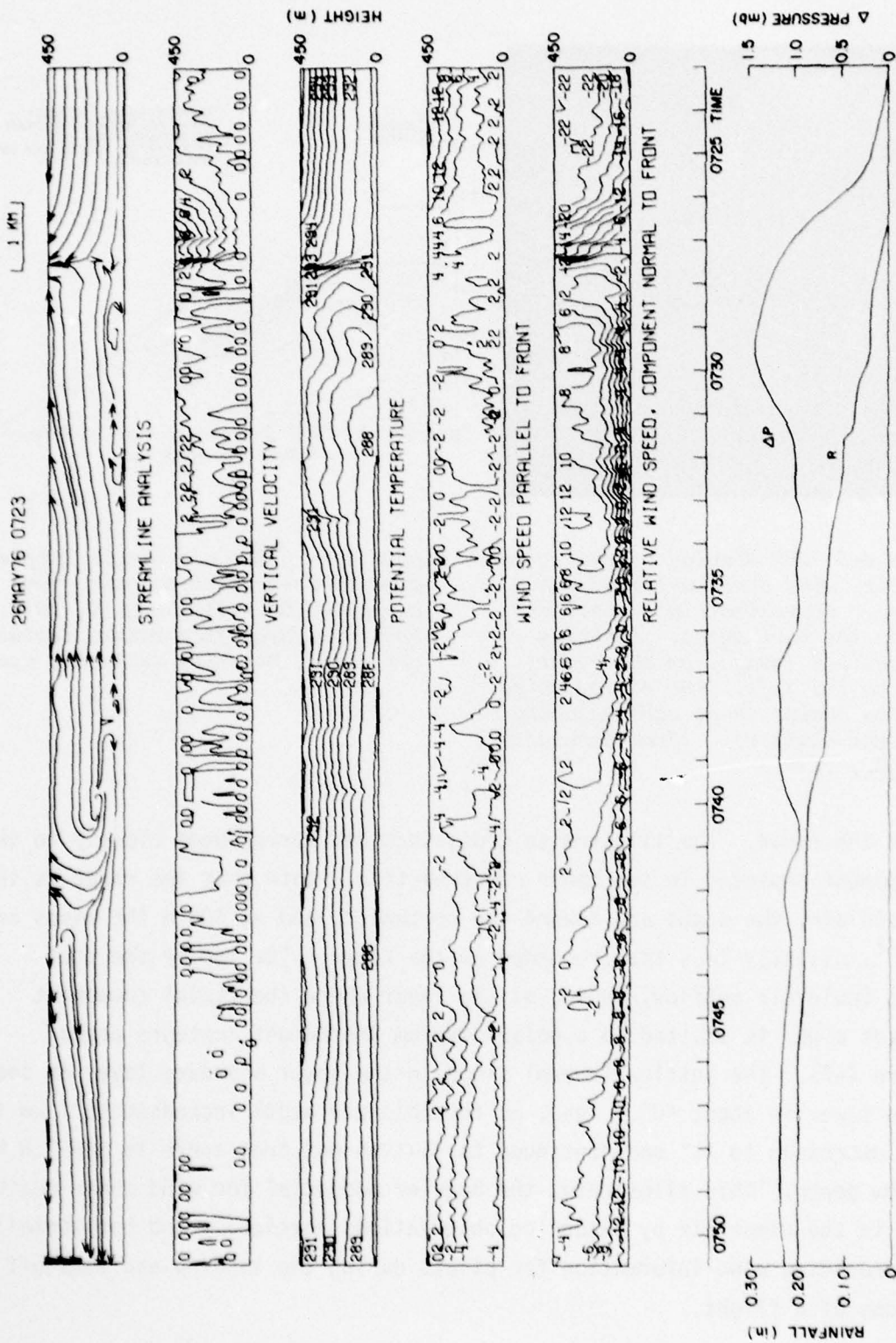
Figure 4-4 Time height cross-section, May 26, 1976, 0723 - 0750 CST.

41
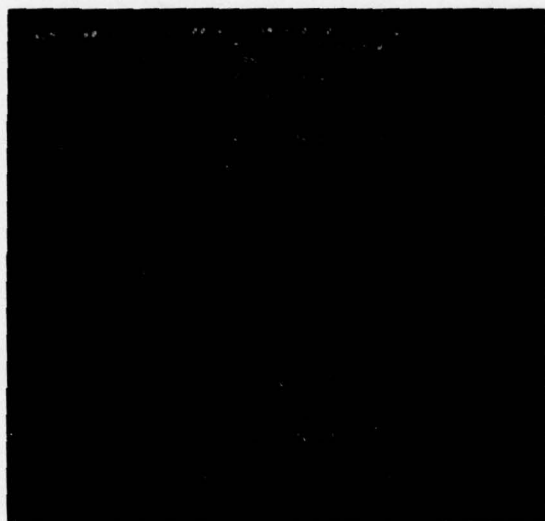
Figure 4-5 CRT display of real time
Doppler wind spectra for 16 range
gates. Approximately 4 m s⁻¹/div
along the horizontal. Positive
velocities (away from the radar)
are to the left. The narrow spike
in the center is at zero velocity
(ground clutter). (From Hennington,
et al., 1976.)
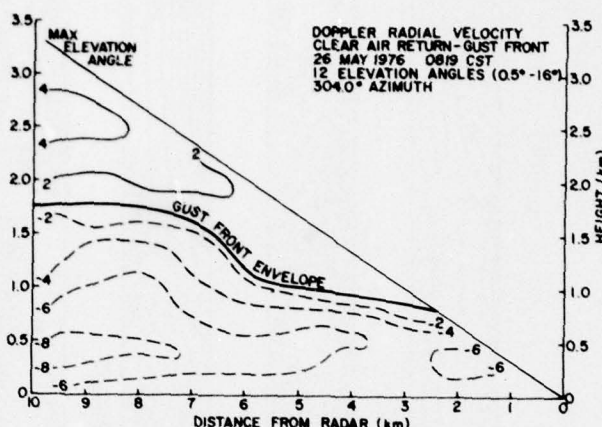
Figure 4-6 Clear air single Doppler
wind cross-section of gust front
along 304.0° radial May 26, 1976.
Positive (away from radar) isotachs
are solid, negative isotachs, dashed.

toward the radar. The illustrated cross-section, corresponds closely to the
u-component depicted in the tower cross-section. Note that the radar is in
the cold air, the scans are toward the northwest, and at 400 m the winds are
8 m s⁻¹, slightly less than recorded at the tower. The top of the gust
front, (cold air outflow) chosen as the layer where the radial component
reverses sign, is plotted on a polar diagram and height contours drawn
(Figure 4-7). The outflow frontal slope in the lower boundary layer as seen
by the tower is about 40°. Thus, as the cold air depth increased to 1 km the
slope decreased to 11° and continued to flatten out from there to the 1.8 km
outflow depth. This illustrates the Doppler potential for wind shear measure-
ments in the clear air by extending observations vertically and horizontally,
thus providing wind information for pilots during the landing and take-off
portions of a flight.

42
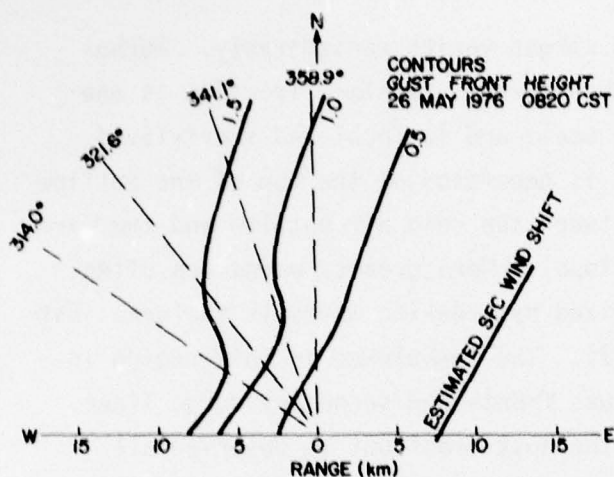
Figure 4-7 Height contours of gust front as determined from vertical cross-sections obtained from Doppler radar May 26, 1976, 0820 CST.

5.0 DESCRIPTIVE GUST FRONT MODEL - THE THUNDERSTORM OUTFLOW IN 3-DIMENSIONS

From analysis of data from towers, aircraft surveillance, and multiple microwave Doppler radars, a 3-dimensional picture of the thunderstorm gust front and outflow emerges. Obviously, characteristics of the outflow differ somewhat in different types of storms. Central Oklahoma is frequented mainly by three types of storms: the squall line, the supercell storm, and the less severe single cell thunderstorm. There is a continuous variation of these types and many combinations that defy simple classification.

Long continuous squall lines are essentially 2-dimensional in the x, z plane but a cellular structure may be observed along the storm axis. Outflows from these storms are generally directed normal to the storm axis diverging under the squall line toward the front or rear of the line. Gust front axes are typically quasi-straight lines in plan view but show bulges directly in front of more intense cells. in squall line thunderstorms outflows tend to propagate farther away from the leading edge of the precipitation (up to 35 km separation in some cases) than in any other type of thunderstorm. The intensity of the outflow in terms of prefrontal updraft, magnitude of the frontal shear zone and turbulence within the outflow, appears to be a strong function of the squall line speed. Also, squall line thunderstorms are often characterized by multiple outflow surges. The further the separation of the gust front from the leading edge of the precipitation, the more secondary surges can be expected. As many as three surges have been observed in the

43

NSSL data. Horizontal spacing between surges varies considerably. Turbulence in the outflow appears to have two sources. Surface friction is one source but this turbulence is of small scale and is local and short-lived. More important, significant turbulence is generated at the top of the outflow along the quasi-horizontal boundary between the cold air outflow and the warm air inflow (called the gust front envelope). Here gravity waves are often observed. One region always characterized by breaking waves is the wake just behind the outflow lead (see Goff, 1977). The turbulence in this region is most intense with fast moving strong gust fronts and secondary surge lines. This turbulence zone moves along with the gust front but is observed all along the axis parallel to the front. It follows the frontal passage by 2 or 3 km.

In supercell storms many of the same features are marked by gust fronts and secondary surge lines, curved outflow interfaces emanating from the mesocyclone (Figure 5-1). Tornadoes, when they occur, are usually associated with the mesocyclone. Since supercell storms are very intense, they produce gust fronts with sharp boundaries marked by very strong horizontal shear. The gust front zone is a preferred region for secondary convective development and, as such, is frequently characterized by deep strong updrafts. The trailing edge of the gust front, though less intense in terms of horizontal shear, is followed by an outflow air mass characteristically extremely turbulent. Here, updraft and downdraft couplets with magnitudes in excess of $5 \, m \, s^{-1}$, have been observed only a few hundred meters above the ground. Since gust fronts do not propagate far from the precipitation's leading edge in supercell storms, it should be easy to avoid the extremely dangerous conditions found there.

Single cell non-severe storms are associated with much temporal and spatial variability in the outflow features they produce.

6.0 SUMMARY

There were few mature daytime thunderstorms in Central Oklahoma during the one month data collection in the spring of 1976. While NSSL was thus

44
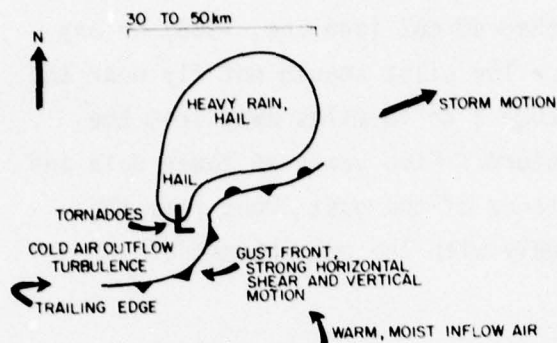
Figure 5-1 Super cell storm,
schematic plan view.

unable to collect coordinated and simultaneous data with the instrumented aircraft (USAF F-4-C), tall tower, and multiple Doppler sensors, some additional information was obtained on the character of the thunderstorm outflow using these sensors singly or in pairs.

Higher resolution tower data compared to that in Goff (1975) showed in more detail inherent outflow shear zones and pockets of updrafts and down-drafts. It is now known that the gust front and its quasi-horizontal envel-ope from the outflow leading edge to the storm's precipitation edge is a zone of high shear and turbulence and thus is often extremely hazardous to low-level aircraft operations. Oklahoma observations indicate near the surface outflow winds behind the gust front typically move normal to the front rather than parallel to it. The mean outflow speed is found to be 1.5 times faster than the gust front propagation speed. In fact the strongest horizontal winds in the cold air outflow are found directly behind the gust front or behind secondary outflow boundaries, if they exist, making these zones particularly hazardous. The same data also reveal that warm pre-gust front updrafts are usually less than 7 m s^{-1} and non-turbulent.

In the cold air outflow immediately following the gust front, high-momentum air is transported downward due to the frontal circulation resulting in strong low-level downdrafts. Secondary surges also are accompanied by high shear, turbulence and strong downdrafts observed to be as strong as 11 m s^{-1} (36 fps, 2165 fpm) from 444 m down to 177 m and as strong as 8.2 m s^{-1} from 177 m down to 89 m.

45

In short, the whole outflow area is to be avoided by aircraft if the storm has central reflectivities higher than 40 dBZ (see Lee, 1965) or any evidence of storm circulation is obvious. The pilot should not fly near the precipitation perimeter and should stay some 5 to 15 miles away from the leading and right forward flanks of the storm. Five years of tower data and 35 outflow cases have shown that the distance of the gust front from the leading edge of precipitation varies roughly with the persistence of an intense storm.

Refinement of these criteria awaits a season when the observing facilities described above are met by appropriately located severe storms during daylight hours.

With accidents and incidents due to the outflow phenomena still recurring, an improved pilot training program reflecting recent thunderstorm outflow findings is imperative. *In* addition, improved flight simulator training is needed.

46

APPENDIX A

Gust Front Cases, 1971-1974

CASE	DATE	TIME (CST)
A	14 May 74	0448
B	2 July 72	1318
C	6 May 72	1734
D	27 May 72	1503
E	31 May 71	1927
F	27 June 72	1936
G	7 June 71	1945
H	23 May 74	1716
I	16 June 73	1509
J	10 June 71	2209
K	2 June 71	2121
L	4 June 73	1803
M	14 June 72	0215
N	12 June 71	0113
O	23 May 72	0440
P	12 May 72	0024
Q	23 May 74	1844
R	19 April 72	1656
S	26 May 71	1901
T	21 April 72	0034

FIGURE LEGEND

Left Pages:

Streamline analysis and time-height sections of vertical velocity (m s^{-1}), wet-bulb potential temperature (°K), potential temperature (°K), horizontal wind speed component parallel to gust front (v) and wind speed component normal and relative to the gust front (u) (m s^{-1}). Each objective analysis is 10 min long and 450 m thick; time increases from right to left. Date and start time of plot is in the upper left and time-to-space converted 1 km distance is indicated in the upper right.

Right Pages:

(Top) 10 cm WSR-57 conventional radar diagram with echo contouring. dBZ values vary from year to year and case to case but shadings roughly represent powers (x) of 10^x mm^6 m^{-3} radar reflectivity. Time clock is in the upper right. Range marks are at 20 n mi intervals in 1971 and 1972 and at 40 km intervals in 1973 and 1974. The WKY-TV tower is located at the isolated ground clutter return at 358° and 20 n mi, best seen in the diagrams for Cases E and K. The radar was on 2° tilt in Case F. There is no radar diagram for Case N.

(Bottom) Quantitative remarks. Speed and orientation error subjectively determined. "Remarks" source is mostly from Storm Data (U. S. Dept. of Commerce) reports; some personal observations. Units correspond to radar range mark units or those used in Storm Data reports. Total rainfall refers to rainfall recorded at tower.
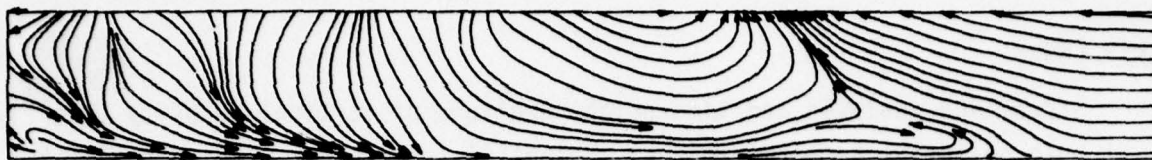
14MAY74 0446   [1 KM _____]

STREAMLINE ANALYSIS
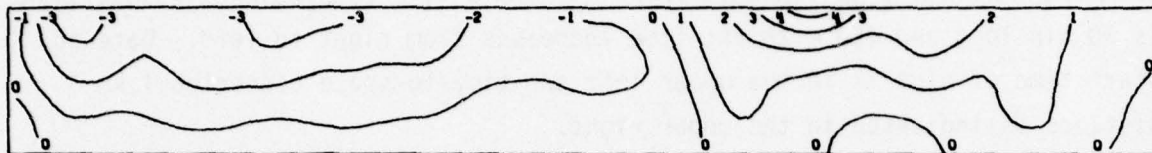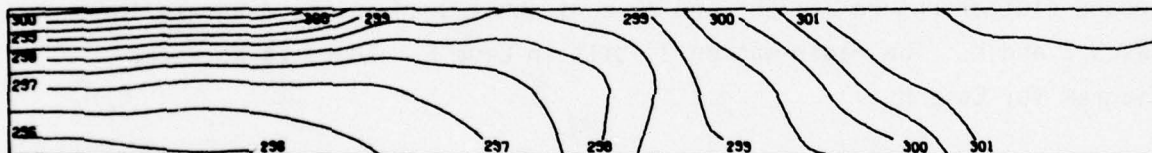
VERTICAL VELOCITY

WET BULB POTENTIAL TEMPERATURE

POTENTIAL TEMPERATURE
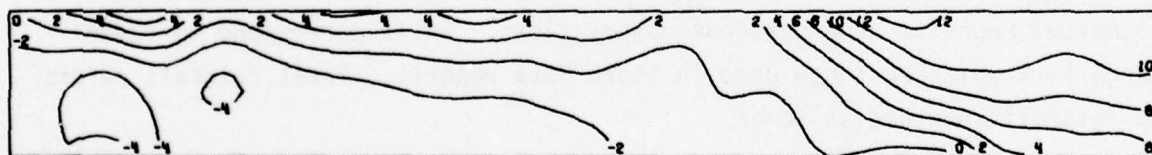
WIND SPEED PARALLEL TO FRONT

RELATIVE WIND SPEED. COMPONENT NORMAL TO FRONT

Figure A-A-1

50
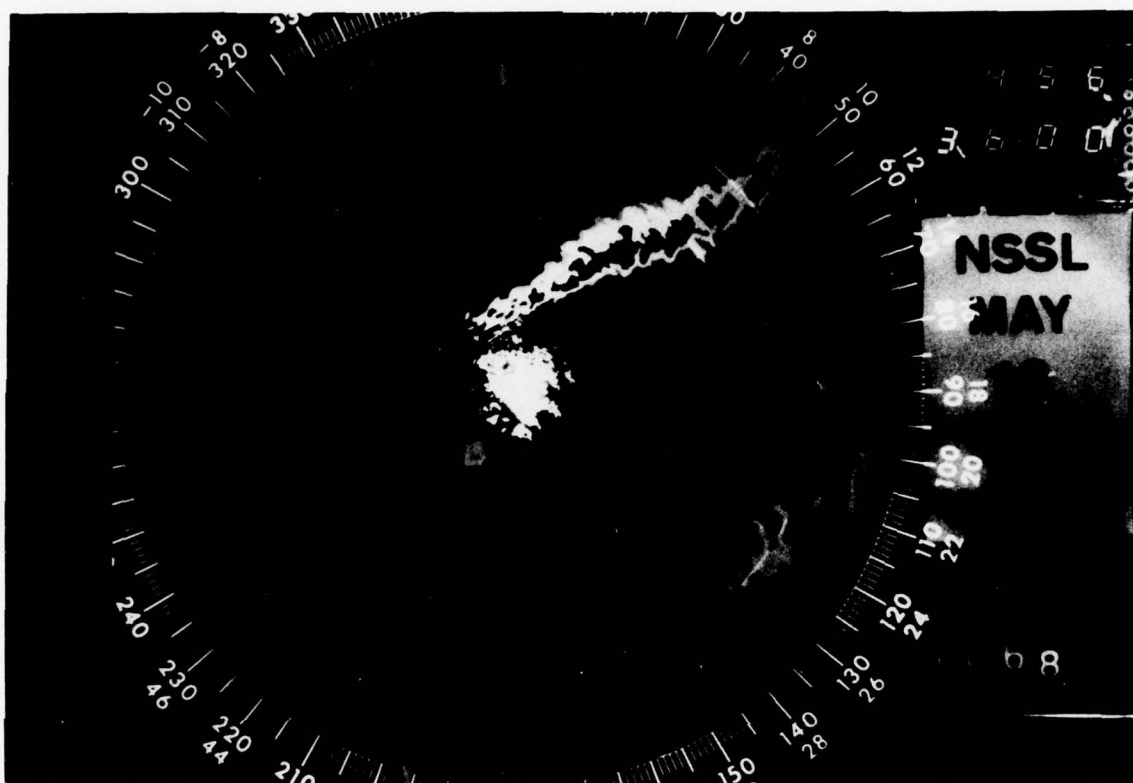
Figure A-A-2

Case A

Date: 14 May 74 (date on radar diagram is incorrect)

Time of gust front: 0448 CST

Speed: 6.1 m s^{-1}

Orientation: 67°

Speed and orientation error less than 10%

Pressure jump: 1.2 mb 0435 - 0451 CST

Total rainfall: Trace

Remarks: Squall line dissipating generally but some new development on southwest end (gust front in formative stage); non-severe storm.
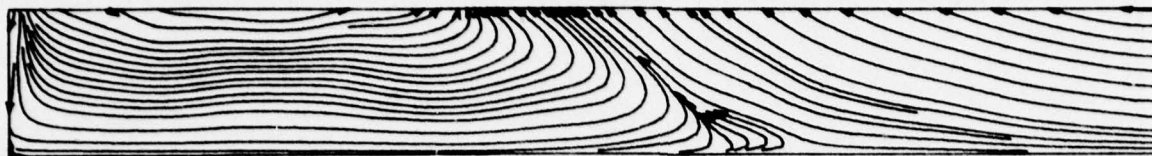
51

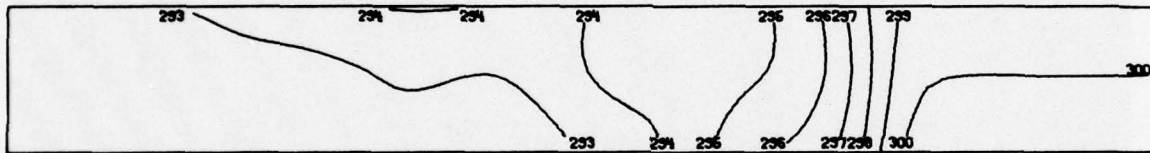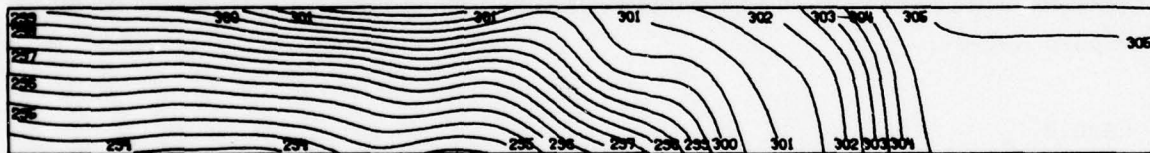02JUL72 1314   1 KM

STREAMLINE ANALYSIS
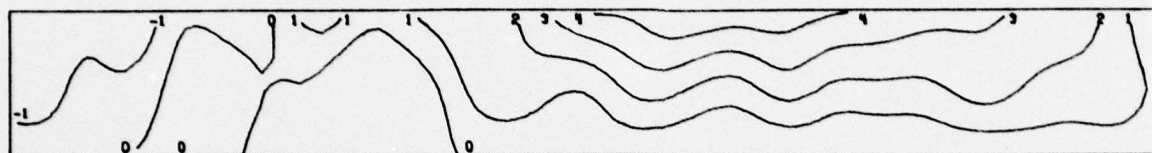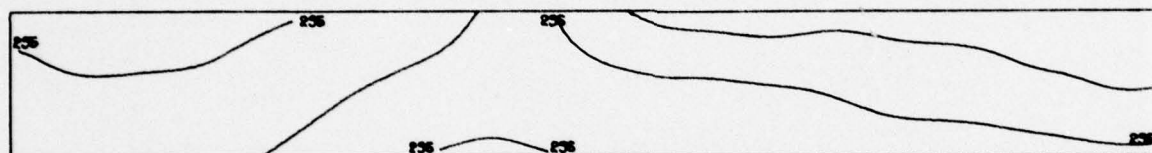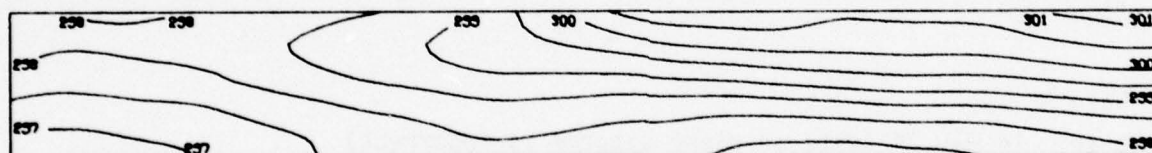
VERTICAL VELOCITY

WET BULB POTENTIAL TEMPERATURE

POTENTIAL TEMPERATURE
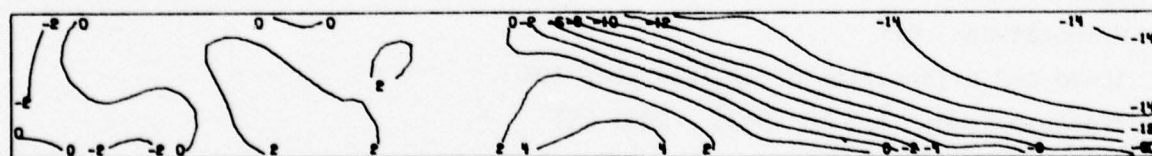
WIND SPEED PARALLEL TO FRONT

RELATIVE WIND SPEED. COMPONENT NORMAL TO FRONT

Figure A-B-1

52
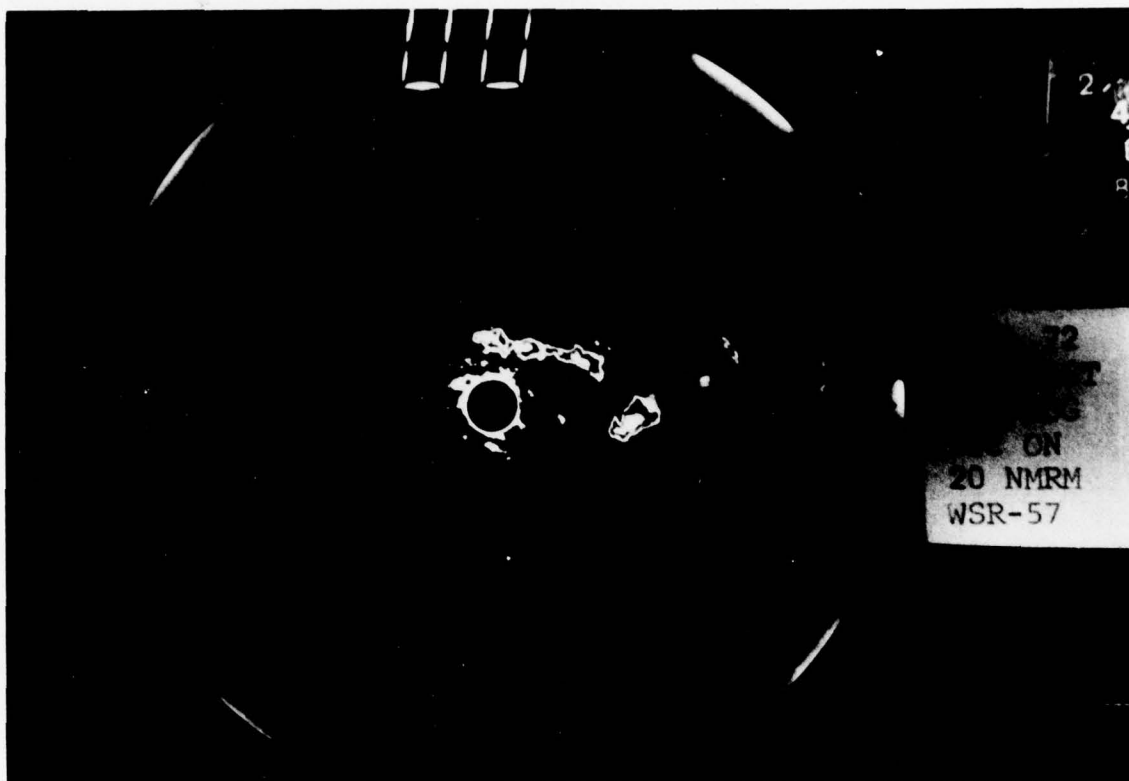
Figure A-B-2

Case B:

Date: 2 July 72

Time of gust front: 1318 CST

Speed: 5.0 m s^{-1}

Orientation: 70°

Speed and orientation error greater than 10%

Pressure jump: 1.3 mb 1312 - 1327 CST

Rain began: 1324 CST ended: 1344 CST

Total rainfall: 0.96 in

Maximum intensity: 6.60 in hr^{-1} 1327 CST

Remarks: Well defined circulation visible on radar (4° tilt); 1 3/4 inch hail 5 n mi north of tower; later developing storms produced 2 3/4 inch hail and winds up to 100 mph in Oklahoma City - Norman area.
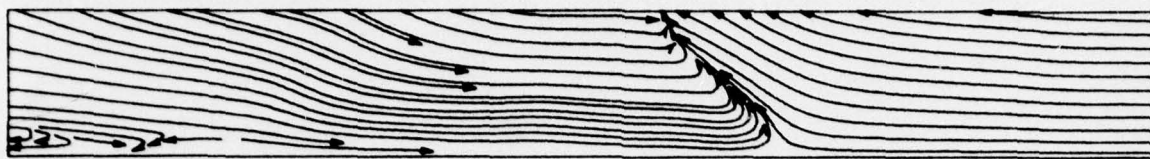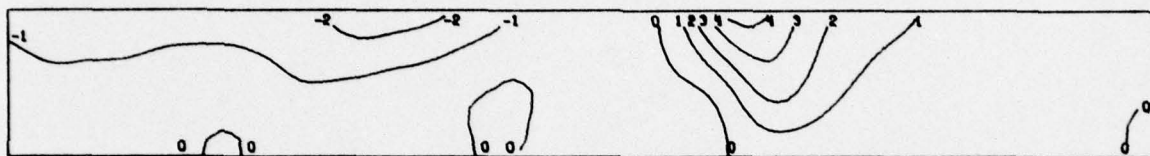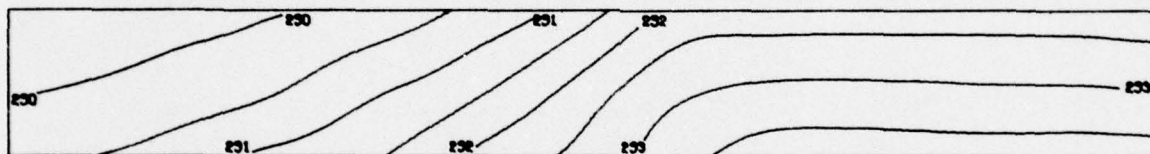
06MAY72 1731   ⊢___ 1 KM ___⊣

STREAMLINE ANALYSIS

VERTICAL VELOCITY

WET BULB POTENTIAL TEMPERATURE
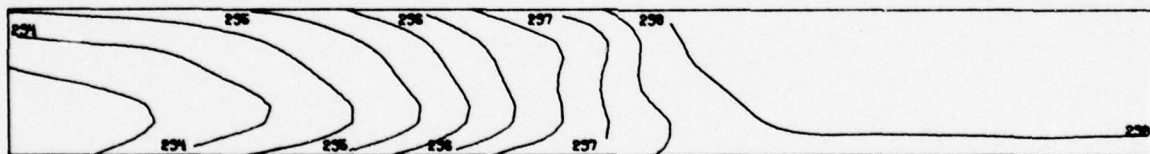
POTENTIAL TEMPERATURE
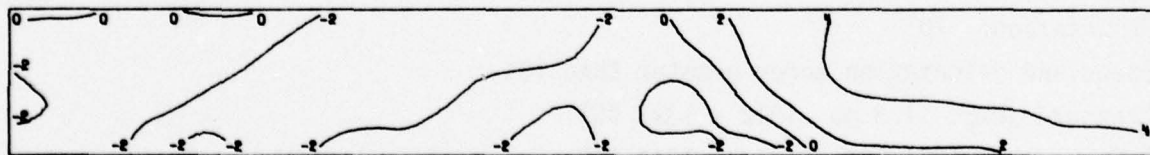
WIND SPEED PARALLEL TO FRONT

RELATIVE WIND SPEED, COMPONENT NORMAL TO FRONT

Figure A-C-1

54
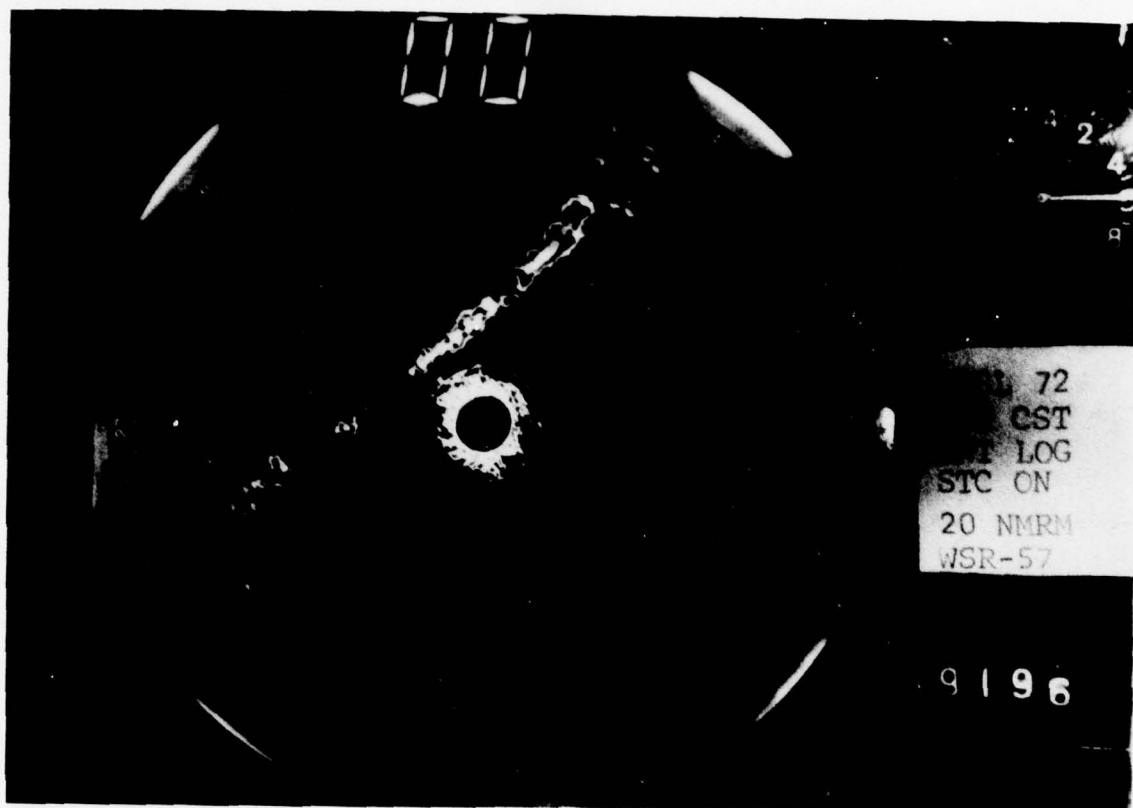
Figure A-C-2

Case C
Date: 6 May 72
Time of gust front: 1734 CST
Speed: 8.6 m s^{-1}
Orientation: 50°
Speed and orientation error less than 10%
Pressure jump: 1.1 mb   1728 - 1742 CST
Rain began: 1801 CST ended: 1837 CST
Total rainfall: 0.43 in
Maximum intensity: 2.40 in hr^{-1} 1811 CST
Remarks: No severe weather

27MAY72 1459   └─ 1 KM ─┘

STREAMLINE ANALYSIS
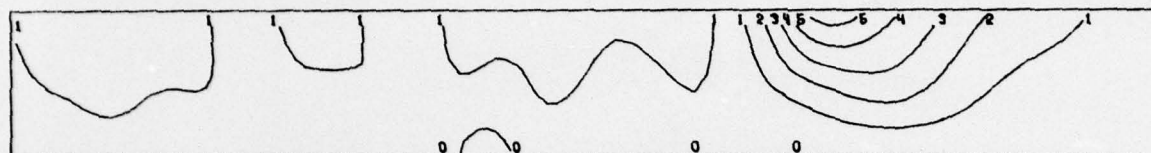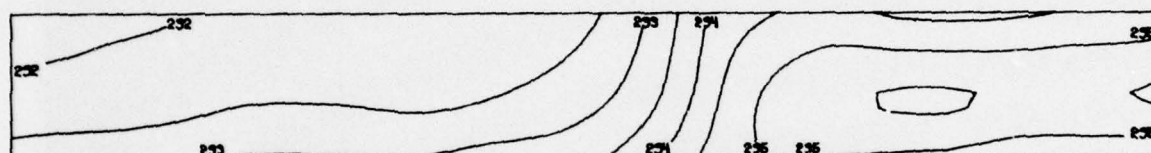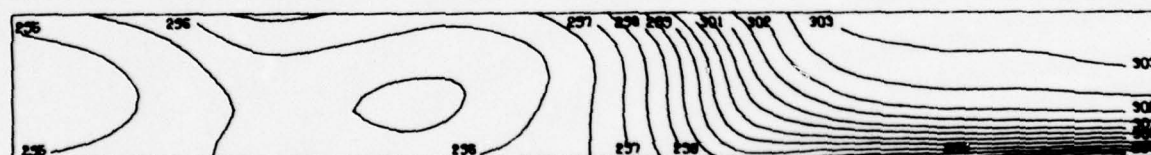
VERTICAL VELOCITY

WET BULB POTENTIAL TEMPERATURE

POTENTIAL TEMPERATURE
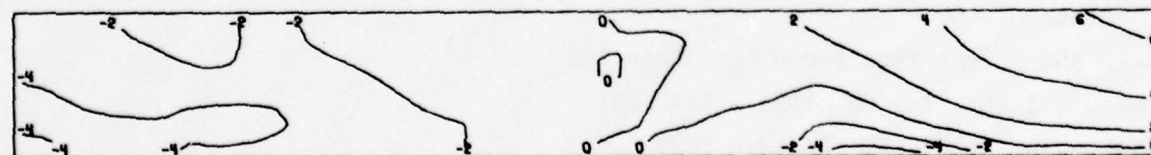
WIND SPEED PARALLEL TO FRONT

RELATIVE WIND SPEED. COMPONENT NORMAL TO FRONT
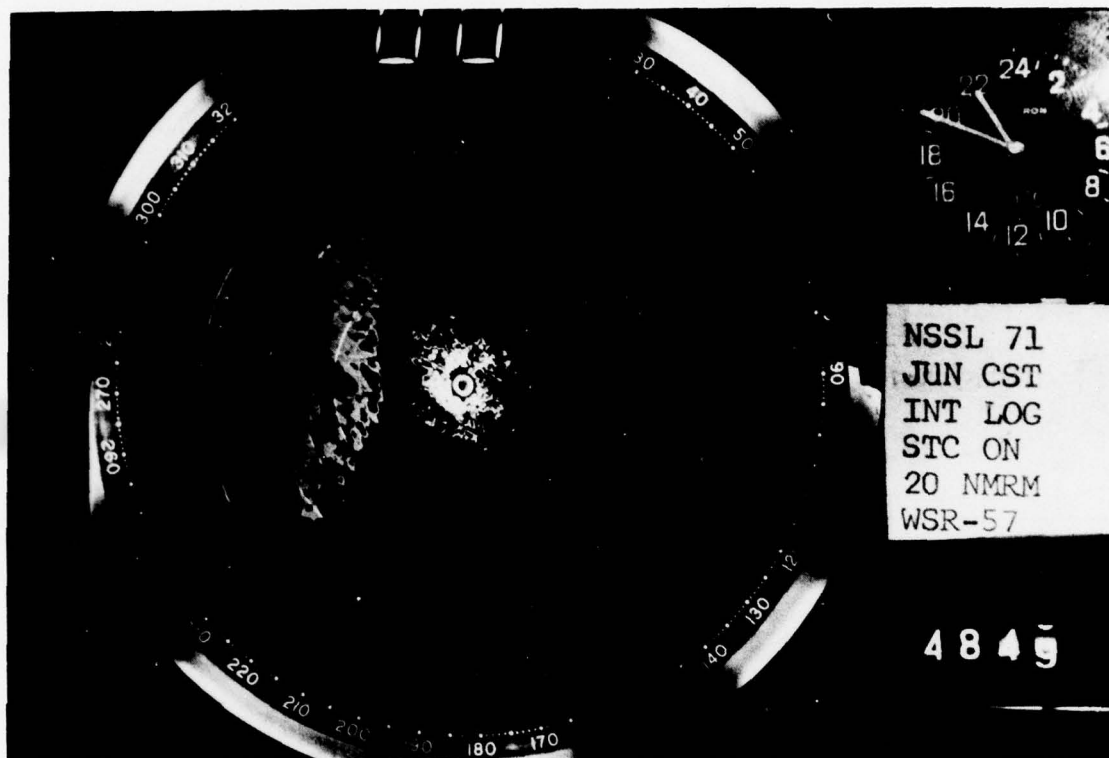
Figure A-D-1

56
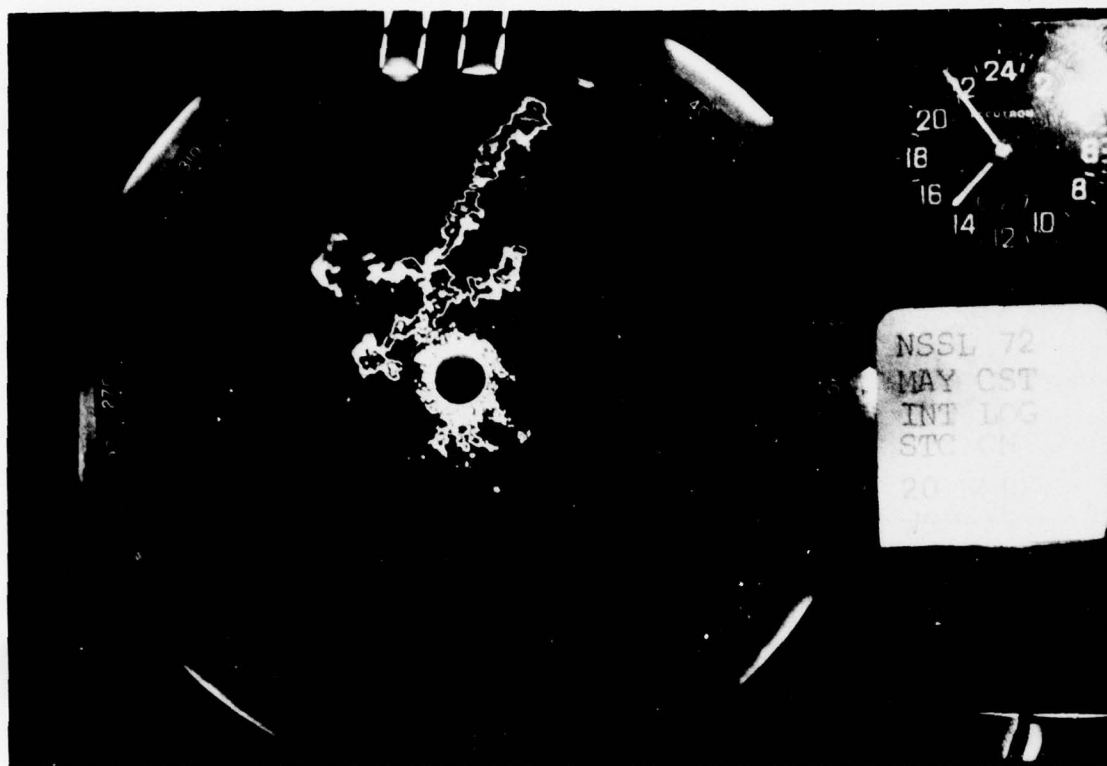
Figure A-D-2

Case D

Date: 27 May 72

Time of gust front: 1503 CST

Speed: 11.6 m s^{-1}

Orientation: 30°

Speed and orientation error about 10%

Pressure jump: 3.0 mb 1451 - 1522 CST

Rain began: 1510 CST ended: unknown

Total rainfall: 1.00 in by 1528 CST

Maximum intensity: 5.40 in hr^{-1}

Remarks: Data collection interrupted at 1528 CST; precipitation records incomplete; 3/4 inch hail 10 n mi west of Norman and 1 3/4 inch hail 10 n mi north of Norman.

31MAY71 1924 | 1 KM
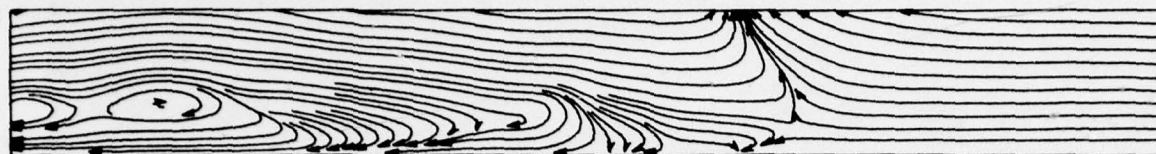
STREAMLINE ANALYSIS
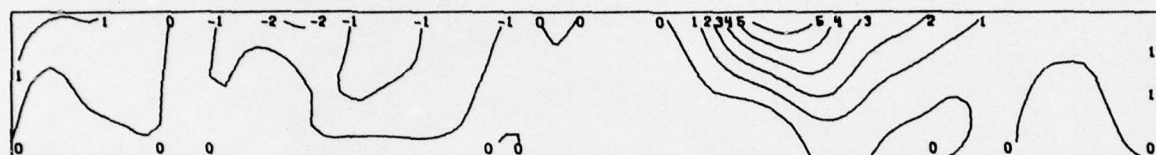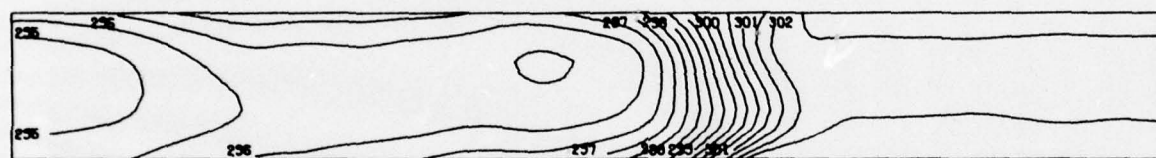
VERTICAL VELOCITY

POTENTIAL TEMPERATURE

WIND SPEED PARALLEL TO FRONT
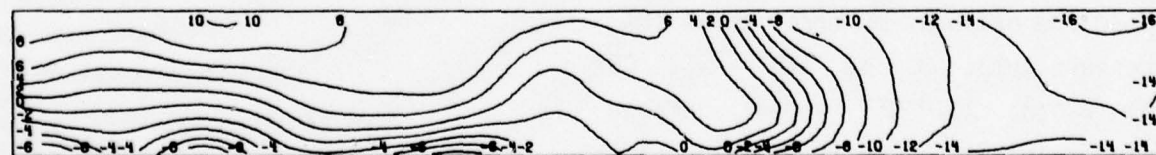
RELATIVE WIND SPEED. COMPONENT NORMAL TO FRONT
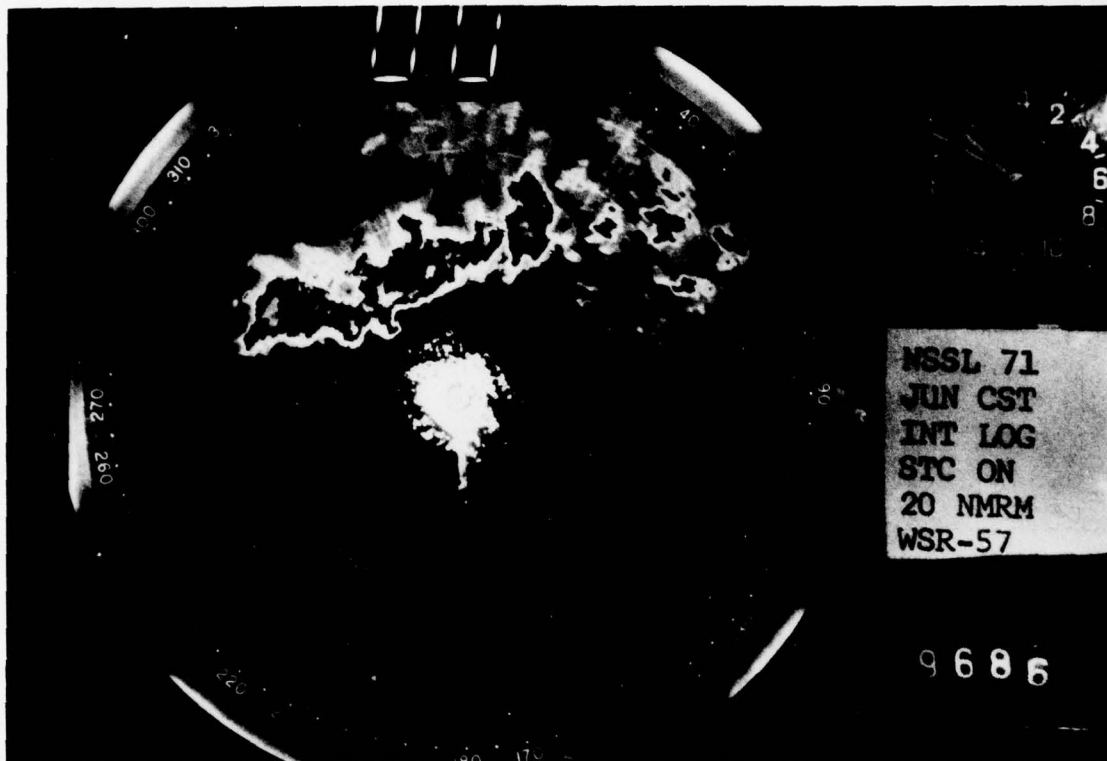
Figure A-E-1

58
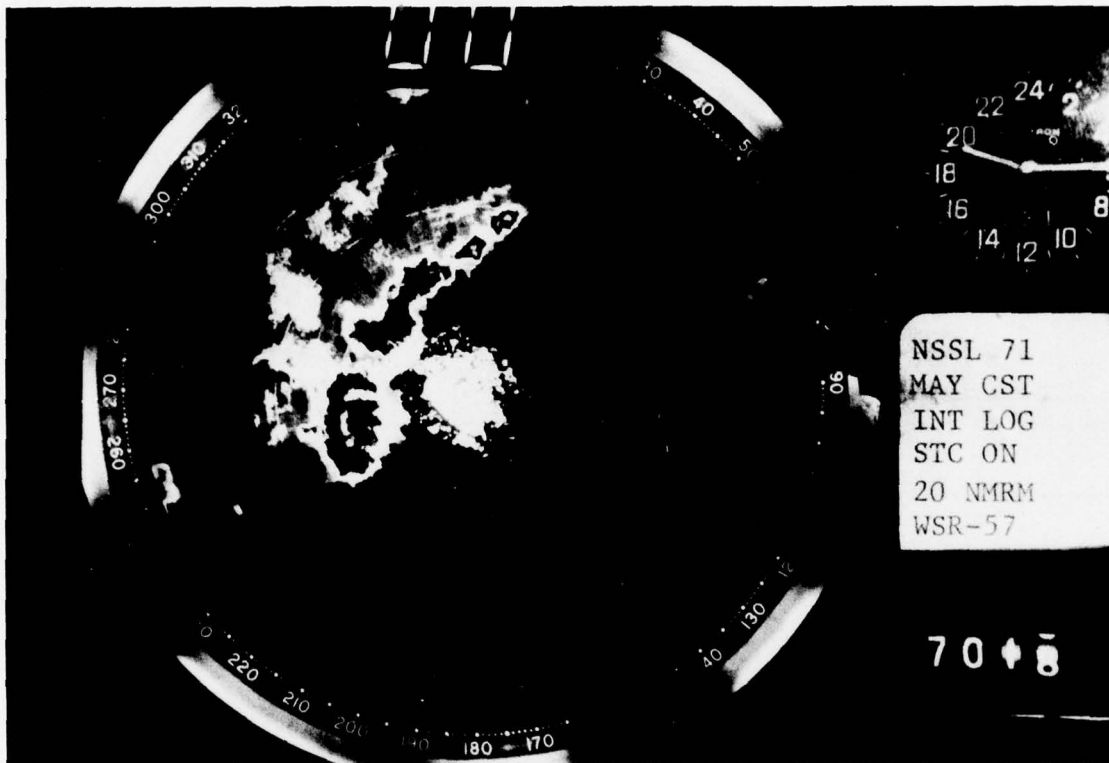
Figure A-E-2

Case E

Date: 31 May 71

Time of gust front: 1927 CST

Speed: 16.7 m s^{-1}

Orientation: 17°

Speed and orientation error about 10%

Pressure jump: 3.9 mb 1911 - 1939 CST

Rain began: 1940 CST ended: 2000 CST

Total rainfall: unknown

Remarks: Precipitation data noisy, cannot determine rainfall intensity; wind damage 10 n mi south of tower; no tornadoes.

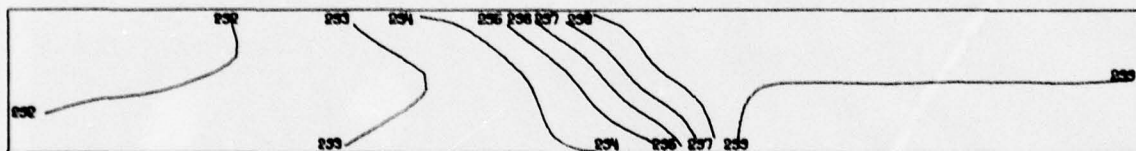27JUN72 1933   ⌐ 1 KM ⌐
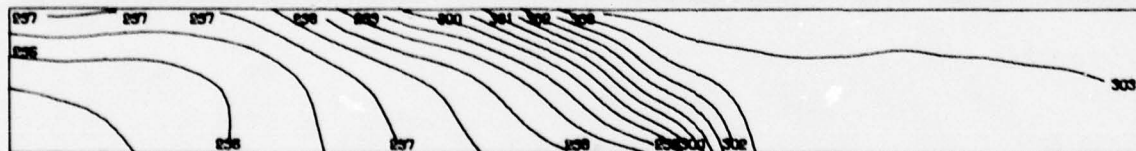

STREAMLINE ANALYSIS
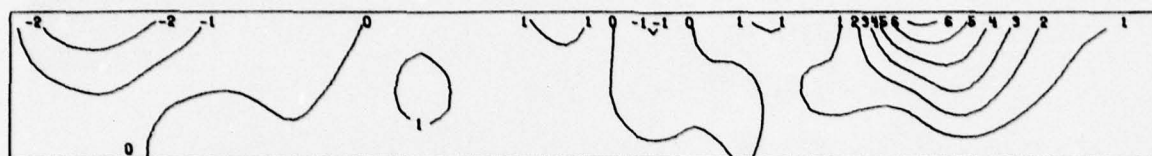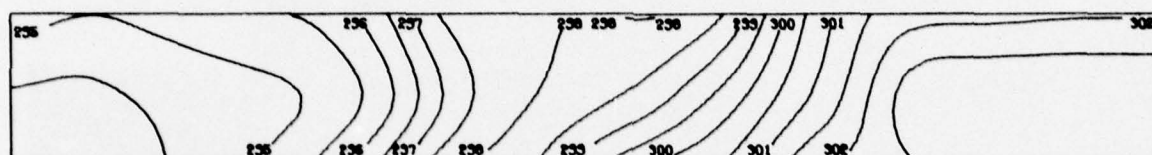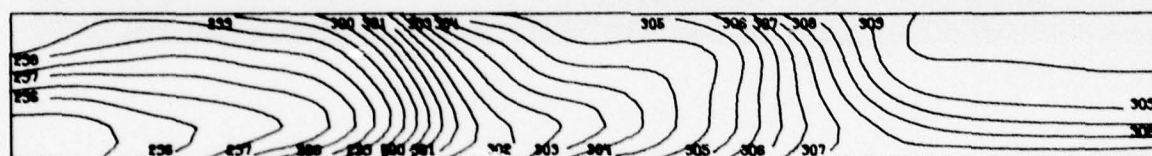
VERTICAL VELOCITY

WET BULB POTENTIAL TEMPERATURE

POTENTIAL TEMPERATURE

WIND SPEED PARALLEL TO FRONT
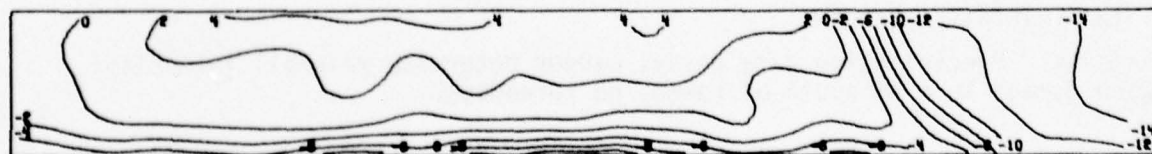
RELATIVE WIND SPEED. COMPONENT NORMAL TO FRONT

Figure A-F-1

60

Figure A-F-2

Case F

Date: 27 Jun 72

Time of gust front: 1936 CST

Speed: 11.0 m s^{-1}

Orientation: 290°

Speed and orientation error less than 10%

Pressure jump: 2.5 mb 1849 - 1942 CST

Rain began: 1940 CST ended: 1944 CST

Total rainfall: 0.09 in

Maximum intensity: 2.40 in hr^{-1} 1941 CST

Remarks: Radar on 2° tilt; left moving cell passes over tower, 3/4 inch hail at Norman. Funnel 10 n mi north of Norman associated with adjacent cell.

07JUN71 1942   ⌊ 1 KM ⌋

STREAMLINE ANALYSIS
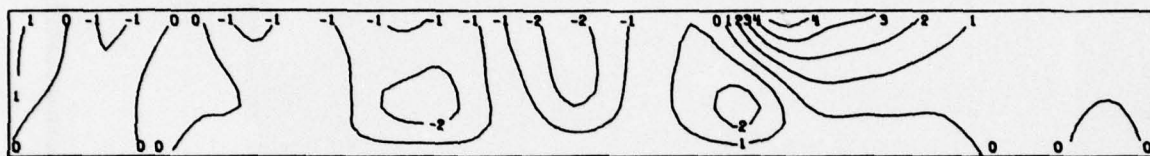
VERTICAL VELOCITY


POTENTIAL TEMPERATURE
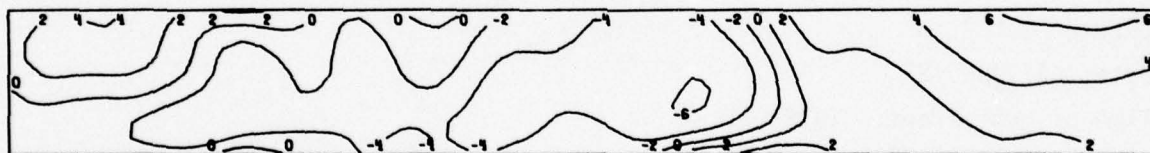
WIND SPEED PARALLEL TO FRONT
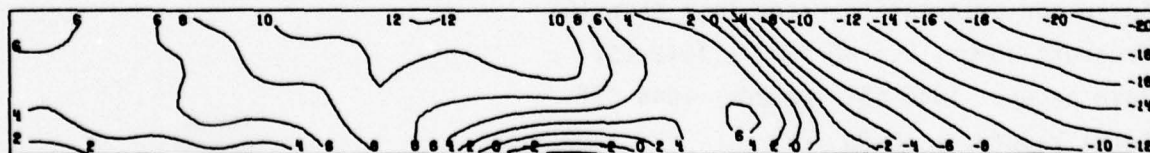
RELATIVE WIND SPEED, COMPONENT NORMAL TO FRONT

Figure A-G-1

62
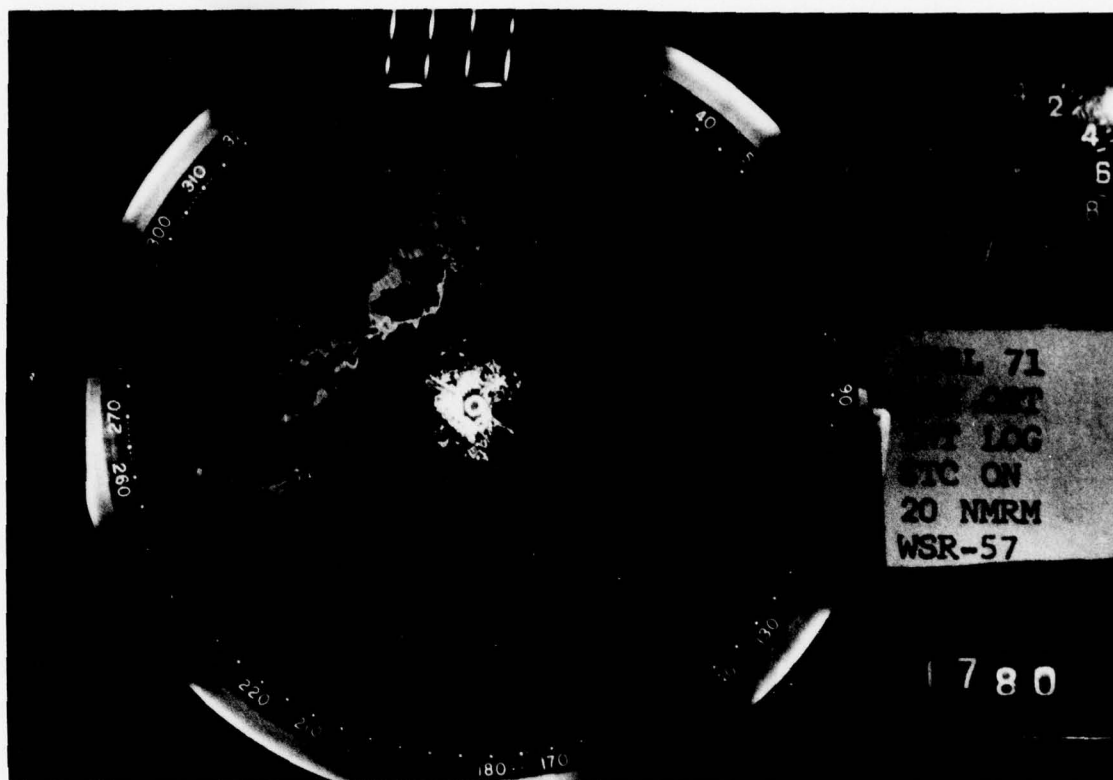
Figure A-G-2

Case G

Date: 7 Jun 71

Time of gust front: 1945 CST

Speed: 1.8 m s^{-1}

Orientation: 50°

Speed and orientation error about 10%

Pressure jump: 5.2 mb 1918 - 2003 CST

Rain began: 2209 CST ended: 2322 CST

Total rainfall: 0.34 in

Maximum intensity: unknown

Remarks: Rainfall data noisy; winds to 65 mph in Oklahoma City, 66 mph at NSSL and 60 mph at Stillwater (30 n mi northeast of tower); no tornadoes.

23MAY74 1712 |___ 1 KM ___|
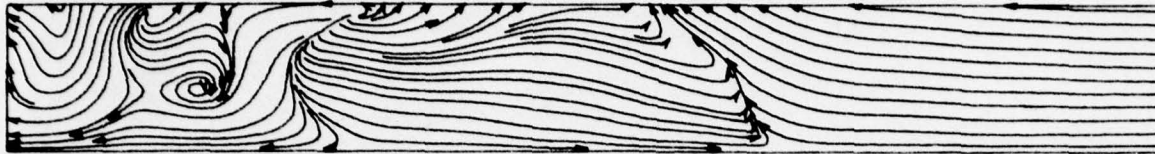
STREAMLINE ANALYSIS
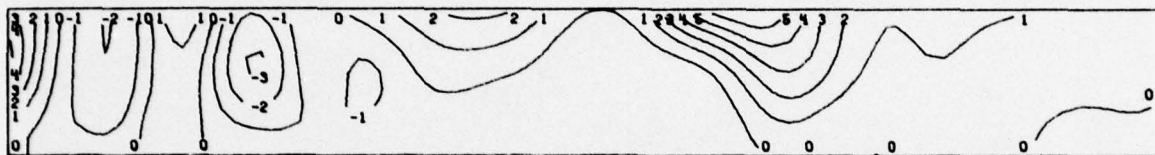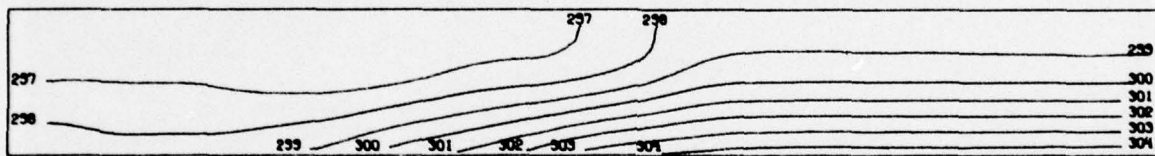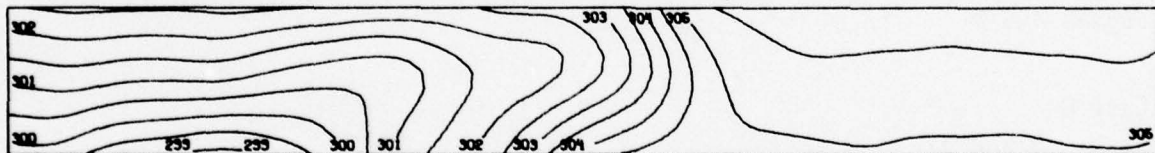
VERTICAL VELOCITY

WET BULB POTENTIAL TEMPERATURE

POTENTIAL TEMPERATURE
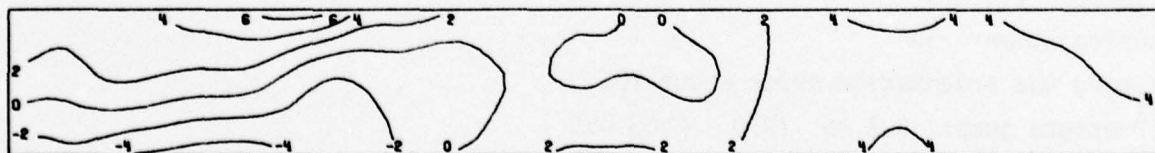
WIND SPEED PARALLEL TO FRONT
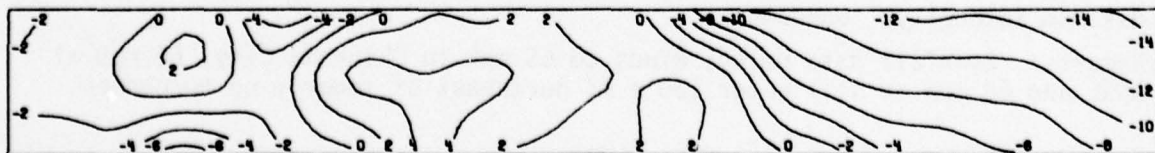
RELATIVE WIND SPEED, COMPONENT NORMAL TO FRONT

Figure A-H-1

64
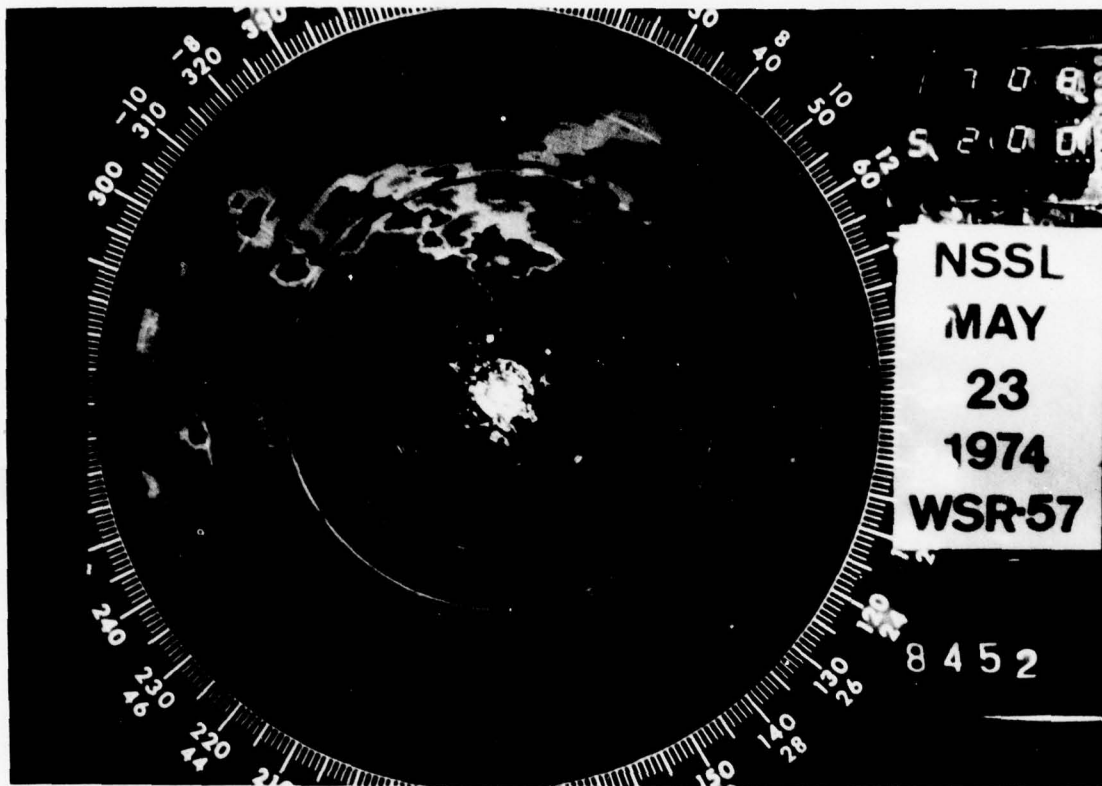
Figure A-H-2

Case H
Date: 23 May 74
Time of gust front: 1716 CST
Speed: 8.5 m s^{-1}
Orientation: 70°
Speed and orientation error greater than 10%
Pressure jump: 2.2 mb 1700 - 1717 CST
Total rainfall: None
Remarks: Funnel and 2 inch hail at Kingfisher (40 km northwest of tower).
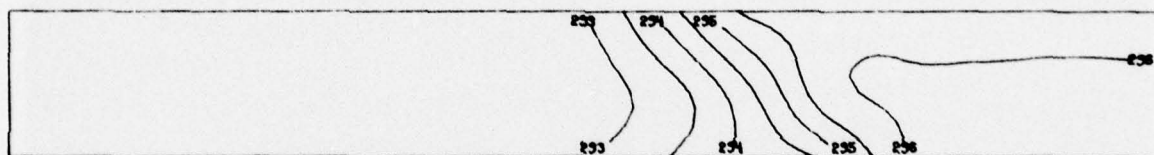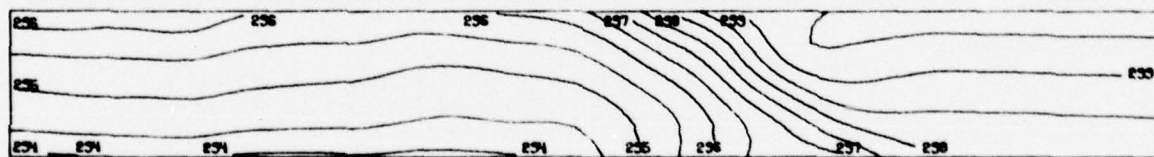
16JUN73 1507 | 1 KM |

STREAMLINE ANALYSIS
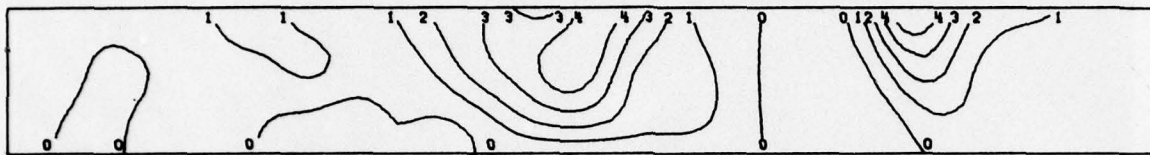
VERTICAL VELOCITY

WET BULB POTENTIAL TEMPERATURE

POTENTIAL TEMPERATURE

WIND SPEED PARALLEL TO FRONT
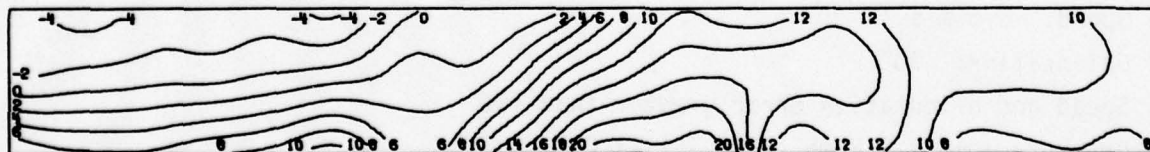
RELATIVE WIND SPEED, COMPONENT NORMAL TO FRONT
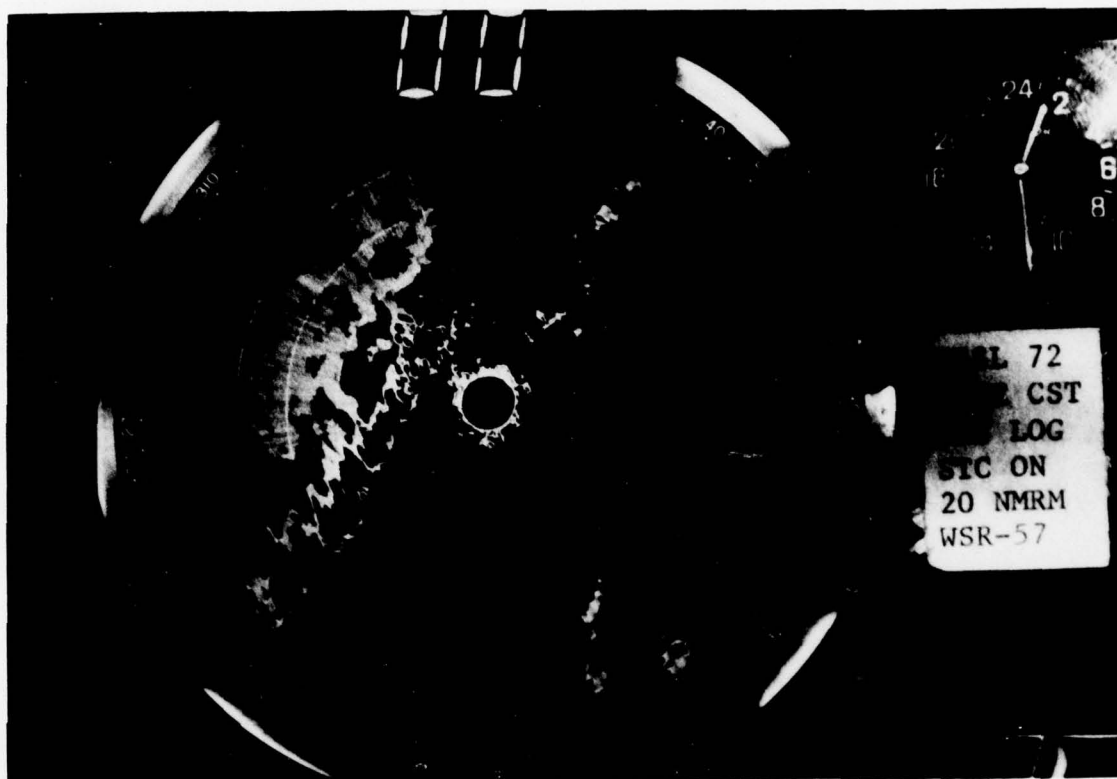
Figure A-I-1

66
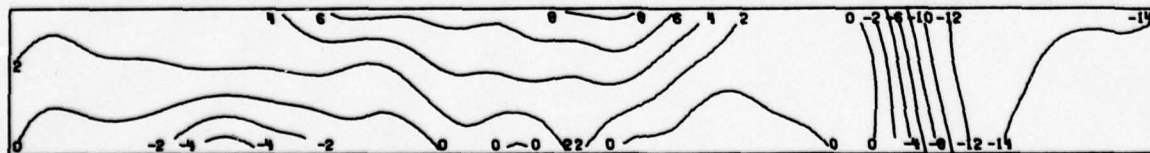
Figure A-I-2

Case I

Date: 16 Jun 73

Time of gust front: 1509 CST

Speed: 11.5 m s^{-1}

Orientation: 22°

Speed and orientation error less than 10%

Pressure jump: 2.8 mb 1505 - 1519 CST

Rain began: 1515 CST ended: 1535 CST

Total rainfall: 0.35 in

Maximum intensity: 2.40 in hr^{-1} 1523 CST

Remarks: Wind damage in Oklahoma City.

67

10JUN71 2206 1 KM

STREAMLINE ANALYSIS

VERTICAL VELOCITY

POTENTIAL TEMPERATURE
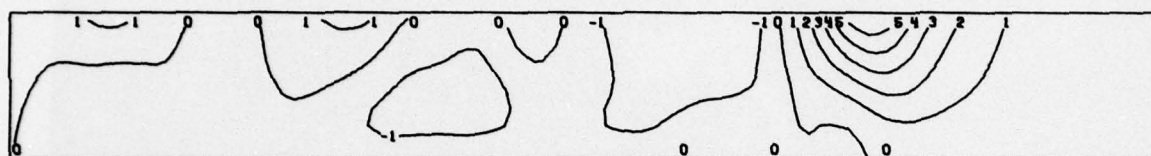
WIND SPEED PARALLEL TO FRONT
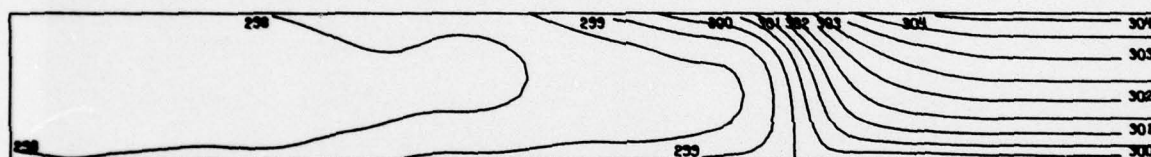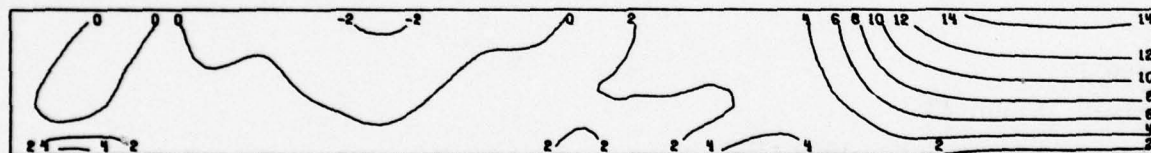
RELATIVE WIND SPEED, COMPONENT NORMAL TO FRONT

Figure A-J-1

68

Figure A-J-2

Case J
Date: 10 Jun 71
Time of gust front: 2209 CST
Speed: 13.1 m s^{-1}
Orientation: 5°
Speed and orientation error less than 10%
Pressure jump: 2.1 mb 2145 - 2213 CST
Rain began: 2249 CST ended: 2304 CST
Total rainfall: 0.08 in
Maximum intensity: unknown
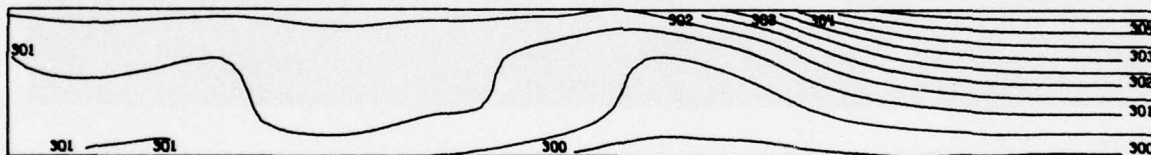Remarks: Rainfall data noisy; no severe weather.

69

02JUN71 2118 1 KM
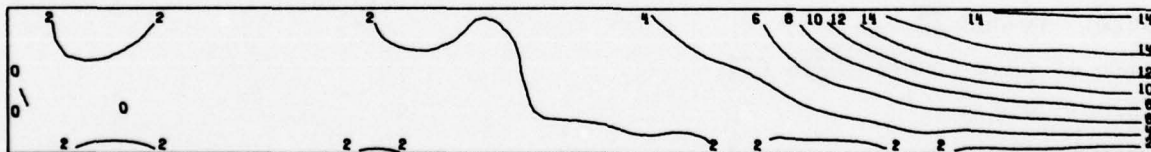
STREAMLINE ANALYSIS
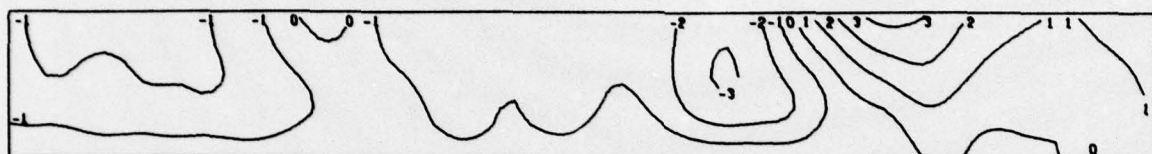
VERTICAL VELOCITY

POTENTIAL TEMPERATURE
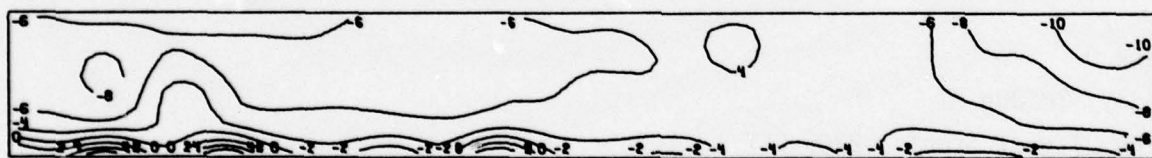
WIND SPEED PARALLEL TO FRONT

RELATIVE WIND SPEED, COMPONENT NORMAL TO FRONT

Figure A-K-1

70

Figure A-K-2

Case K

Date: 2 Jun 71

Time of gust front: 2121 CST

Speed: 12.4 m s^{-1}

Orientation: 70°

Speed and orientation error about 10%

Pressure jump: 6.6 mb 2052 - 2137 CST

Rain began: 2126 CST ended: 2300 CST

Total rainfall: 2.05 in

Maximum intensity: 8.40 in hr^{-1} 2133 CST

Remarks: Gusts to 100 mph recorded at Stillwater 30 n mi northeast of tower; funnel northwest of Guthrie, 20 n mi north of tower; funnel 5 n mi north Yukon, 15 n mi west of tower; winds to 70 mph in Oklahoma City; 3/4 inch hail at airport.

71

04JUN73 1759 |___ 1 KM _____|
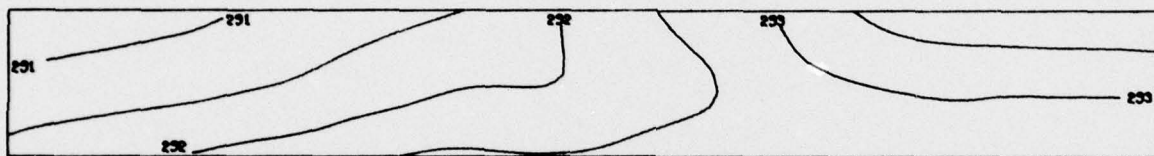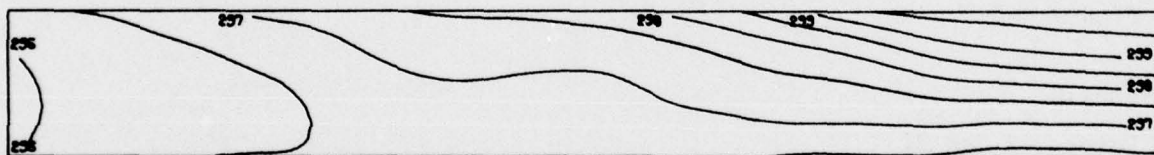
STREAMLINE ANALYSIS
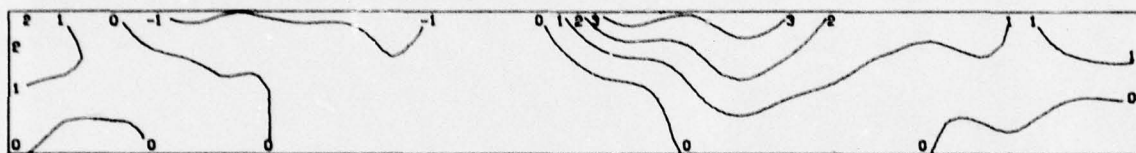
VERTICAL VELOCITY

WET BULB POTENTIAL TEMPERATURE

POTENTIAL TEMPERATURE

WIND SPEED PARALLEL TO FRONT

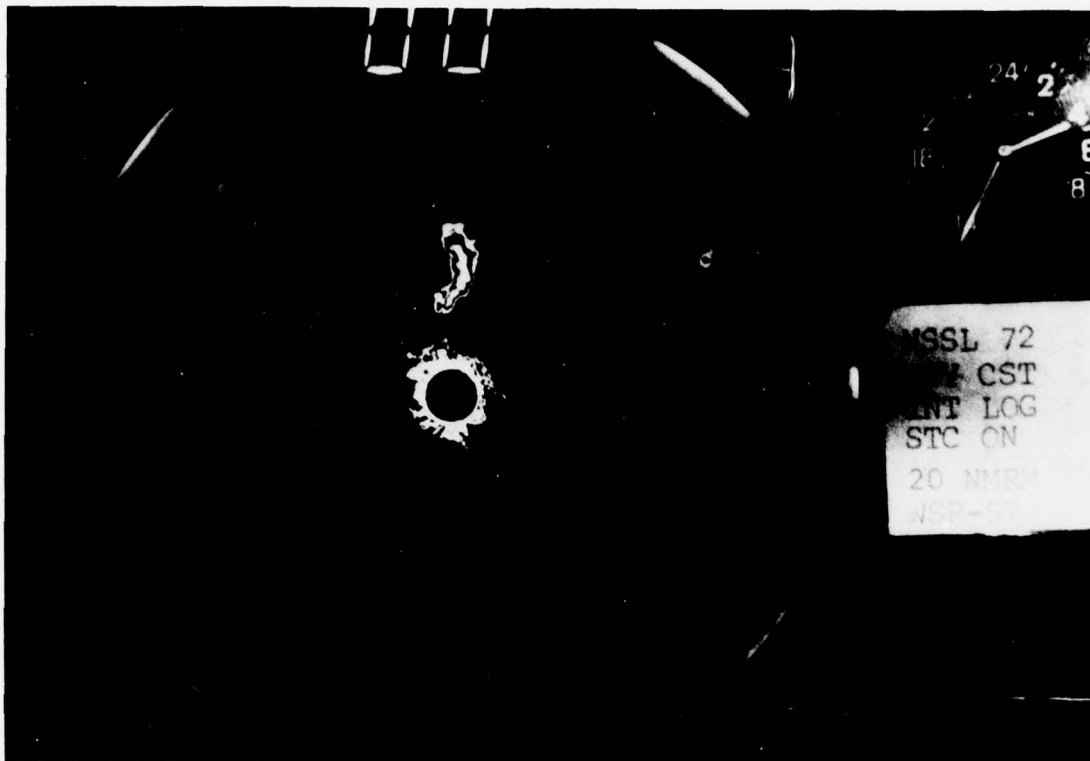RELATIVE WIND SPEED. COMPONENT NORMAL TO FRONT

72
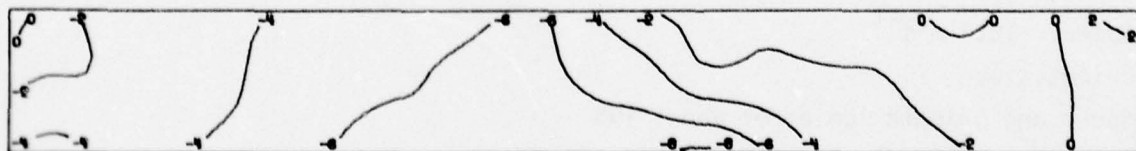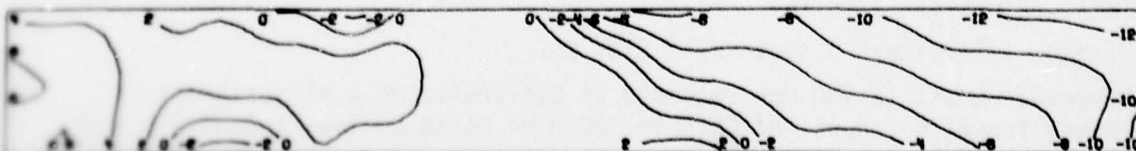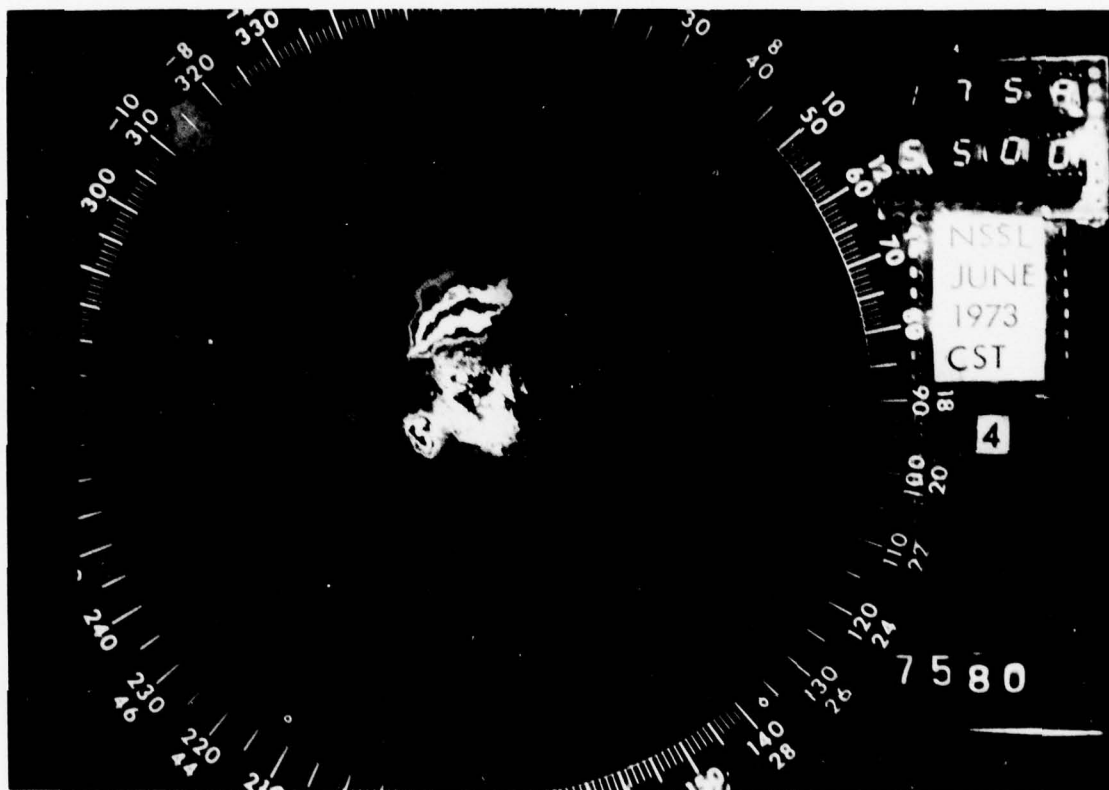
Figure A-L-2

Case L

Date: 4 Jun 73

Time of gust front: 1803 CST

Speed: 5.5 m s^{-1}

Orientation: 60°

Speed and orientation error about 10%

Pressure jump: 2.8 mb 1721 - 1802 CST

Rain began: 1834 CST ended: 2150 CST

Total rainfall: 1.52 in

Maximum intensity: 4.20 in hr^{-1} 1838 CST

Remarks: Hail damage 40 km northwest of tower; wind damage, funnel in Stillwater 60 km northeast of tower; baseball sized hail, 2 funnels in Moore 20 km south of tower; wind damage, funnel and tornado damage at Yukon 30 km west of tower; hail, wind damage and 2 funnels in Oklahoma City; hail, tornado observed at NSSL.
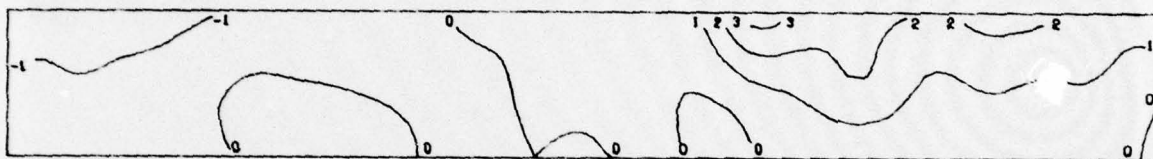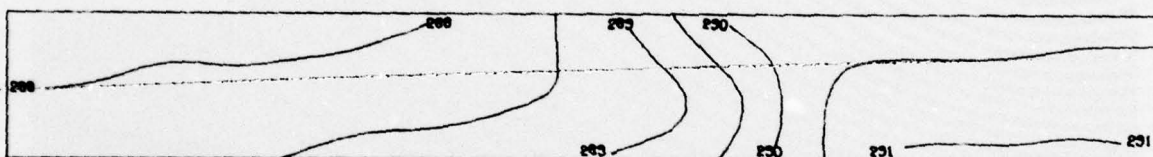
14JUN72 0211   [1 KM]
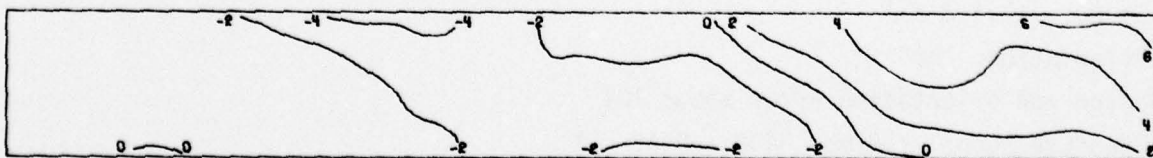
STREAMLINE ANALYSIS
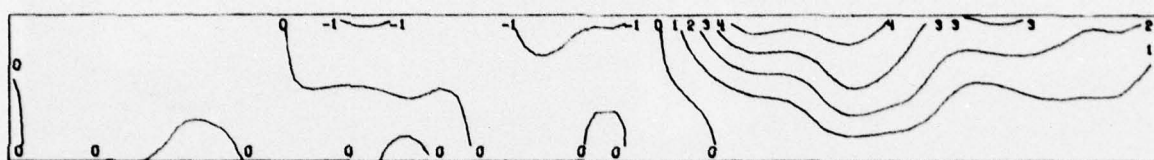
VERTICAL VELOCITY

WET BULB POTENTIAL TEMPERATURE

POTENTIAL TEMPERATURE

WIND SPEED PARALLEL TO FRONT

RELATIVE WIND SPEED. COMPONENT NORMAL TO FRONT
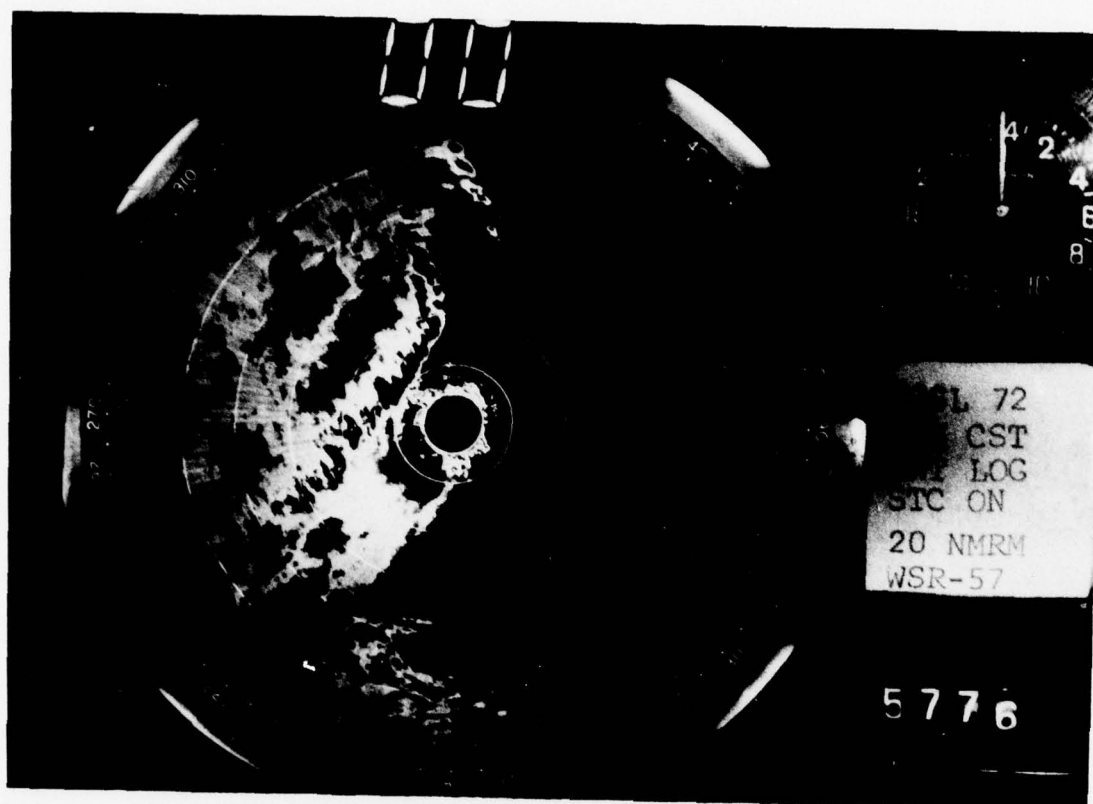
Figure A-M-1

74

Figure A-M-2

Case M

Date: 14 Jun 72

Time of gust front: 0215 CST

Speed: 9.6 m s^{-1}

Orientation: 0°

Speed and orientation error less than 10%

Pressure jump: 1.2 mb 0206 - 0227 CST

Rain began: 0217 CST ended: 0242 CST

Total rainfall: 0.34 in

Maximum intensity: 1.80 in hr^{-1} 0230 CST

Remarks: Shear-gravity waves observed after squall lines (0310 CST); no severe weather.

12JUN71 0109   ⊢——— 1 KM ———⊣

STREAMLINE ANALYSIS
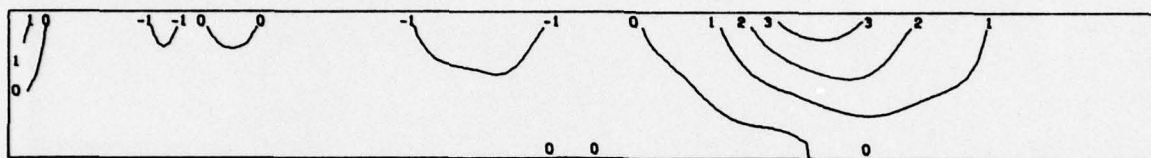
VERTICAL VELOCITY

POTENTIAL TEMPERATURE

WIND SPEED PARALLEL TO FRONT

RELATIVE WIND SPEED, COMPONENT NORMAL TO FRONT

Figure A-N-1

76

(NO NSSL RADAR DATA AVAILABLE)

Figure A-N-2

Case N
Date: 12 Jun 71
Time of gust front: 0113 CST
Speed: 8.0 m s^{-1}
Orientation: 0°
Speed and orientation error about 10%
Pressure jump: 1.2 mb 0107 - 0130 CST
Total rainfall: None
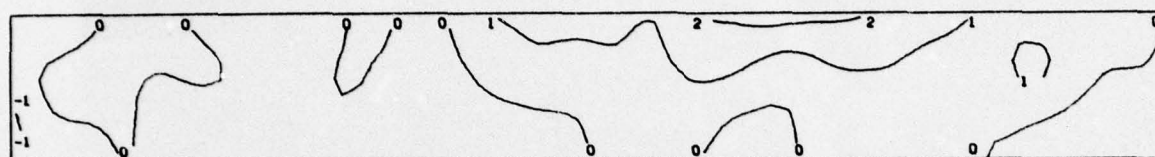Remarks: No severe weather.

23MAY72 0436 | 1 KM |
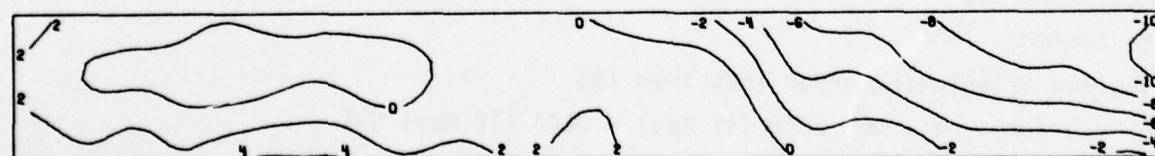

STREAMLINE ANALYSIS
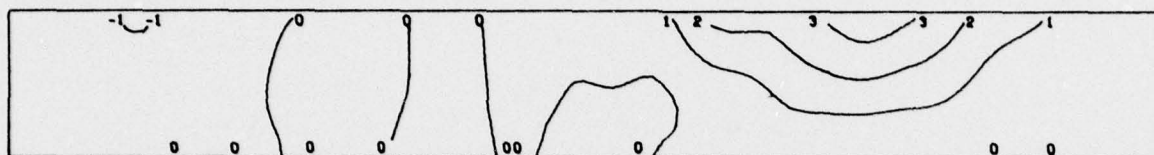
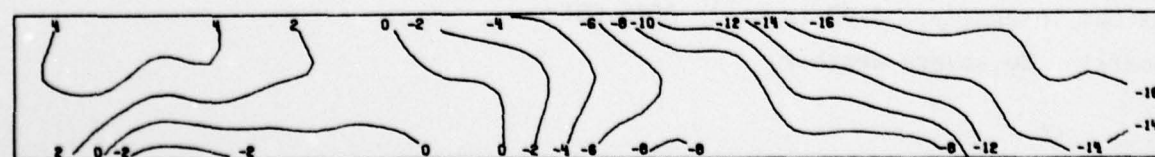

VERTICAL VELOCITY

WET BULB POTENTIAL TEMPERATURE

POTENTIAL TEMPERATURE

WIND SPEED PARALLEL TO FRONT

RELATIVE WIND SPEED. COMPONENT NORMAL TO FRONT

Figure A-0-1

Figure A-0-2

Case 0

Date: 23 May 72

Time of gust front: 0440 CST

Speed: 11.4 m s^{-1}

Orientation: 50°

Speed and orientation error about 10%

Pressure jump: 1.9 mb 0430 - 0445 CST

Total rainfall: None

Remarks: No severe weather.

12MAY72 0020

1 KM
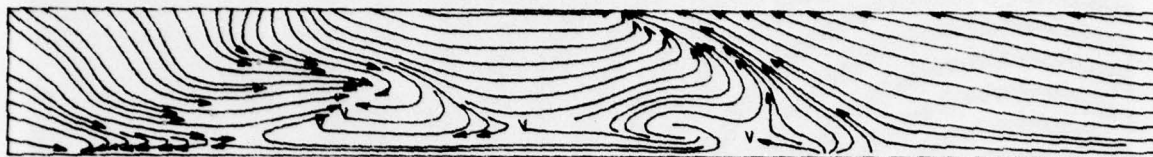
STREAMLINE ANALYSIS

VERTICAL VELOCITY

WET BULB POTENTIAL TEMPERATURE

POTENTIAL TEMPERATURE

WIND SPEED PARALLEL TO FRONT

RELATIVE WIND SPEED. COMPONENT NORMAL TO FRONT

Figure A-P-1

Figure A-P-2

Case P

Date: 12 May 72 (date incorrect on time clock)

Time of gust front: 0024 CST

Speed: 6.9 m s^{-1}

Orientation: 10°

Speed and orientation error less than 10%

Pressure jump: 2.3 mb 2354 (11 May) - 0044 (12 May) CST

Rain began: 0030 CST ended: 0612 CST

Total rainfall: 2.07 in

Maximum intensity: 3.60 in hr^{-1} 0045 CST

Remarks: No severe weather.

23MAY74 1837   ⌞ 1 KM

STREAMLINE ANALYSIS

VERTICAL VELOCITY

WET BULB POTENTIAL TEMPERATURE


POTENTIAL TEMPERATURE

WIND SPEED PARALLEL TO FRONT

RELATIVE WIND SPEED. COMPONENT NORMAL TO FRONT

Figure A-Q-1

82
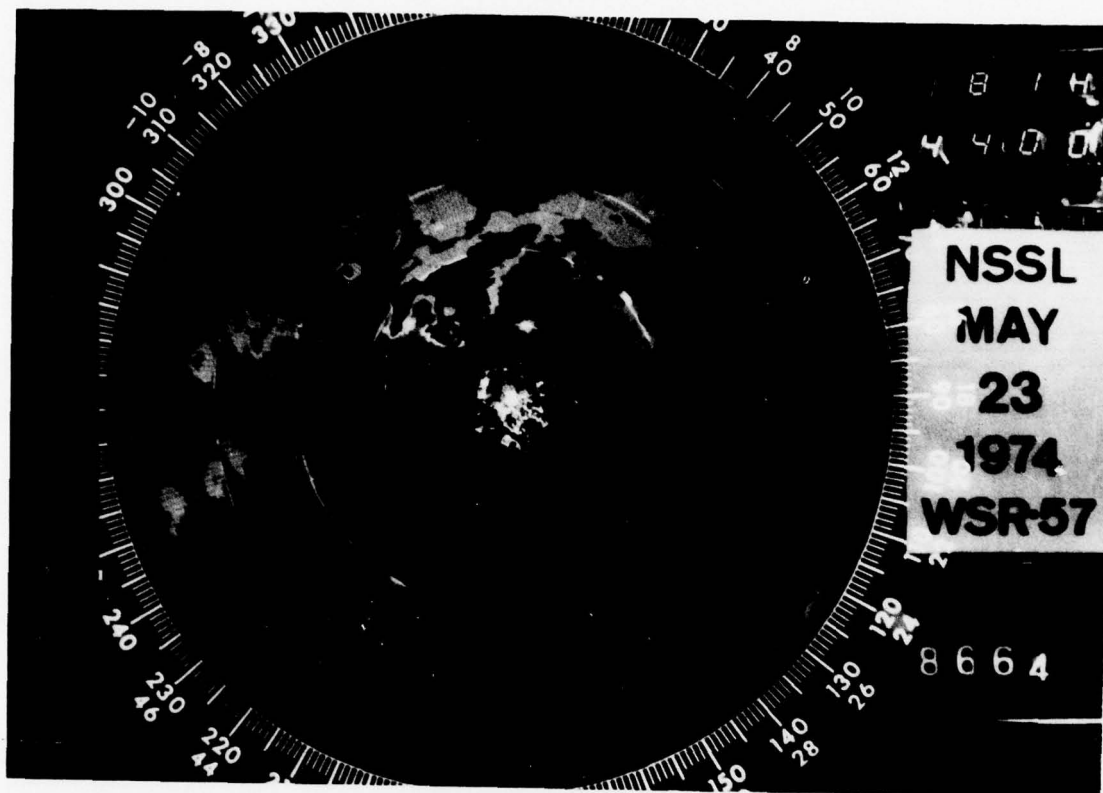
Figure A-Q-2

Case Q

Date: 23 May 74

Time of gust front: 1844 CST

Speed: 17.5 m s^{-1}

Orientation: 50°

Speed and orientation error about 10%

Pressure jump: 3.9 mb 1816 - 1844 CST

Rain began: 1836 CST ended: about 1920 CST

Total rainfall: 2.19 in

Maximum intensity: 7.20 in hr^{-1} 1859 CST

Remarks: Telemetry equipment failures produced several gaps in data; tornado 30 km west of tower, funnel at Tinker Air Force Base 21 km southeast of tower.
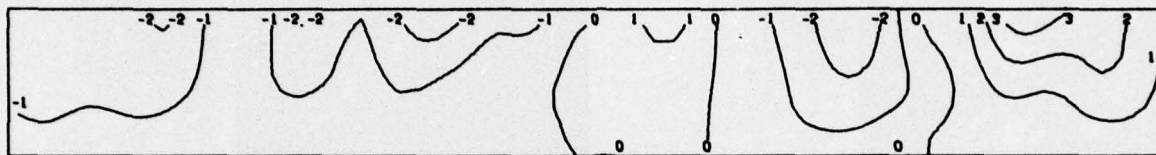
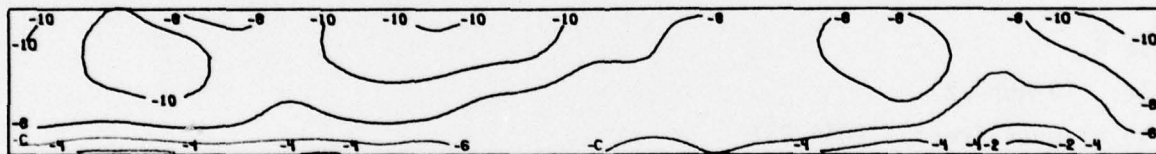19APR72 1651   └ 1 ┘ KM
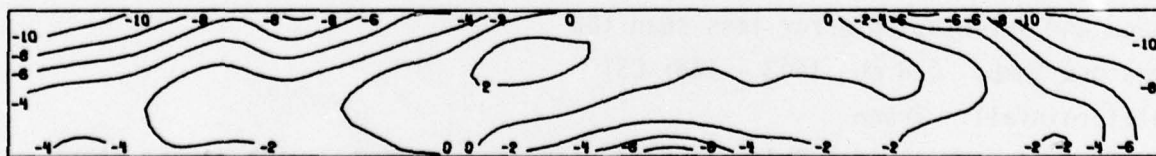

STREAMLINE ANALYSIS
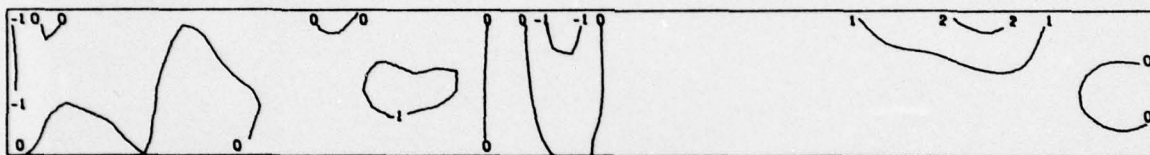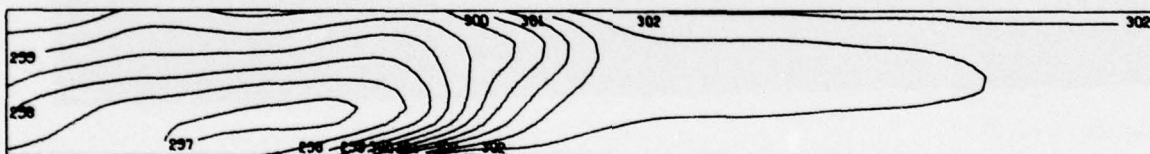
VERTICAL VELOCITY

POTENTIAL TEMPERATURE

WIND SPEED PARALLEL TO FRONT
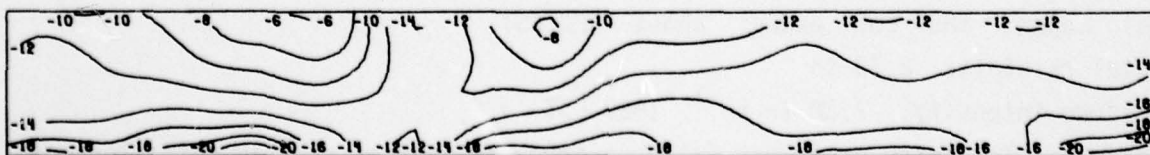
RELATIVE WIND SPEED, COMPONENT NORMAL TO FRONT

Figure A-R-1

84
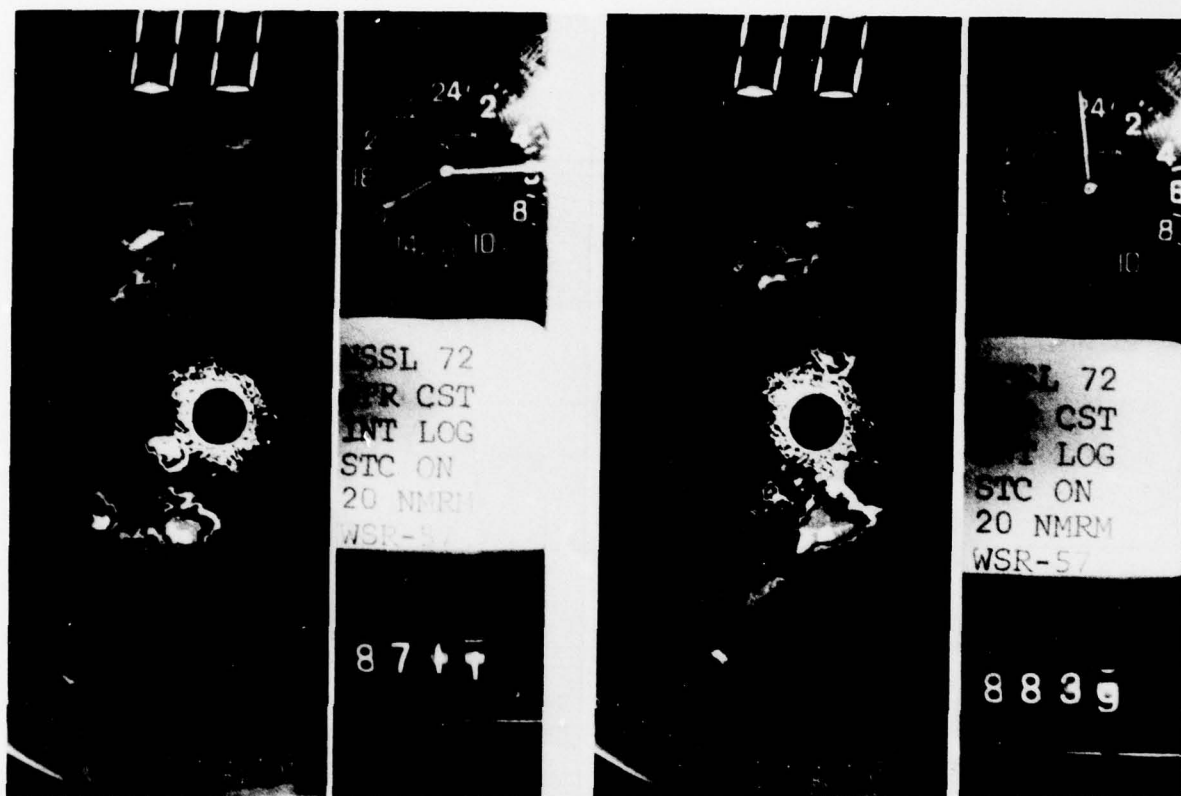
Figure A-R-2

Case R

Date: 19 Apr 72

Time of gust front: 1656 CST

Speed: 25.0 m s^{-1}

Orientation: 290°

Speed and orientation error less than 10%

Pressure jump: 0.8 mb 1643 - 1651 CST

Total rainfall: Trace

Remarks: 1 inch hail at Oklahoma City; tornado associated with parent storm killed 5 people, 60 n mi south of tower.

AD-A056 151   NATIONAL SEVERE STORMS LAB NORMAN OKLA   F/G 1/2
                GUST FRONT ANALYTICAL STUDY.(U)
                DEC 77   R C GOFF , J T LEE, E A BRANDES   DOT-FA76WAI-622
UNCLASSIFIED   FAA-RD-77-119   NL

2 OF 2
AD
A056 151

END
DATE
FILMED
8 -78
DDC

26MAY71 1904   ⌊ 1 KM ⌋

STREAMLINE ANALYSIS

VERTICAL VELOCITY

POTENTIAL TEMPERATURE

WIND SPEED PARALLEL TO FRONT

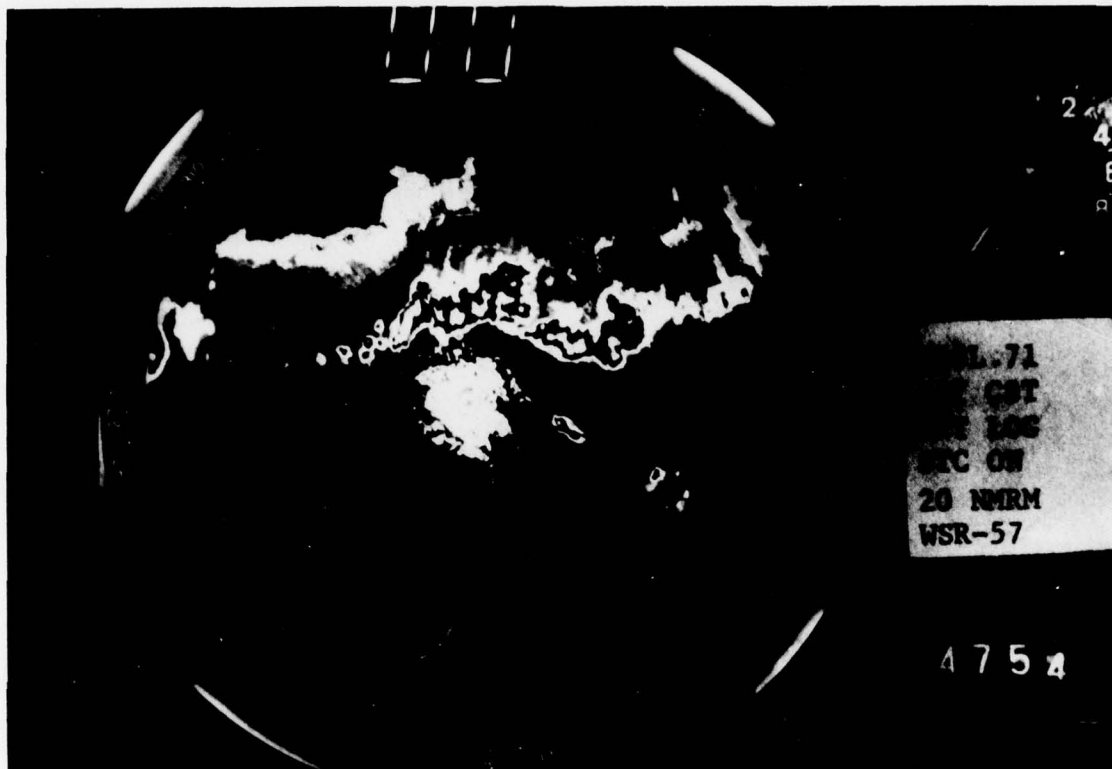RELATIVE WIND SPEED, COMPONENT NORMAL TO FRONT

Figure A-S-1

86

Figure A-S-2

Case S

Date: 26 May 71

Time of gust front: 1906 CST

Speed: 11.0 m s^{-1}

Orientation: 120°

Speed and orientation error about 10%

Pressure jump: 1.9 mb   1819 - 1910 CST

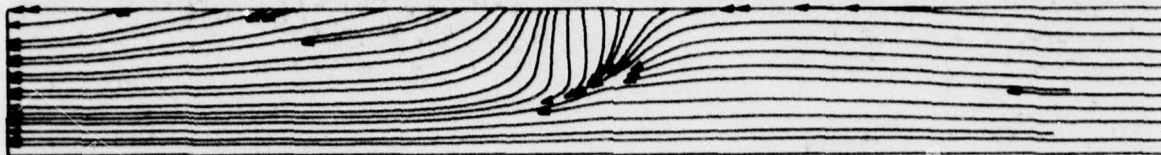Rain began: 1942 CST   ended: unknown time

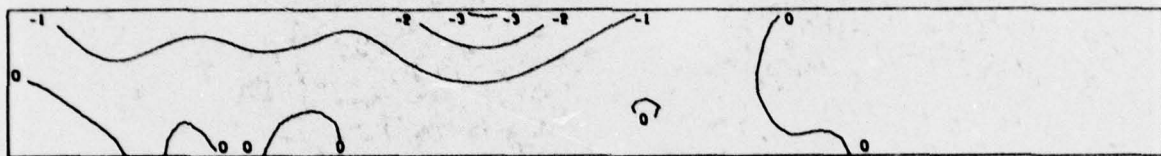Total rainfall: 0.50 in

Maximum intensity: Unknown

Remarks: Winds up to 75 mph in Oklahoma City; funnel 10 n mi east southeast of tower; 1/4 inch hail in Oklahoma City; wind caused considerable damage in Norman, 20 n mi south of tower; tower records incomplete because of power failure.
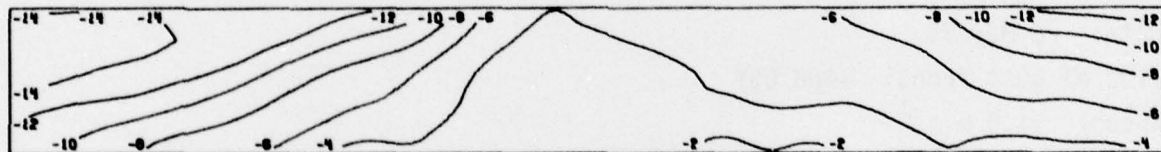
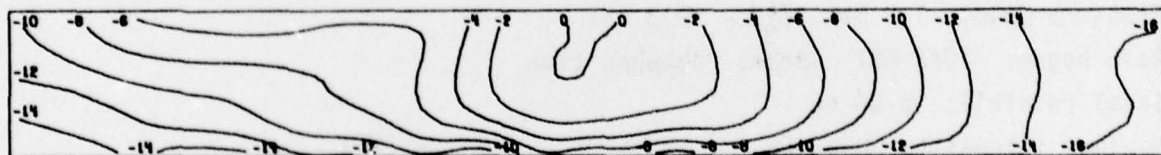21APR72 0029   └─┘ 1 KM

STREAMLINE ANALYSIS

VERTICAL VELOCITY

POTENTIAL TEMPERATURE

WIND SPEED PARALLEL TO FRONT

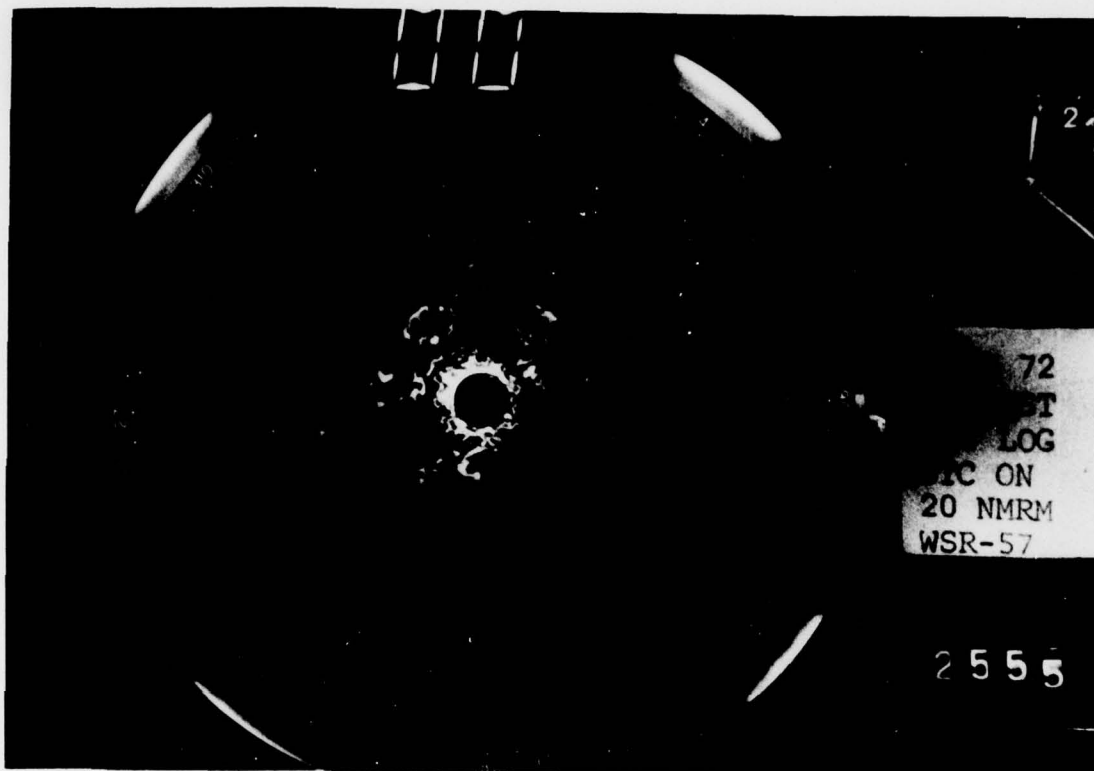RELATIVE WIND SPEED. COMPONENT NORMAL TO FRONT

Figure A-T-1

Figure A-T-2

Case T

Date: 21 Apr 72

Time of gust front: 0034 CST

Speed: 19.9 m s^{-1}

Orientation: 5°

Speed and orientation error about 10%

Pressure jump: 3.0 mb 0028 - 0035 CST

Rain began: 0033 CST ended: 0044 CST

Total rainfall: 0.13 in

Maximum intensity: 2.40 in hr^{-1}

Remarks: No severe weather.

APPENDIX B
Gust Front Cases, 1976

CASE	DATE	TIME (CST)
A	10 May	0144
B	12 May	0844
C	22 May	2208
D	26 May	0014
E	26 May	0727
F	29 May	2109
G	29 May	2359
H	30 May	1828
I	13 Jun	1925
J	23 Jun	2140

APPENDIX B

FIGURE LEGEND

Left Pages:

Streamline analysis and time-height sections of vertical velocity (m s^{-1}), wet-bulb potential temperature (°K), potential temperature (°K), horizontal wind speed component parallel to gust front (v) and wind speed component normal and relative to the gust front (u) (m s^{-1}). Each objective analysis is 10 min long and 450 m thick; time increases from right to left. Date and start time of plot is in the upper left and time-to-space converted 1 km distance is indicated in the upper right.

Right Pages:

(Top) 10 cm WSR-57 conventional radar diagram with echo contouring. dBZ values vary from year to year and case to case but shadings roughly represent powers (x) of 10^x mm^6 m^{-3} radar reflectivity. Time clock is in the upper right. Range marks are at 40 km. The KTVY-TV tower is located at the isolated ground clutter return at 358° and 38 km.

(Bottom) Quantitative remarks. Speed and orientation error subjectively determined. "Remarks" source is mostly from Storm Data (U. S. Dept. of Commerce) reports; some personal observations. Units correspond to radar range mark units or those used in Storm Data reports.
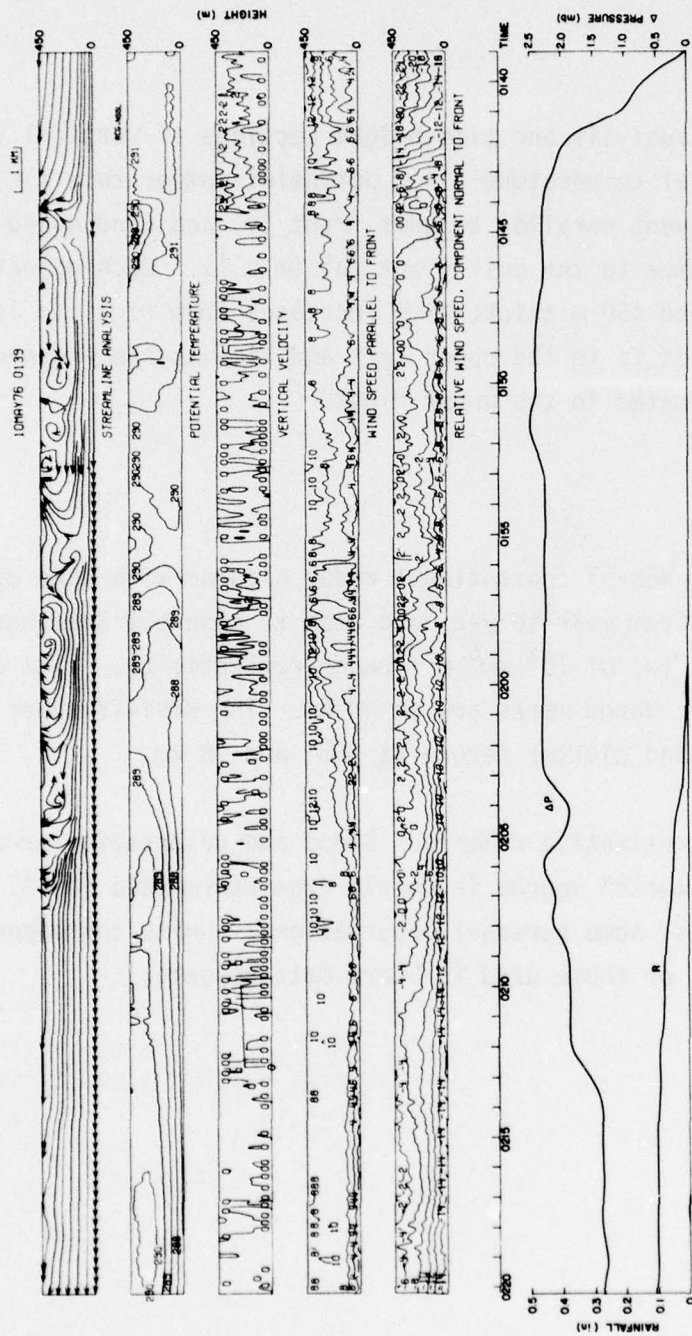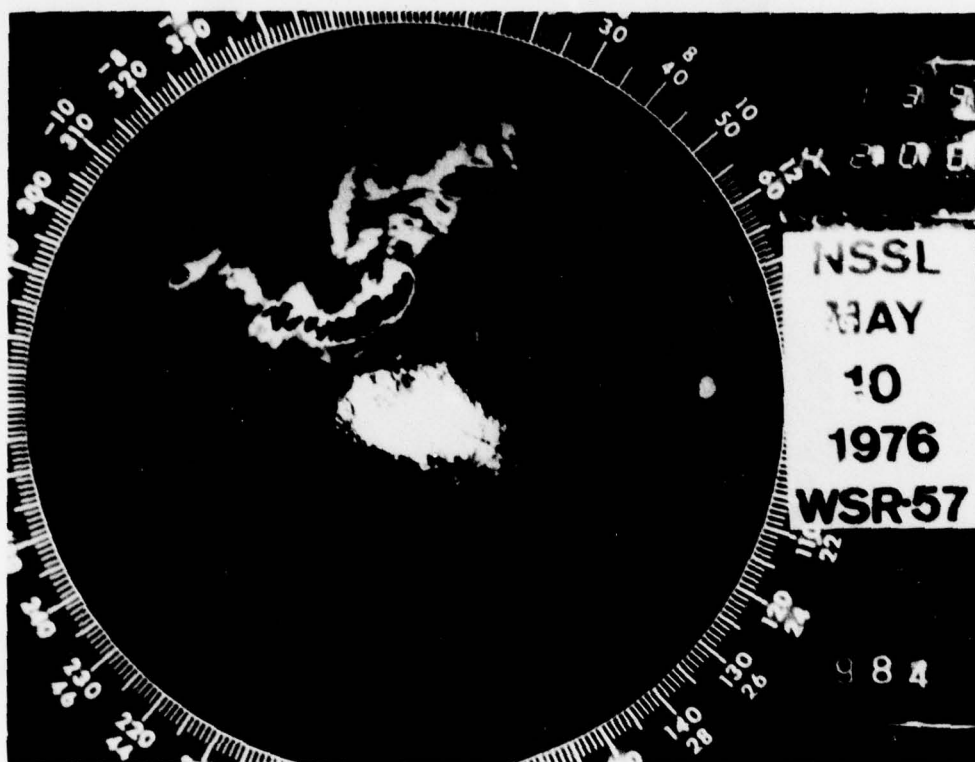
Figure B-A-1

94

Figure B-A-8

Case A

10 May 1976   0144   c = 14.2 m/sec   α = 65°

Moderately strong outflow associated with fast moving but dissipating squall line. Gust front identified on radar by thin line. Gust front shear zone and pressure jump are strong but near-surface temperature discontinuity is almost non-existent. Wave in potential temperature at 0145 indicates highly unstable layer associated with gust front. Weak secondary surge accompanies rainfall onset. Weak turbulence in outflow.
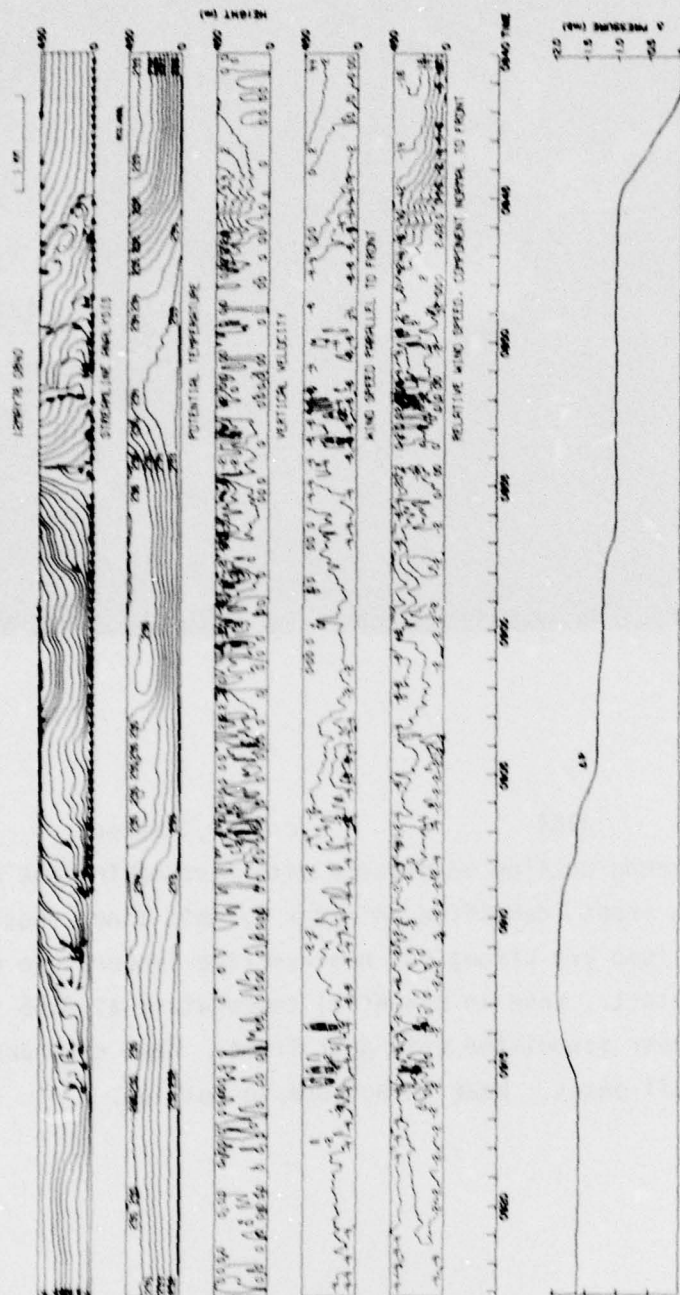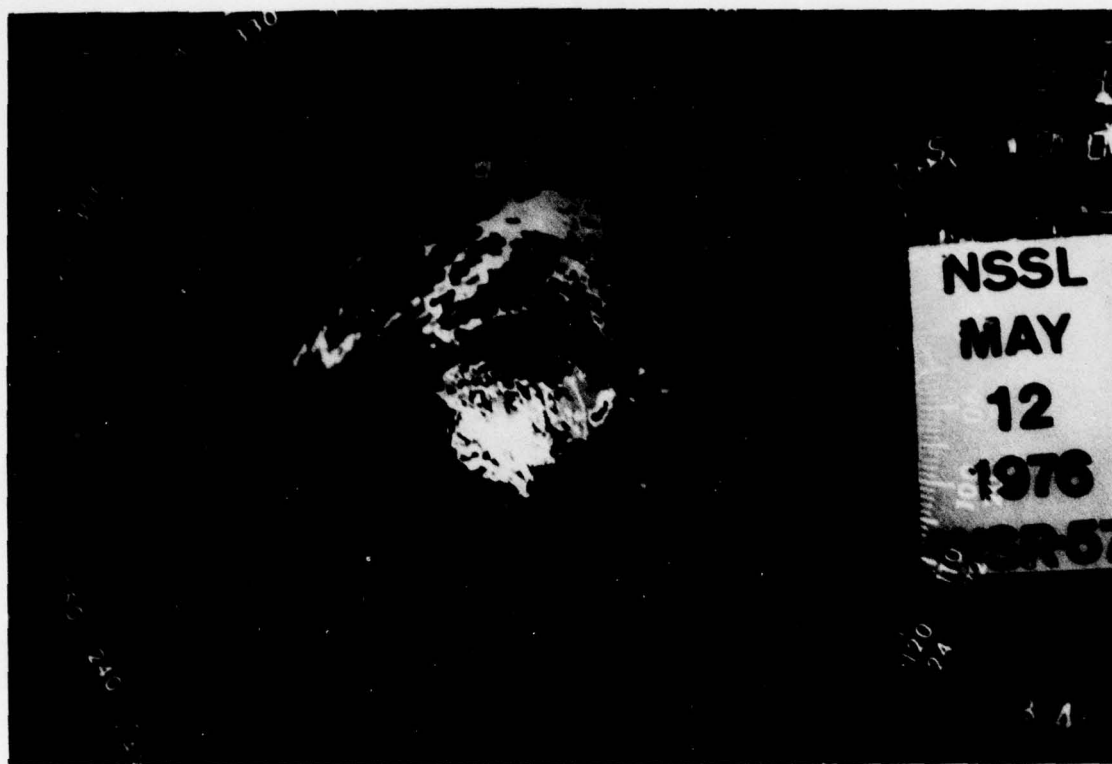
Figure B-B-1

Figure B-B-2

Case B

12 May 1976	0844	c = 6.6 m/sec	α = 65°

Strong and highly turbulent outflow associated with short (50 mi long) but intense squall line. Squall line is along leading edge of cold front. Most intense portion of squall line passes to east of tower. No measurable precipitation at tower. No secondary outflow surges. Outflow depth is unusually shallow (less than 200 m) after 0854. This may represent outflow left behind storm rather than pre-storm outflow. Main thunderstorm downdraft axis associated with squall line passes tower 0853-0855.
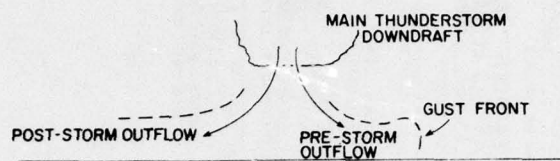
MAIN THUNDERSTORM
DOWNDRAFT

GUST FRONT

POST-STORM OUTFLOW

PRE-STORM
OUTFLOW

Figure B-B-3 Outflow schematic for Case B.

Vertical velocity fluctuations are large along elevated boundary of post-storm outflow. Extreme turbulence evident in horizontal wind due to instrument noise. Gust front has shallow slope even though inflow air has strong temperature inversion.
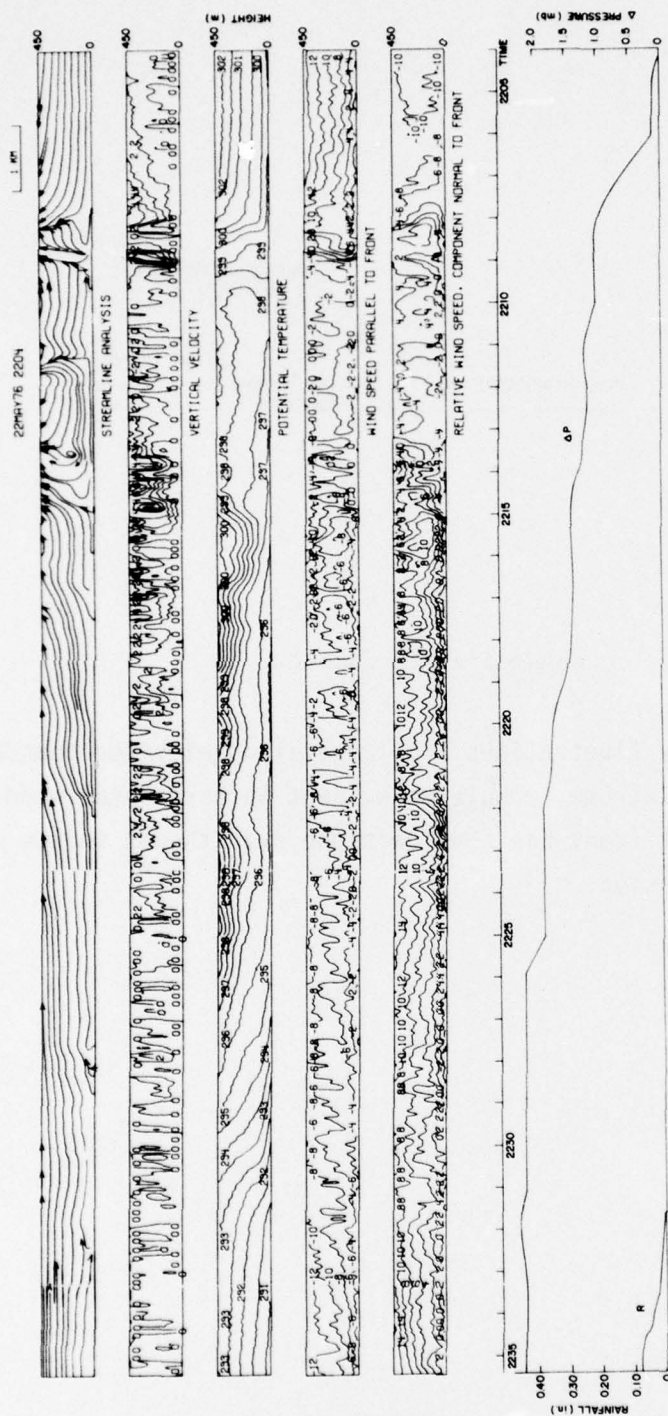
Figure B-C-1

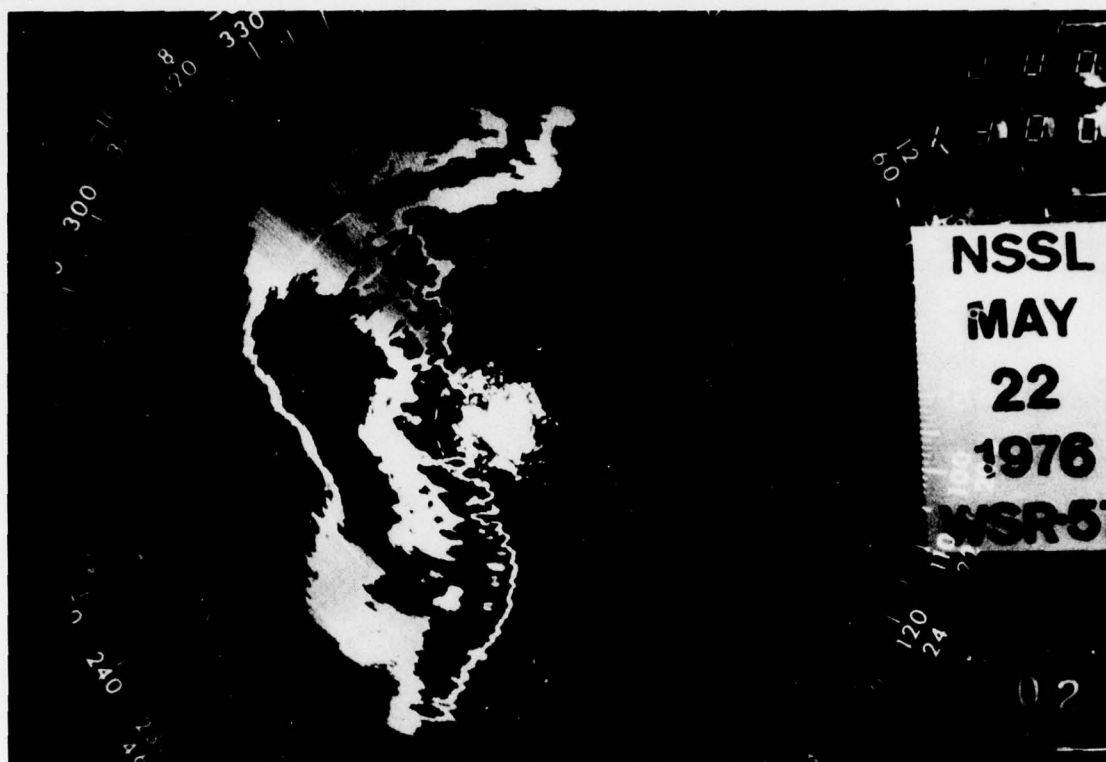*Figure B-C-2*

Case C

22 May 1976   2208 $c = 16.3$ m s^{-1} $\alpha = 352°$

Highly turbulent, relatively shallow outflow associated with long unbroken north-south squall line. Gust front at 2208 is followed 1 min. later by secondary surge. Strong updrafts precede both discontinuities. Potential temperature cross section after 2215 illustrates shallowness of outflow. Center of outflow wake occurs at 2216. Thickness of outflow is only 200 m at this point. Vertical velocity indicates wake region is highly turbulent. Wake is associated with third surge at 2214. Horizontal wind is strong after third surge compared with first two. Undulations on outflowtop (gust front envelope) after 2215 have 500 m amplitude. Coldest temperatures associated with onset of rainfall at 2231. No gust surge with rainfall onset. Gust front envelope rises above tower 6 min. prior to rainfall. Tower layer relatively tranquil thereafter, although strong horizontal winds accompany rainfall. No strong downdraft in rainfall.
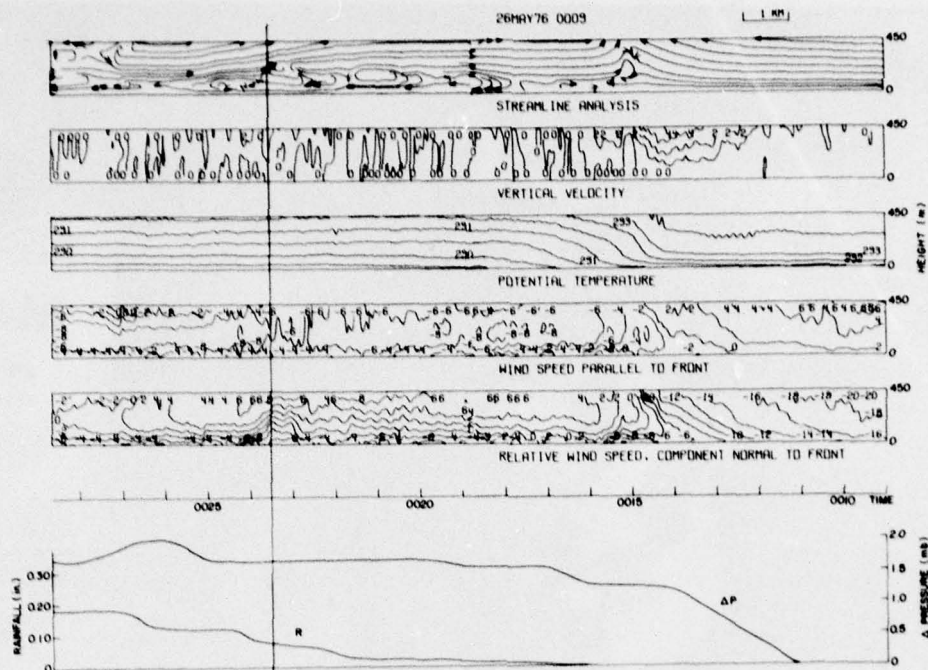
Figure B-D-1a   Time height cross section, May 26, 1976, 0009 - 0028 CST.
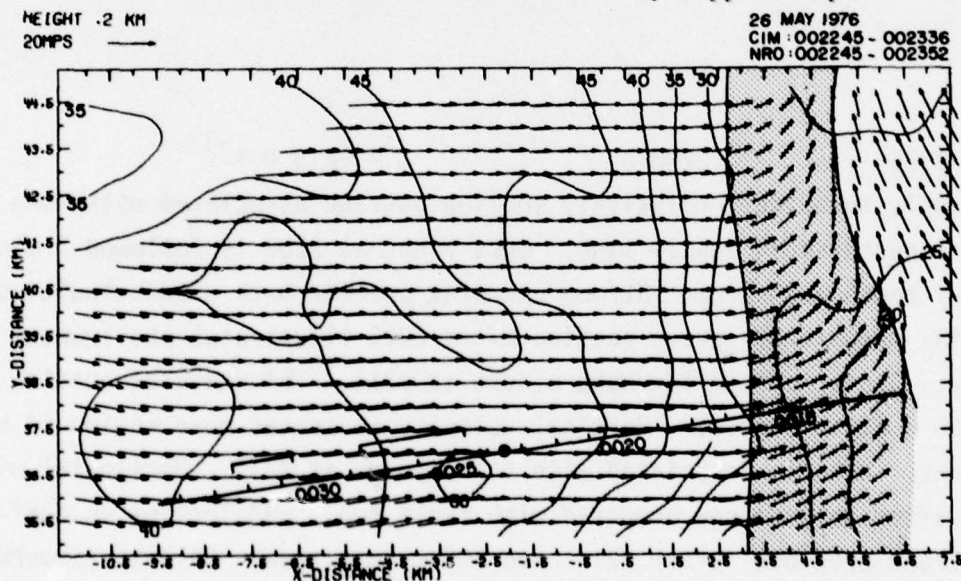Vertical line indicates mean time of Doppler map.

Figure B-D-1b   Horizontal wind field at 0.2 km deduced from Doppler radars at
Norman (NRO) and Cimarron (CIM) airfield, Oklahoma. Times of
data collection at NRO and CIM are given in the upper right.
The frontal zone is shaded. Tower positions relative to the
storm are along the solid line drawn. The tower position is
given by a dot. Zones of the most intense precipitation are
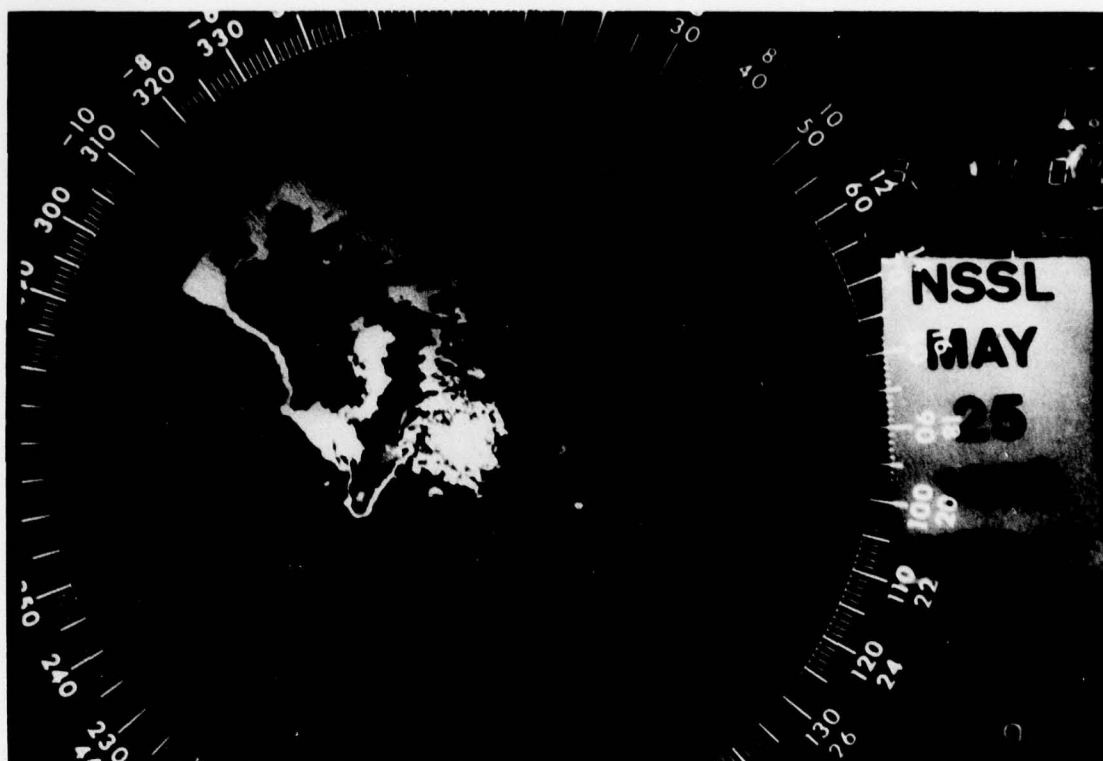shown by the bracketed line.

102

Figure B-D-2

Case D

26 May 1976   0014 $c = 13.8 \text{ m s}^{-1}$ $\alpha = 355°$

Moderately strong outflow associated with moderate to strong squall line. Most intense portion of squall line passes to south of tower. Gust front has only weak temperature discontinuity but strong shear boundary. Weak turbulence in outflow. No strong downdraft even though rainfall intensity is in excess of 2 in per hour (0022 to 0027). Most of pressure jump associated with gust front is in advance of boundary so strong surface gusts in cold air are not observed. No secondary outflow surges.
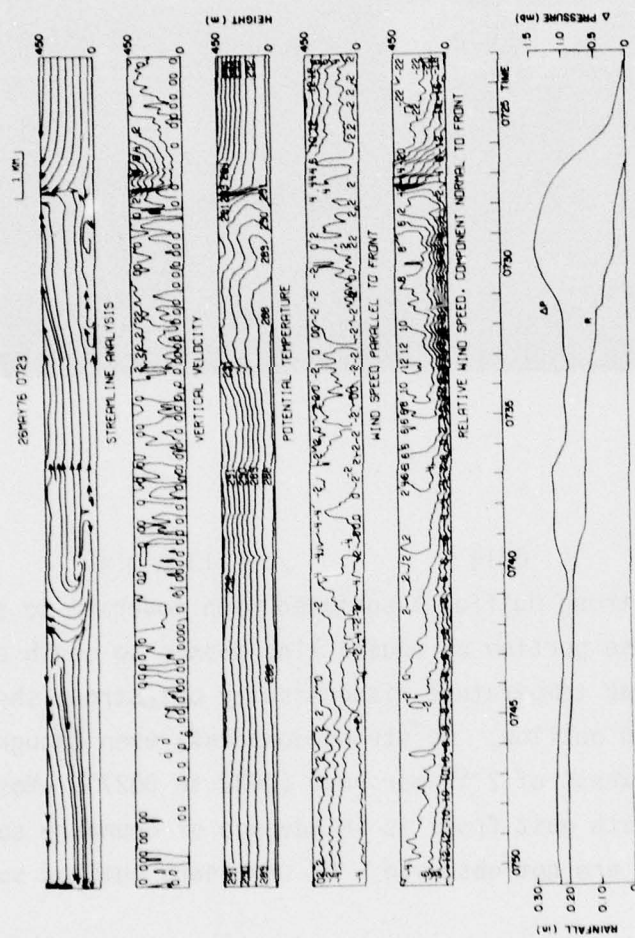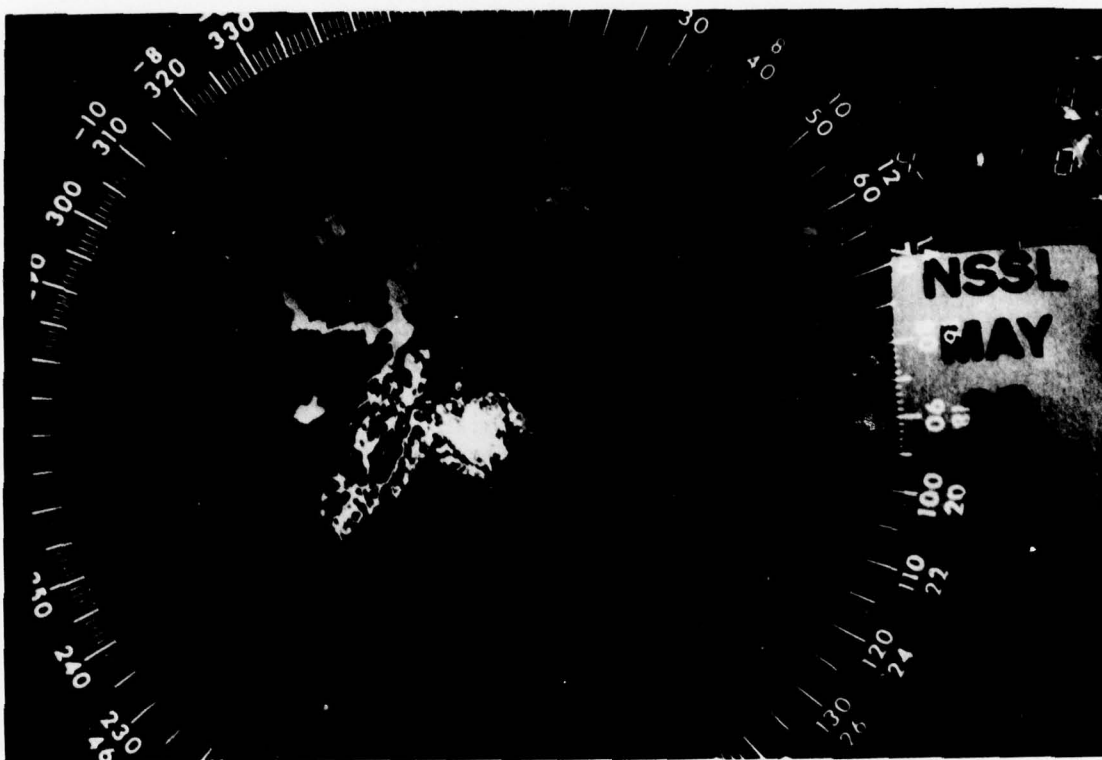
Figure B-E-1

104

Figure B-E-2

Case E

26 May 1976   0727   c = 13.3 m s^{-1} α = 30°

   Classical strong gust front and outflow associated with strong squall
line type thunderstorm. Early morning hour is atypical of such strong
thunderstorms in Oklahoma. Gust front associated with leading edge of
precipitation. Pre-gust front updraft of over 8 m s^{-1} is strongest ever
observed at tower. Large pressure jump accompanies gust front. Turbulence
in outflow is relatively weak, but horizontal flow is strong. Gust front
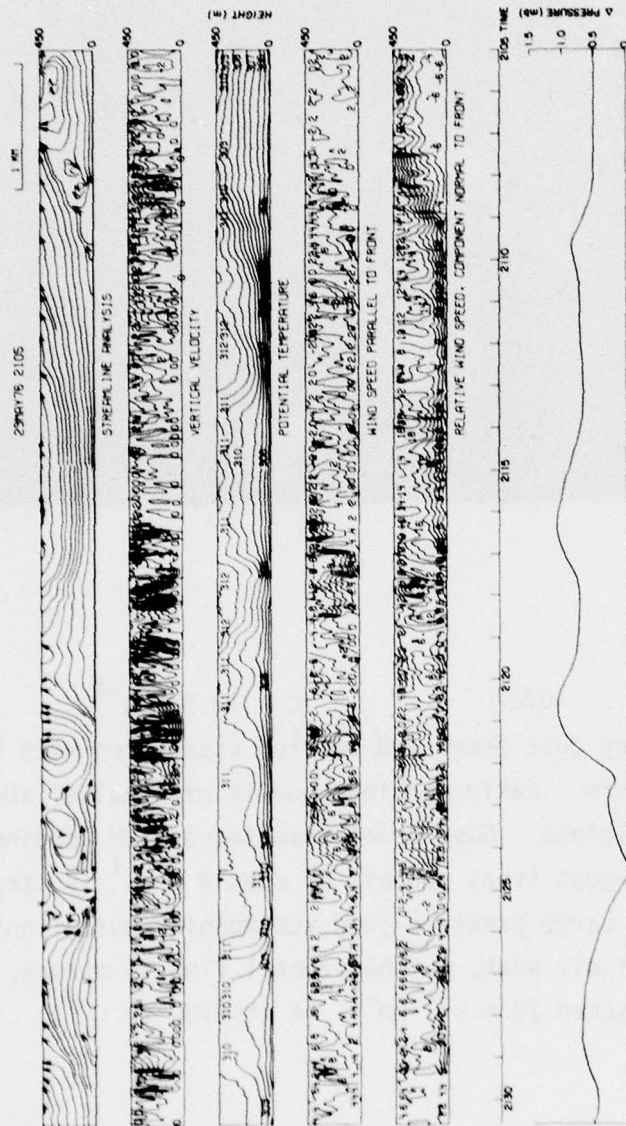horizontal shears exceed 20 m s^{-1} km^{-1}. (4 kts/100 m)

Figure B-F-1a

106

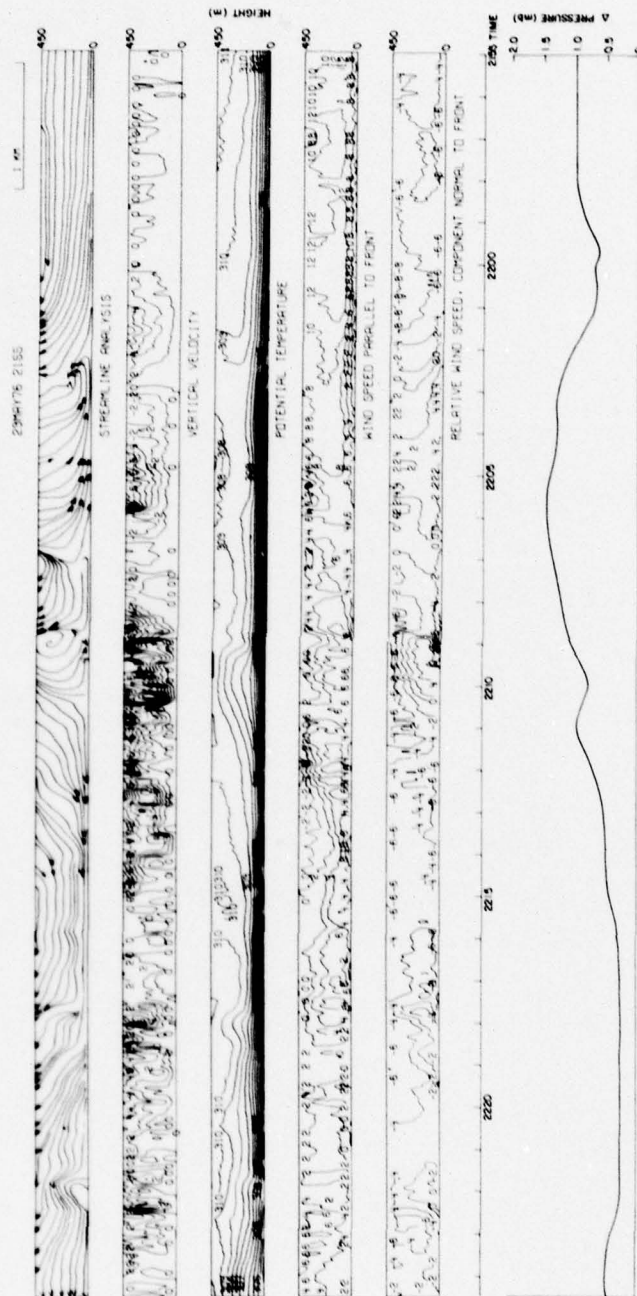Figure B-F-1b

107

Figure B-F-2

Case F

29 May 1976   2109 $c = 5$ m s^{-1} $\alpha = 300°$

Part I

So-called heat burst phenomenon. Relatively unknown feature believed produced by strong subsidence covering large area associated with thunderstorm south of tower. Subsidence outside thunderstorm precipitation zone produces extremely warm and dry air mass.

Such a feature passes by tower at 2109. Shape of heat burst leading edge resembles a very strong warm front (note how slope of front has sign opposite that of gust front.

Turbulence in warm, dry air is most intense ever observed in tower layer. Downdrafts in excess of 8 m s^{-1} at 2117. Band of updrafts greater than 8 m s^{-1} last one min (2120-2121). Very strong and highly fluctuating

109

horizontal wind from frontal zone (2109) to 2125. Despite darkness, temperature in the tower layer rises to 94°F from 85°F in approximately ten minutes. No significant pressure jump with front but large pressure oscillations after 2121.

Part II

Tower layer is relatively tranquil 2130 to 2201. Extreme turbulence begins again at 2201. Lasts more than 20 min. Although fluctuations in horizontal wind are not as large as in Part I, vertical velocity fluctuations are larger (greater than 9 m s^{-1} at 2210). Analysis of NSSL mesonetwork and subsynoptic data (not shown) indicates heat burst pehnomenon covered 10,000 sq mi area in Central Oklahoma. Extreme turbulence possibly caused by combination of downdraft shafts and large eddy mixing of warm air undercutting colder ambient air.

Heat burst front is not to be considered a thunderstorm gust front.

Figure B-G-1

112

Figure B-G-2

Case G

29 May 1976   2359 $c = 5.0 \text{ m s}^{-1}$ $\alpha = 75°$

Relatively weak outflow precedes dissipating squall line. Outflow leading edge at 2359, 29 May and secondary surge at 0024, 30 May identified by two distinct radar thin lines. Gust front precedes precipitation by 20 to 25 km. Horizontal winds behind gust front are weak but turbulence (vertical velocity fluctuations) are strong, possibly due to undulating gust front envelope. Horizontal winds stronger behind secondary surge. A third surge (not shown) accompanies leading edge of precipitation. Large pressure jump is associated with weak gust front but smaller pressure jump observed with stronger secondary surge.
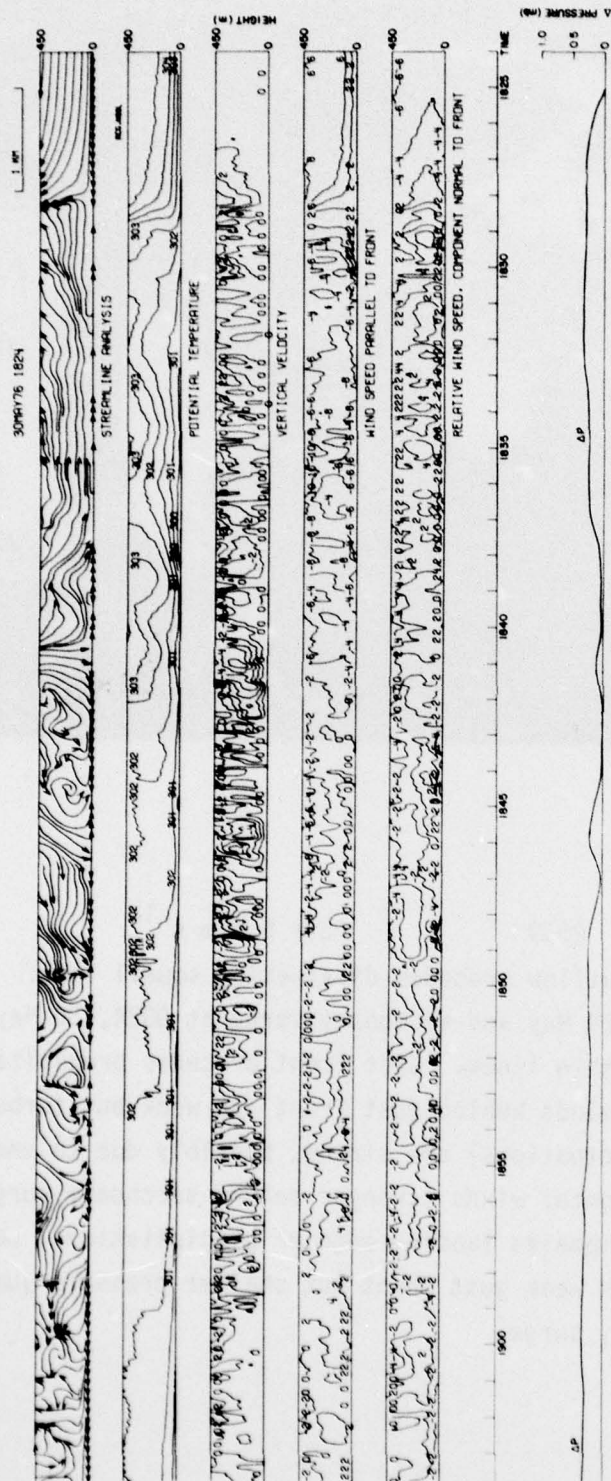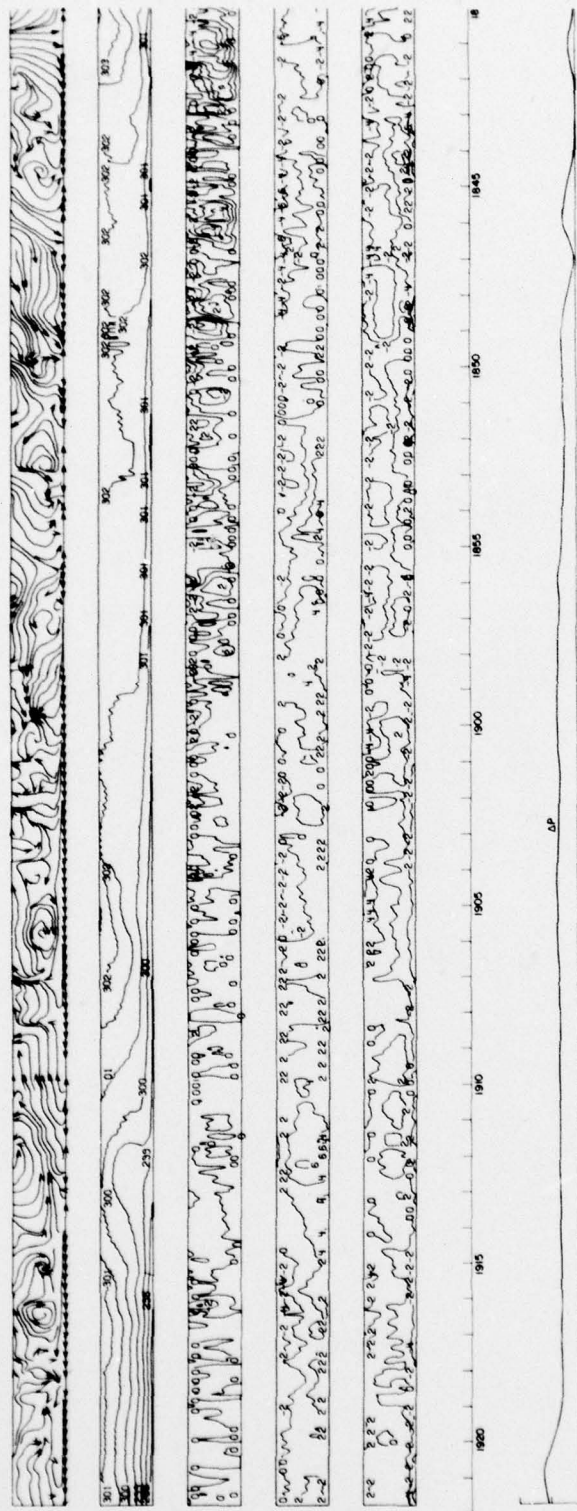
Figure B-H-1a

114

Figure B-H-1b

115

Figure B-H-2

Case H

30 May 1976   1828 $c = 6.1 \text{ m s}^{-1}$ $\alpha = 240°$

Weak to moderately strong outflow associated with broken squall line oriented northeast to southwest. Cells moving toward northeast along squall line axis. Western extension of large cell and attendant outflow brush tower. Gust front shear boundary is weak; pressure jump is small (less than 0.3 mb), however, outflow contains extremely strong turbulence (updraft and downdraft oscillations). Greater than 4 m s^{-1} downdrafts observed only 100 m above ground (1842 and 1846). Maximum downdraft greater than 5 m s^{-1} (1841). Strong turbulence in otherwise weak outflow associated with storm flank appears consistent with several other cases. Here, outflow air may be mixing with ambient air moving past storm. Turbulence diminishes after 1900.
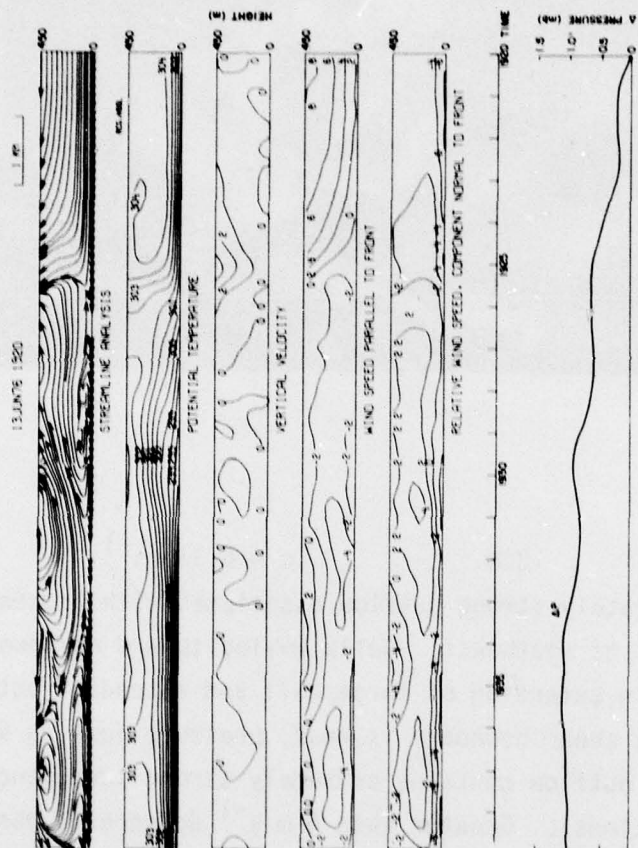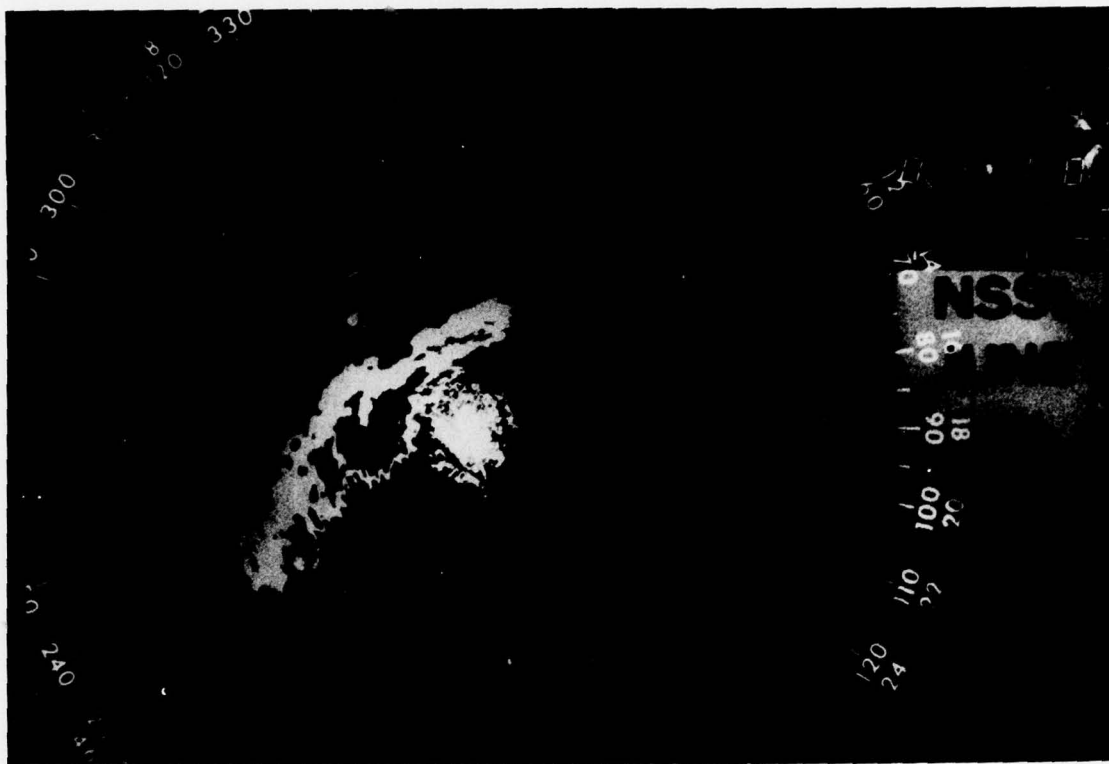
Figure B-I-1a

Figure B-I-1b

119

Figure B-I-2

Case I
13 June 1976   1925   c = 9.0 m s^{-1} α = 0°
Part I

North end of short dissipating squall line produces weak outflow. No measureable rainfall. Horizontal shear associated with gust front, temperature discontinuity and pre-gust front updrafts are weak. No turbulence in outflow.

Part II

Weak secondary surge accompanies rainfall onset. Updrafts in advance of surge are strong (greater than 4 m s^{-1}). Large pressure jump (greater than 2 mb) associated with onset of rainfall. Rainfall very light.

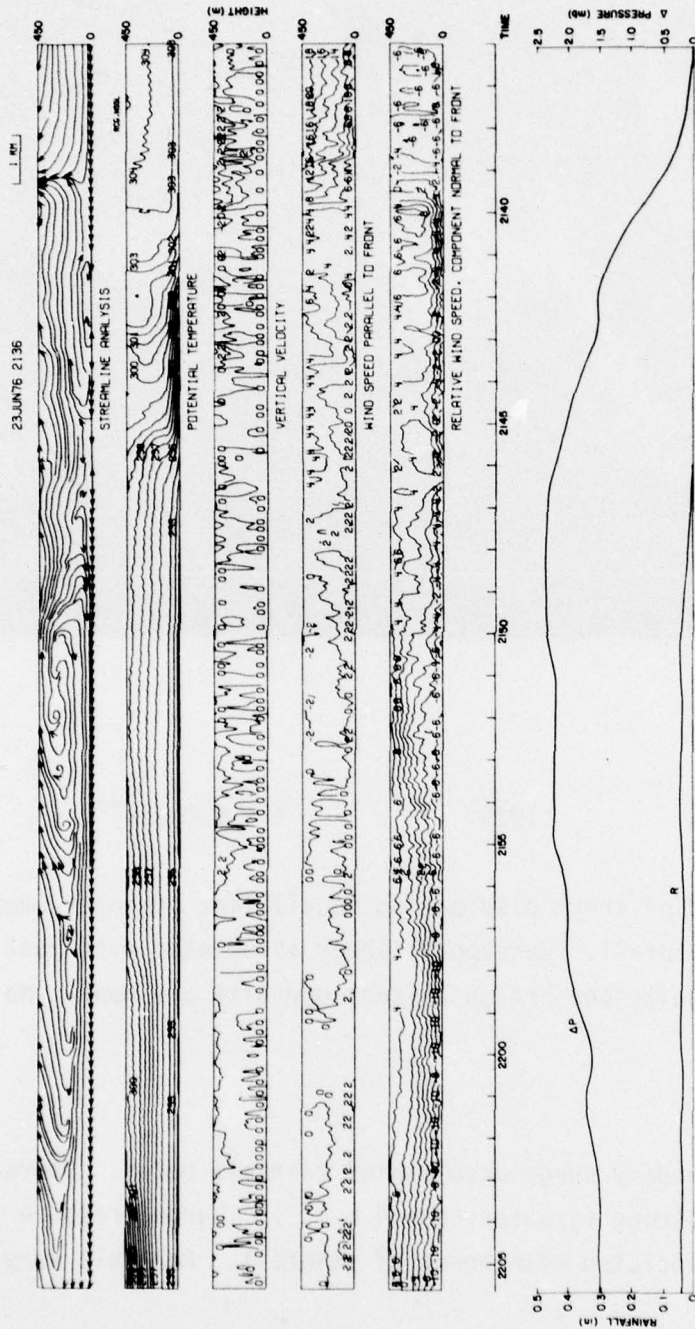Figure B-J-1

122

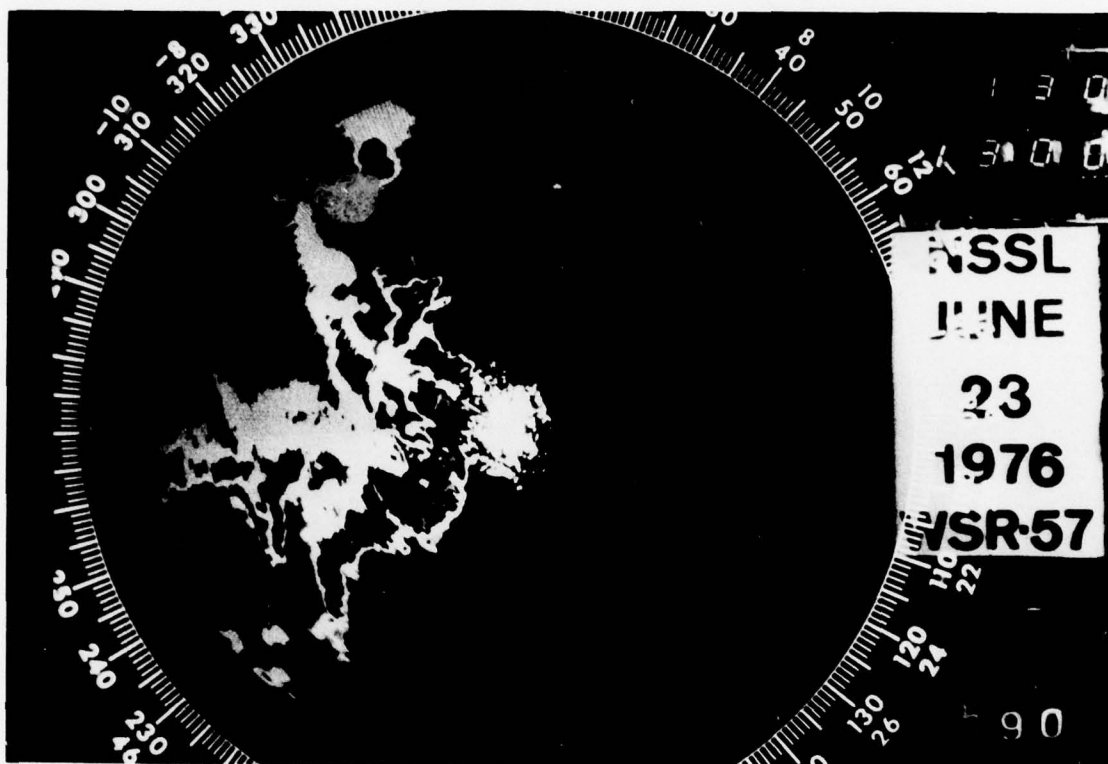*Figure B-J-2*

Case J

23 June 1976   2140 $c = 13.0 \text{ m s}^{-1}$ $\alpha = 350°$

Moderately strong outflow associated with broken squall line. Gust front is unusual in that it precedes temperature discontinuity by up to six minutes or about 5 km. This is the only known observation of such a sequence. Pressure jump is large (2.3 mb). Appears to be two temperature discontinuities but only one wind surge. Light turbulence only in outflow. Light rainfall indicates intense cells in squall line miss the tower.

REFERENCES

Barnes, S. L. (1964). "A technique for maximizing details in numerical weather map analysis." J. Appl. Meteor., 3, 396-409.

Brandes, E. A. (1977). "Flow in severe thunderstorms observed by dual-Doppler radar." Mon. Wea. Rev., 105, 113-120.

Browning, K. A. (1964). "Airflow and precipitation trajectories within severe local storms which travel to the right of the winds." J. Atmos. Sci., 4, 634-639.

Burgess, D. W., L. Hennington, R. J. Doviak, and P. S. Ray (1976) "Multimoment Doppler display for severe storm identification." J. Appl. Meteor., 15, 12, 1302-1306.

Byers, H. R. and R. R. Braham, Jr. (1949). "The Thunderstorm - A Report of the Thunderstorm Project, U. S. Government Printing Office, 287 pp.

Charba, J. (1974). "Application of gravity current model to analysis of squall-line gust front." Mon. Wea. Rev., 102, 140-156.

Goff, R. C. (1975). "Thunderstorm-Outflow Kinematics and Dynamics." NOAA Tech. Memo. ERL NSSL-75, 63 pp.

Goff, R. C. (1976). "Some observations of thunderstorm induced low-level wind variations." Proc. Ninth AIAA Fluid and Plasma Dynamics Conf., San Diego, Calif., 423-427.

Hennington, L., R. J. Doviak, D. Sirmans, D. Zrnic, and R. Strauch (1976). "Measurements of Winds in the optically clear air with microwave pulse-Doppler radar." Preprints, 17th Radar Conf., Amer. Meteor. Soc., Boston, Mass., 342-348.

Lee, J. T. (1965). "Thunderstorms Turbulence and Radar Echoes--1964 Data Studies." Proc. Fifth Annual National Conf. on Environmental Effects on Aircraft and Propulsion Systems, U. S. Naval Air Turbine Test Station, Supt. of Documents, 19 pp.

Lee, J. T. (1972). "Thunderstorm turbulence and drafts." Preprints, International Conference on Aerospace and Aeronautical Meteorology of the Amer. Meteor. Soc., Boston, Mass., 276-280.

Marwitz, J. D. (1972). "The structure and motion of severe hailstorms. Part 1: Supercell storms." J. Appl. Meteor., 11, 166-179.

Mitchell, K. E. and J. B. Hovermale (1977). "A Numerical Investigation of the Severe thunderstorm Gust Front." Mon. Wea. Rev., 105, 657-675.

Shuman, F. G. (1957). "Numerical Methods in Weather Prediction: II. Smoothing and filtering." Mon. Wea. Rev., 85, 357-361.

Sirmans, D. (1973). "Real-time estimate of mean velocity by averaging quantized phase displacements of Doppler radar echoes." 1973 SWIEEECO Record of Technical Papers. 25th Annual Southwestern IEEE Conference, 71-72.

126